

Species Distribution Models of Intertidal Benthos

Tools for Assessing the Impact of Physical and Morphological Drivers on Benthos and Birds in the Wadden Sea

Eelke Folmer, Anne Dekinga, Sander Holthuijsen,
Jaap van der Meer, Dennis Mosk, Theunis Piersma, Henk van der Veer

Texel, August 2017
NIOZ Royal Netherlands Institute for Sea Research

Species Distribution Models of Intertidal Benthos - Tools for Assessing the Impact of Physical and Morphological Drivers on Benthos and Birds in the Wadden Sea

Eelke Folmer, Anne Dekinga, Sander Holthuijsen, Jaap van der Meer, Dennis Mosk, Theunis Piersma, Henk van der Veer

Summary

Introduction The Wadden Sea and its coastal area is threatened by relative sea level rise (RSLR). Particularly, the risk that intertidal flats will drown and that the main land may flood increases with rising sea level and subsidence of the land and seafloor. Dutch authorities are investigating how sediment nourishments in the outer deltas of the Wadden Sea may help avoid the drowning of intertidal flats and reduce the risk of floods. RSLR by itself and in combination with nourishments will affect the morphology of the system, its hydrodynamics and the sediment composition of the subtidal and intertidal seafloor. These changes are expected to influence the distribution of benthos and shorebirds. This report investigates possible responses of benthos communities on the basis of analysis of the distribution of intertidal benthos and relationships with physical drivers. Expected responses of a number of shorebird species are based on their diets and expected changes in benthos abundance and distribution.

Methods We use data from a large scale synoptic monitoring program (SIBES) to provide insight into the spatial and temporal variability of sediment characteristics and macrozoobenthos in the Dutch Wadden Sea. We use six physical predictor variables (i.e. exposure time, shear stress, wave forcing, salinity, sediment, median grain size and mud fraction) to statistically model the benthos community by means of correspondence analysis and constrained correspondence analysis. We also develop species distribution models (SDMs) by means of regression for 27 benthos species using five different machine learning algorithms. The models are tuned by means of cross validation with spatially distinct subsets. On the basis of the individual model predictions we compute a consensus prediction (a weighted average of the predictions). Partial dependence plots are constructed on the basis of the SDMs to provide insight into species-specific responses to possible changes in the physical conditions at the intertidal flats. The partial dependence plots can be used to postulate expectations of the benthos and bird communities in response to changing physical conditions.

In addition to the physical variables we also analyze the relationship between residual (based on the machine learning consensus model) benthos biomass for the bivalve species *Cerastoderma edule*, *Mya arenaria*, *Limecola balthica* and *Peringia ulvae* and pelagic chlorophyll-a concentrations.

Results We show that the intertidal flats have become sandier in the period 2009-2015; particularly median grain size of the sediment has increased and the mud fraction has decreased. We present the biomass, numeric abundance and site occupancy of the 27 intertidal benthos species that are most important in terms of biomass. We show that the abundance (biomass, number of specimens, occupancy) of benthos varies widely between years and over a broad range of environmental conditions. Despite the yearly variability, the relationships between occupancy and the environmental variables are constant between years. This observation justifies the use of the average abundance per sampling site to analyze the relationships with the environmental variables.

Correspondence analysis shows that there are gradients over which the species tend to co-occur but that there are no distinct clusters of species. Constrained correspondence analysis shows that the main axes explaining differences between benthos species are related to the sediment

properties of the intertidal flats and to exposure time, shear stress and wave forcing.

For most species, the SDMs are able to capture the main distribution patterns of the benthos species. However, the consensus predictions, based on the five machine learning algorithms, are systematically lower than the high biomass values (underprediction) and higher than the low density values (overprediction). The level of spatial autocorrelation in the residuals is significantly lower than the spatial autocorrelation in the observations for the species where the SDMs captured signal.

We found positive but weak relationships between chlorophyll-a concentrations and the densities of the residuals of the biomass of *Cerastoderma edule* and *Limecola balthica* but not between *Mya arenaria* and *Peringia ulvae*. Within tidal basins, there were both positive and negative relationships between biomass and chlorophyll-a.

The partial dependence plots show that three main prey species of red knot (i.e. *Limecola balthica, Cerastoderma edule, Peringia ulvae*) show similar positive relationships with exposure time. If the total area of intertidal flats with high exposure time were to be reduced, the important red knot prey species are expected to decline. Oystercatchers' main prey items (*Cerastoderma edule*, *Limecola balthica* and *Hediste diversicolor*) are also expected to decrease if exposure time decreases. Additionally, if the areas with relatively high shear stress expand, the biomass of *Hediste diversicolor* is expected to be reduced and of *Ensis leei* it might increase.

Conclusion The finding that most benthos species occur over broad ranges of environmental conditions and that the temporal variabilities are relatively large suggests that the benthos communities are quite irrepressible to moderate changes in the environmental variables on short timescales. However, the dependence relationships suggest that if there are significant and permanent changes in the environmental variables, changes in the benthos community are to be expected in the long term. The variability of the benthos densities under relatively constant abiotic conditions (i.e. the conditions considered in this report) suggests that it will take long time and many observations to detect systematic shifts in benthos distributions related to changes in the physical variables. Models simulating the physical environment may provide more detailed insight into possible future conditions. On the basis of such scenario's more detailed prognoses about the benthos and shorebird communities can be developed which can be used to support decision making with regards to sediment nourishments in a more tangible manner.

Contents

1 Introduction

The Wadden Sea is the largest coherent system of intertidal flats in the temperate zones of the world. It is highly valued for its natural values and it provides important ecosystem services such as protection against storm surges. The Wadden Sea and its hinterland is threatened by relative sea level rise (RSLR) (Kabat *et al.*, 2009). Particularly, under future rates of RSLR it is unlikely that natural sedimentation rates are sufficient to compensate for RSLR. Authorities in the Netherlands are investigating how sediment nourishments can support sustainable persistence of the Wadden Sea area and its ecosystem services.

The high primary productivity of the Wadden Sea and North Sea ecosystems support high productivity and abundance of secondary producers such as macrozoobenthos and predators such as shorebirds, fish and crustaceans. The benthic macrofauna is composed of molluscs, polychaetes, crustaceans and other groups (Compton *et al.*, 2013a). Typical numerical densities are in the order of several thousands of individuals per m^2 and biomass typically ranges between 1 and 100 g ash-free dry weight per m^2 (Heip *et al.*, 1995; Compton *et al.*, 2013a). The spatial distribution of macrozoobenthos strongly depends on the properties of its environment such as inundation time and sediment grain size (e.g. Kraan *et al.*, 2010; Compton *et al.*, 2013a). The temporal variability in biomass may span multiple orders of magnitude which is mainly driven by episodic recruitment events (van der Meer *et al.*, 2001).

Large-scale changes in the system, including anthropogenically induced changes due to for example dredging and sediment nourishments, will affect the morphology, hydrodynamics and the sediment properties of the seafloor and thereby affect the distribution and community composition of benthos. Although there is regularity in benthos distributions and community composition, there is no theory that can be used to deduce quantitative forms of relationships between environmental variables and the distributions of benthos species and communties. Therefore, the modelling of benthos distributions is a highly empirical data-driven enterprise. To analyze and interpret system changes for purposes of predictive modelling, long-term large scale data about system changes and the distribution of benthos are essential (Herman *et al.*, 1999).

Changing sea levels in isolation or in combination with sediment nourishments will cause the system morphology and local physical conditions to change. To identify the areas where specific species and communities are likely to establish, species distribution models (SDMs) can be used (Elith & Leathwick, 2009; Guisan *et al.*, 2013; Folmer *et al.*, 2016). SDMs are based on statistical relationships between the abundance of organisms and environmental conditions. The quality of the predictor variables, in the sense that they adequately represent the relevant physical conditions, is crucial to the development of useful SDMs. Important abiotic predictor variables for benthos include the hydrodynamic conditions such as inundation time, shear stress and wave forcing, the seafloor sediment properties and salinity.

In this report we 1. provide detailed insight into the spatial and temporal variability of the sediment properties and macrozoobenthos in the Dutch Wadden Sea (Fig. 2) over the years 2008-2013 on the basis of a large scale synoptic monitoring program (SIBES); 2. use physical predictor variables to model the community distributions by means of correspondence analysis

and constrained correspondence analysis; 4. develop (consensus) species distribtution models by means of machine learning algorithms and analyse the residuals for spatial autocorrelation; 5. analyze the relationships between the benthos biomass residuals and chlorophyll-a concentrations; 6. construct partial dependence plots to develop insight into the response of the benthos and bird communities under possible changing environmental conditions; 7. provide recommendations for management and suggestions for further research.

2 Methods

2.1 Study area

The Wadden Sea is located in the south-eastern coastal zone of the North Sea and borders Denmark, Germany and the Netherlands. It was designated an UNESCO World Heritage site because of its 'universally outstanding natural values'. It consists of intertidal flats, shallow subtidal flats, drainage gullies and deeper inlets and channels. Tidal currents and exposure to waves strongly differ between regions due to differences in tidal range, geomorphology, fetch and the occurrence of barrier islands. The intertidal flats consist of sand mixed with fine-grained muddy sediments; the fractions of fine-grained particles increase towards the shores.

Figure 1: Exposed intertidal mudflat in the Wadden Sea (photo: Roos Kentie).

2.2 Field sampling and laboratory analysis

Within the Synoptic Intertidal Benthic Survey (SIBES), sediment and benthos was sampled throughout the entire intertidal Dutch Wadden Sea (Fig. 2). Sampling was performed over 500 m grids. Randomly located sites within the grid were also sampled for the improvement of the fine-scale accuracy of spatial interpolations (Bijleveld *et al.*, 2012). Sampling sites were visited by foot during low tide and by boat during high tide.

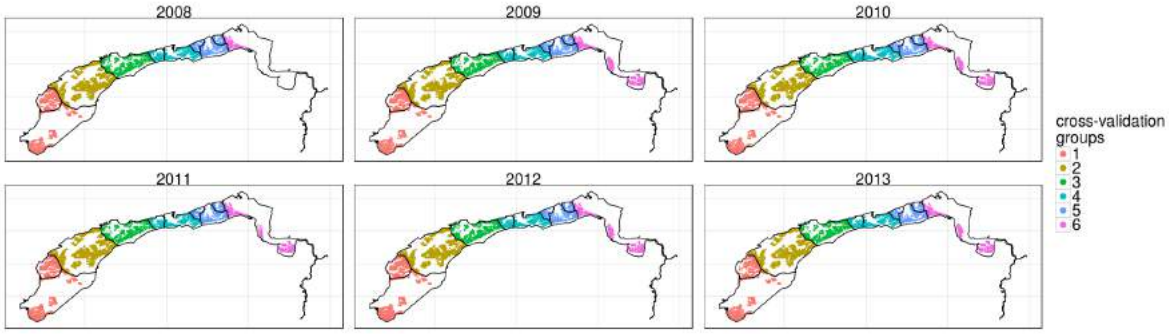

Figure 2: Sites sampled in the Dutch Wadden Sea within the SIBES monitoring programme between 2008 and 2013. The boundaries of the tidal basins are included. The tidal basins or sets of tidal basins used to split the data for spatial cross-validation are indicated by different colours (see Section 2.5). In 2008 the Ems and Dollard in the eastern Wadden Sea were not sampled.

2.2.1 Sediment

Sediment samples were taken at 500 m grid intervals and at the random sites in the period 2009-2015[1]and at 1 km grid intervals in 2008. Sediment samples were taken from the surface of the intertidal flats to a depth of 4 cm and then frozen at -20 °C. Sediment samples were freeze-dried for up to 96 h and then homogenized with a mortar and pestle. Homogenized samples were weighed and placed into 13 ml polypropylene auto-sampler tubes with degassed reversed osmosis water. Grain size distributions were measured by means of a particle size analyzer which uses laser diffraction and Polarization Intensity Differential Scattering technology (Coulter LS 13 320, optical module 'grey', grain sizes from 0.04 to 2000 µm in 126 size classes). Mud fraction of the sample is defined as the volume fraction between 0.04 and 63.00 µm. For further details concerning sediment analysis we refer to Compton *et al.* (2013b).

2.2.2 Benthos

At the sites sampled by boat, two cores were taken to a depth of approximately 25 cm (total area of 0.0173 m^2). At the sites sampled by foot, a core of 0.0177 m^2 was taken. Samples were sieved in the field on a 1 mm round mesh. Bivalves were separated from the other macrofaunal species and stored frozen until laboratory analysis. The remaining species were preserved using a 4% formaldehyde solution.

Molluscs were identified to species level. Other organisms (mainly crustaceans, polychaetes, oligochaetes) were identified to the finest taxonomic level possible. Polychaetes and crustaceans were identified to either genus or species level; oligochaetes were identified to class level. For further details concerning species identification we refer to Compton *et al.* (2013b).

[1]the reason that sediment data until 2015 are included and benthos until 2013 is that sediment is faster to process.

After identification, the lengths of all molluscs, crabs and shrimp were measured to the nearest 0.1 mm and the biomasses were determined to the nearest 0.1 mg. Some polychaete species are divided into large and small size classes. In the cases that there were multiple individuals of the same mollusc species with shell length less than 8 mm in one sample, the total weight of the small, same-sized individuals was determined. The flesh of molluscs with shell length larger than 8 mm was separated from the shell and dried for 2 to 3 days at 60 °C in a ventilated stove. After weighing the dried flesh to the nearest 0.1 mg, the flesh was incinerated at 560 °C for 5 h. After incineration, the weights of the ashes were measured again (to the nearest 0.1 mg). In this way species and length-specific values for ash-free dry mass (AFDM) were obtained.

2.3 Predictor variables

Hydrodynamics with GETM The hydrodynamic predictors were developed within the PACE project which had the goal of accurately modelling the physics and salinity conditions of the entire Wadden Sea. In the PACE project the hydrodynamics were simulated by means of the General Estuarine Transport Model (GETM, Burchard & Bolding, 2002). GETM is designed for coastal ocean simulations with drying and flooding of intertidal flats. The numerical set-up - based on a 200 x 200 m topography - is the end member of a hierarchy of four nested models covering the North Atlantic, the North Sea, and the southern North Sea (Gräwe *et al.*, 2015). Simulations were run for the period 2008–2011; the year 2008 was not included in the computation of the summary statistics used here since it was considered as spin up for the hydrodynamics. Further modelling details and postprocessing are described in (Gräwe *et al.*, 2016; Folmer *et al.*, 2016).

The model output was used to obtain estimates of mean exposure time[1] (***expt***, i.e. the mean fraction of time that the seabed is exposed to the air) and mean shear stress (***shear***, Nm^{-2}) due to currents and mean salinity (***sal***, *psu*) at the sea floor over the period 2009–2011 (Fig. 3).

Wave forcing Donker (2015) simulated wave forcing in the Dutch Wadden Sea by means of the wave model SWAN (version 40.91AB). SWAN is a 2D horizontal wave model which solves the wave action balance in the horizontal domain. In SWAN, waves are generated by wind and energy is transfered through wave-wave interactions. Waves dissipate energy via depth-induced wave breaking; white capping and bottom friction is included in the model. The model is unable to model flow velocities. For further description we refer to Donker (2015) and references therein.

[1]Peter Herman suggested to make use of the most accurate depth measurements (vaklodingen) to model the densities of benthos. We investigated the relationship between depth and inundation time to judge whether this might lead to more accurate modelling of benthos distributions. The correlation between the two variables is too low to justify the use of depth as a predictor variable. Results are presented in Appendix A. The possibility to apply the inundation model of Janine Nauw and others has not been followed up.

Donker (2015) used SWAN to determine the spatial distribution of wave forcing, in terms of the root mean squared near-bed wave orbital velocity amplitude for 1480 representative environmental scenarios. Particularly, Donker used combinations of five windspeeds (4, 8, 12, 16 and 20 ms^{-1}), eight wind directions (N, NE, E, SE, S, SW, W, NW) and 37 sea levels (from -0.9 to 2.7 m with step size 0.1 m around mean sea level). Obtained model results were, subsequently, related to frequency of occurrence of the environmental scenarios to obtain statistically representative estimates of wave exposure for the entire Dutch Wadden Sea for the period 2006-2013.

In this report we briefly considered the yearly variability of the mean, median, 90^{th} and 95^{th} percentile orbital velocity values for all locations where benthos was sampled. The yearly variations in the mean, median, 90^{th} and 95^{th} percentile values are low compared to the spatial variations (Appendix B shows scatterplots of the median and 95^{th} percentiles of wave forcing between years). Furthermore, the mean, median, 90^{th} and 95^{th} percentile values are strongly correlated. Therefore we used the averages of the 95^{th} percentile values over the years 2006-2013 in the remainder of the report (Fig. 3); we label the variable ***wave*** (ms^{-1}).

Sediment We used mud fraction (***mud***) and median grain size (***mgs***, μm) obtained from the sediment samples described in Section 2.2.1 as predictor variables for the benthos community. We used the average values of mud and mgs per location over the years 2008-2013 as predictors for the benthos community (for which the average densities and biomasses over the period are also used). Section 3.1 shows that the yearly differences in sediment composition are very small in comparison with the spatial differences which justifies the use of the average over the period 2008-2013.

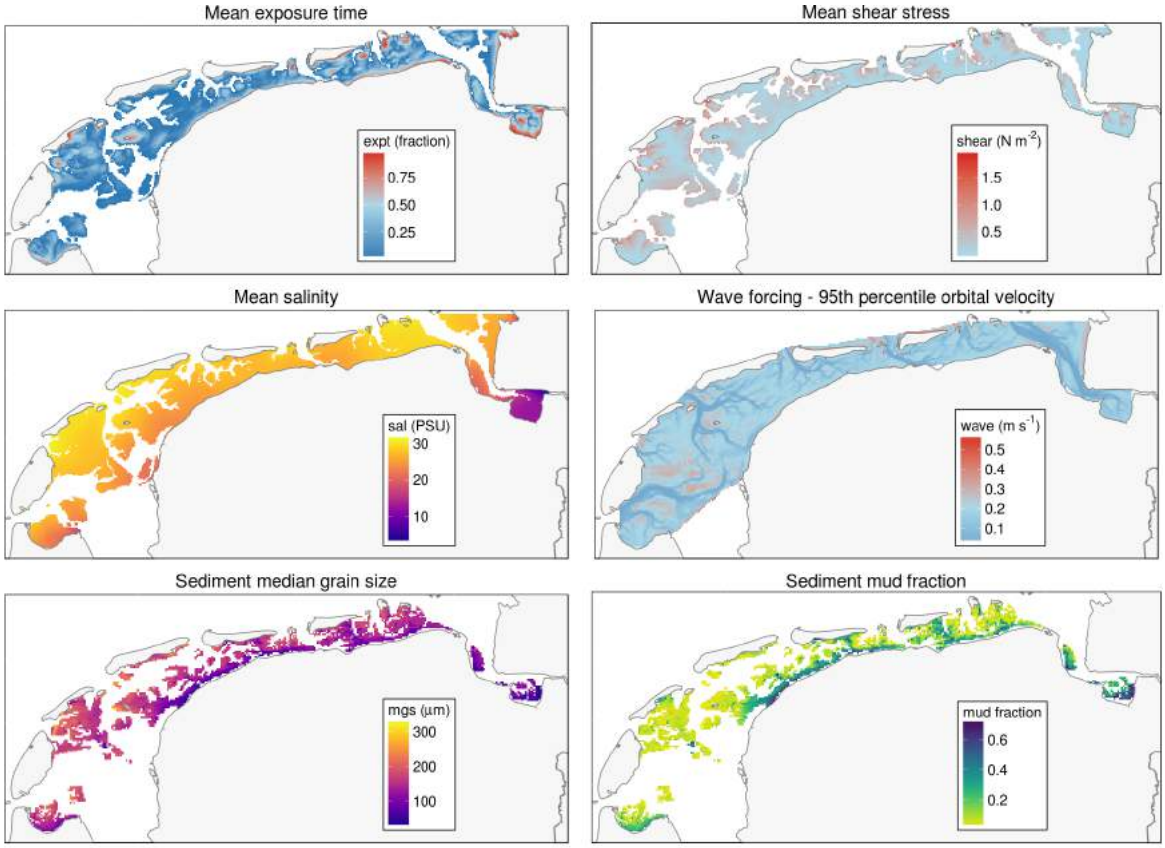

Figure 3: Physical predictor variables used for modelling benthos distributions. Mean exposure time, mean shear stress and mean salinity are products from the PACE project; data provided by Ulf Gräwe from the Leibniz-Institute for Baltic Sea Research (IOW). Near-bed wave forcing data provided by J. Donker (see Donker, 2015), University of Utrecht. Sediment median grain size and mud fraction are from the NIOZ SIBES program.

2.4 Statistical analysis

2.4.1 Imputation

For a number of cases of the benthos data length or biomass measurements were missing (Fig. 24). We used the R package 'mice' (Buuren & Groothuis-Oudshoorn, 2011) for imputing missing values with plausible data values. Plausible values are drawn from distributions which are specifically designed for each missing data point.

For the bivalve species, mudsnail (*Peringia ulvae*), and shore crab (*Carcinus maenas*) there are strong linear relationships between lengths and the cubic root of biomass but the relationships vary between years. Therefore imputation was done for each species and year separately. For the polychaetes length measurements are lacking although for some species two size classes are used. Imputation was done on the basis of this information. Figures 25 and 26 show the density distributions of the original biomass and the resulting imputations.

2.4.2 Sediment dynamics

We analysed the spatio-temporal dynamics of *mgs* and *mud* by means of mixed-effects models. To obtain insight into where the changes occured the analyses were done on a pixel-by-pixel basis. As median grain size appeared normally distributed we used a linear mixed-effects model. The location (i.e. pixel id) is taken as a random effect. Because *mud* is expressed as a fraction of the total volume of the sample we logit-transformed (i.e. $logit(y) = log(\frac{y}{1-y})$) *mud* and estimated the yearly change per pixel with a linear mixed-effects model. In the entire sediment dataset from the period 2009-2015 there were 813 cases (out of 26674) for which *mud* was 0.00. Therefore, we added 0.001 to all measurements to avoid having 0 values in logit-transformation. We centered the variable *year* by subtracting 2012 so that the intercepts of the invididual random effects correspond to the mean *mgs* and mean *mud* fraction. We used the R package 'lme4' (Bates *et al.*, 2012) for estimating the mixed-effects models.

2.4.3 Multivariate analysis of predictors and benthos community

To develop insight into the the distribution of the benthos community and the relationships with the abiotic predictor variables we make use of a number of multivariate techniques. In these analyses we only consider the values of the predictor variables at the benthos sampling sites.

We used principal component analysis (PCA) to analyse the covariance structure in the environmental predictor variables set. PCA uses a linear transformation of the variables into a lower dimensional space which retains maximal amount of information about the variables (Venables & Ripley, 2002). We present biplots to show component loadings of the variables and component scores of the benthos sampling sites simultaneously.

We used correspondence analysis to analyse the benthos communities. Correspondence analysis is similar to PCA but it is based on chi-squared distance rather than on variance (Legendre

& Legendre, 1998) [1]. The chi-square distance transformation reduces the values of abundant species more than that of rare species. Because the numeric density (number of specimens per meter squared) of the benthos is variable and strongly influenced by several high values (particularly *Ensis leei* in 2011) the data were square-root transformed prior correspondence analysis. In a biplot of a correspondence analysis the species scores are the weighted averages of site scores.

Constrained correspondence analysis (CCA) is a form of direct comparison analysis where the ordination vectors are maximally related to environmental predictor variables (Legendre & Legendre, 1998). CCA is also known as canonical correspondence analysis. CCA displays the variation in the data that can be explained by the used constraints. We used CCA, implemented in the R-package 'vegan' (Oksanen *et al.*, 2007), to describe how the variation in the benthos community may be explained by the variables *expt*, *shear*, *wave*, *sal*, *mud* and *mgs*.

2.5 Species distribution modelling

Because the benthos data are overdispersed, show strong zero-inflation and are spatially autocorrelated it is hard to develop parametric regression models. Lyashevska *et al.* (2016), however, show an application of modelling the density of *Limecola balthica* in the Dutch Wadden Sea by means of a geostatistical mixture-model where Bernoulli processes and Poisson processes are combined. The method of Lyashevska *et al.* (2016) requires intensive MCMC simulation which would be impractical for the current study.

In this paper we develop models for the spatial distributions of the average benthos biomass over the period 2009-2013[2] by means of "distribution free" machine learning algorithms. When species distribution models (SDM) are developed to predict distributions of species under new conditions machine learning algorithms are often preferred due to their predictive accuracy (Barry & Elith, 2006; Hastie *et al.*, 2009; McCue *et al.*, 2014; Folmer *et al.*, 2016). Another practical advantage of using machine learning algorithms is that they are distribution free and require little manual tuning (Kuhn, 2014). An important goal of this research project is the assessment of the relationships between benthos biomass and the predictor variables. Adequate assessment of these relationships requires general and robust models that are able to predict benthos distributions under new conditions. Therefore, we tuned the SDMs on the basis of their predictive capacity using non-random, spatial cross-validation. In a similar vein to Wenger & Olden (2012); Folmer *et al.* (2016), we split the data into regionally distinct subsets which are more independent than random subsets. We used the borders of the tidal basins of the Dutch Wadden Sea to delineate the regions; some of the smaller neighbouring tidal basins were combined to have more equal number of data points per group. The spatial cross-validation groups are presented in Fig. 2. An advantage of tuning models in this way is that the models are guarded against overfitting and possible bias which may result from

[1] note that other distance measures are possible.

[2] 2008 is excluded in these analyses because in that year the Ems-Dollard estuary was not sampled.

spatial autocorrelation (Wenger & Olden, 2012; Folmer *et al.*, 2016). We model the average biomass of 27 benthos species with the predictor variables described in Section 2.3.

2.5.1 Model tuning procedure

The following model tuning procedure was used to find the best models and predictions for the biomass of each of the benthos species separately.

1. The area was split into six cross-validation groups (Fig. 2).
2. Cross-validation: one of the data subsets was held-out and each of the five modelling frameworks (Section 2.5.3) were fitted to the remaining dataset by means of a grid-search over the algorithm specific hyperparameters. For each parameter combination and for each fold the performance metric RMSE (root mean squared error) was computed.
3. For each of the modeling frameworks, the mean RMSE of each hyper-parameter combination is computed over the six folds.
4. The parameter combination with the lowest mean RMSE was considered the best parameterization for the model.
5. The models were then fitted to the entire data set.

The procedure resulted in five sets of predictions which were used to compute the consensus predictions. For each data point, the consensus prediction was computed by taking the average of the five predicted values, S_{mi}, weighted by the inverse of the individual variances, i.e. $\overline{S_i} = \frac{\sum_{m=1}^{m=5} w_{mi} S_{mi}}{\sum_{m=1}^{m=5} w_{mi}}$ and $w_{mi} = \sigma_{mi}^{-2}$.

The residuals were analysed for spatial pattern by means of correlograms which describe the spatial autocorrelation by spatial lags.

2.5.2 Partial dependence plots

We analysed the nature of the relationships between response variables and predictor variables by means of partial dependence plots. Partial dependence plots show the marginal effect of a response variable after accounting for the average effects of the other variables on the response (Hastie *et al.*, 2009; Zhao & Hastie, 2017). We used the models obtained via the procedure described in Section 2.5.1.

In the following sections follows a brief description of the modelling frameworks.

2.5.3 Machine Learning Frameworks

Generalized Additive Models with Splines Generalized Additive Models with Splines (GAM) is a modelling approach that combines generalized linear models and additive models to account for nonlinear relationships (Wood, 2006; Hastie *et al.*, 2009). In a GAM, the linear predictor is given by a sum of smooth functions of the covariates. GAM is popular because of the flexibility to capture nonlinear effects and is therefore commonly used in ecology. We used the R package *mgcv* (Wood, 2015). We used the identity link function and smoothing splines for each predictor. The smoothing parameters were selected by Generalized Cross Validation (GCV) (Wood, 2015). We used the option to penalize terms to zero so that smoothing parameter estimation - which is part of fitting - can completely remove terms from the model (Marra & Wood, 2011).

Multivariate Adaptive Regression Splines Multivariate Adaptive Regression Splines (MARS) is a regression technique that works similar to regression trees but uses piecewise linear basis functions instead of step functions (Friedman, 1991; Hastie *et al.*, 2009; Kuhn & Johnson, 2013). The basis functions are defined in pairs where a knot sets the cut point along the predictor variable. The basis function has zero value on one side of the knot and is non-zero on the other side. The basis functions are added to a basic linear regression model and estimated coefficients determine the slopes (within the range of the basis function where it is greater than 0). The algorithm progresses in a forward stepwise fashion where knots with corresponding pairs of basis functions are selected on the basis of the largest decrease in prediction error. Terms (i.e. basis functions) are added to the regression model until a stopping point is reached. At this point the model contains many terms and it overfits the data. Therefore a deletion process of terms (pruning) is initiated to reduce model complexity and to improve parsimoniousness. Terms are pruned in order of increasing error reduction. The error metric is the generalized cross validation (GCV) statistic which approximates leave-one-out cross-validation (Kuhn & Johnson, 2013). The degree of the features that are added to the model and number of terms to prune are hyperparameters to be tuned. The degree was set to 1 and 2 and the number of terms to prune was set to 2,3,...,20. We used the R package "earth" for MARS (Milborrow, 2015).

Random Forest The random forest (RF) algorithm (Breiman, 2001; Prasad *et al.*, 2006; Cutler *et al.*, 2007; Hastie *et al.*, 2009) is suitable for SDM because of its ability to model non-linear relationships and complex interactions among predictor variables. Also in the case of multicollinearity, prediction accuracy is usually high which is crucial to the development of reliable models. RF is an ensemble learning method in that it fits many regression trees and then combines the predictions from the trees (Cutler *et al.*, 2007; Hastie *et al.*, 2009). Each tree in a RF is generated by a bootstrap sample of about 67% of the overall sample; about 33% of the sample is used for validation (i.e. the out-of-bag [OOB] sample). At each split point, a fixed number of variables (labeled m_{try}) from all predictors is selected randomly. Per split point the best variable is chosen from the random subset of variables. We followed the recommendation by Hastie *et al.* (2009) to treat m_{try} as a tuning hyperparameter which took

all integer values in the range between 1 and 6 (i.e. the number of predictor variables: *expt*, *shear*, *sal*, *wave*, *mgs*, *mud*). The optimal m_{try} was found by minimizing the prediction error as described above. The number of trees was set on the basis of OOB error convergence. Plots of error against the number of trees suggested that 500 trees was sufficient to stabilize the errors. We used the R package "RandomForest" (Liaw & Wiener, 2002).

An advantage of fitting many regression trees is the possibility to determine the prediction power of variables (Cutler *et al.*, 2007; Hastie *et al.*, 2009). First, the prediction accuracy (mean squared error, MSE) is calculated on the basis of OOB samples. Then, in the OOB sample, the values of the predictor variable are randomly permuted and prediction accuracy is computed again. If a variable is important, then permutation has a negative impact on prediction accuracy. The difference between the two accuracies, averaged over all trees, and normalized by the standard deviation of the differences is the increased mean square error (%incMSE). Another measure of the importance of a variable is the increase in node purity which is computed as the reduction in the residual sum of squares (RSS) before and after the split. The node purity is computed by averaging the RSS's over all trees.

Gradient Boosting Machines We also used Gradient Boosting Machines (GBM) (Elith *et al.*, 2008; Hastie *et al.*, 2009; Kuhn & Johnson, 2013) implemented in the R package "gbm" (Ridgeway, 2013). GBM is also known as Boosted Regression Trees. GBM combines many weak regression trees (by restricting tree depth) in a successive fashion (i.e. boosting) to optimize predictive performance. In GBM, regression trees are sequentially fitted to residuals to minimize the loss function (here the sum of the squared residuals) after which the new tree is added to the model; hence – in contrast to RF – new trees depend on past trees. Boosting may easily lead to overfitting of the data. To avoid overfitting, the contribution of each added tree to the predicted value of the iteration in the step before, is shrunk by the learning rate λ. Shrinkage can be thought of as a penalty for complexity. The disadvantage of shrinkage is that computation time increases with decreasing λ. However, regularization with small values of λ works best to attain optimal models (Elith *et al.*, 2008). Tree depth, learning rate and number of trees are the only hyperparameters to be tuned. Tree depth was set to the values 1 - 8; λ: 0.01, 0.02, ..., 0.1; number of trees: 100, 150, ... 1000. GBM models were fitted to all combinations of hyperparameters and the best model was selected on the basis of RMSE of the test sets.

Support Vector Machines Support Vector Machines (SVM) were originally developed for solving classification problems (Vapnik, 1998) but they have been extended to regression problems with a quantitative response (Hastie *et al.*, 2009; Kuhn & Johnson, 2013). SVMs are popular because they require little tuning, standard algorithms can be used for optimization and they perform well with high dimensional data. Furthermore, SVMs can be applied to simple linear and very complex nonlinear functions by using kernels to map the original inseparable low dimensional feature space to a higher dimension, which is separable. SVMs have been applied in a wide range of scientific domains including ecology, notably species distribution modelling (Drake *et al.*, 2006). For detailed and technical explanations of support

vector regression we refer to Smola & Schölkopf (2004); Hastie *et al.* (2009); Kuhn & Johnson (2013).

The function *ksvm* in the R package "kernlab" (Karatzoglou *et al.*, 2004) was used for SVM regression modelling. We selected the radial basis function kernel because it is very effective and requires only one hyperparameter (σ), which is automatically estimated by the function *kvsm* (Kuhn & Johnson, 2013). The C parameter controls the cost of errors and thus the flexibility of the model; ε controls the width of the insensitive error band. We followed the suggestion by Kuhn & Johnson (2013) to fix ε and to tune over the hyperparameter C because of the relationship between C and ε. C was set to the values 2^{-2}, 2^{-1}, ... , 2^{11}.

2.6 Nutrients and primary production

The species distribution models based on physical predictor variables did not fully capture the spatial patterns of the benthos distributions. We attempted to explain the unexplained variability by means of primary productivity. To analyse the impact of productivity on the macrozoobenthos community we compiled nutrient and chlorophyll-a data from various locations in the Wadden Sea (Figs. 4a and 4b). We analysed the relationships between the SDM residuals and the chlorophyll-a concentrations; nutrient trends are included for reasons of completeness.

2.6.1 Data

Chlorophyll-a and nutrient concentrations in the Wadden Sea were monitored by the Dutch Ministry of Transport and Public Works at a number of locations (Fig. 4a). Data were obtained from the Deltares opendap server which mirrors the waterbase water quality monitoring database[1]. The unit for for chlorophyll-a concentration is µg/l and for nutrient concentrations it is µmol/l.

The purpose of the data handling described below is to obtain estimates of winter nutrient and summer chlorophyll-a concentrations at the monitoring stations and to link them to the benthos sampling sites. To compute summer chlorophyll-a concentrations we used measurements from the months April until August. The winter nutrient concentrations are based on the months December until March. The nutrient concentrations for the month December are considered to be part of the winter of the year after. For example, when chlorophyll-a concentrations of 2010 are matched up with the nutrients, the concentrations of December 2009 and January until March of 2010 are used.

The frequency at which monitoring occured differed between periods and stations which led to temporally irregular timeseries. This may result in differences in the reliability of computed averages. Two methods were used to overcome this difficulty which helps to make robust

[1] opendap: http://opendap.deltares.nl/thredds/fileServer/opendap/rijkswaterstaat/waterbase/
waterbase: http://www.watergegevens.rws.nl

comparisons between stations. The first method comprised of computing average yearly concentrations only when there were more than two measurements within the relevant season (summer concentrations of chlorophyll-a and winter concentrations of nutrients). Although this improves the reliability of the computed averages, the method is not perfect because within seasons the concentrations may also strongly differ. For instance, differences in estimates of chlorophyll-a concentrations can result from the inclusion or exclusion of measurements during phytoplankton blooms (which are easy to miss due to their short durations). The second method aims to overcome this possible bias by means of interpolation of the timeseries. Particularly, the temporally irregular measurements were used to compute regular daily concentrations by means of Stineman interpolation which is a robust method that prevents overshooting (Stineman, 1980). Figure 4b presents the estimates of yearly averages by means of both methods. It shows that the way in which the yearly concentrations are measured is not strongly influenced by the chosen method (x for using the raw data; $y.stine$ for the interpolated data).

To analyse the relationships between yearly benthos biomass and chlorophyll-a concentration we assumed that the benthos biomass in a particular year was influenced by the chlorophyll-a concentration in that year and the two preceding years. The chlorophyll-a concentrations at benthos sampling sites i were computed on the basis of the average concentrations measured at the chlorophyll-a sampling stations j. The benthos sites and pelagic stations were linked on the basis of the weighted inverse squared distance between them, i.e. $Chla_i = \frac{\sum_{j=1}^{j=9} d_{ij}^{-2} \cdot Chla_j}{\sum_{j=1}^{j=9} d_{ij}^{-2}}$.

2.7 Shorebird distributions and diets

The consequences of changing environmental conditions for three shorebird species were investigated using the partial dependence plots for their benthos prey species. We selected three shorebird species which forage on a mix of bivalves and polychaetes (for a review see Folmer *et al.*, 2010). We analyze the response of the prey species that constitute an important portion of the diet and are abundant and accurately monitored in the SIBES program in the Wadden Sea.

- Red knot (*Calidris canutus*): *Limecola balthica, Cerastoderma edule, Peringia ulvae*
- Oystercatcher (*Haematopus ostralegus*): *Cerastoderma edule, Limecola balthica, Ensis leei, Hediste diversicolor*
- Bar-tailed godwit (*Limosa lapponica*): *Hediste diversicolor, Nephtys hombergii, Scoloplos armiger, Arenicola marina, Lanice conchilega, Limecola balthica, Carcinus maenas*

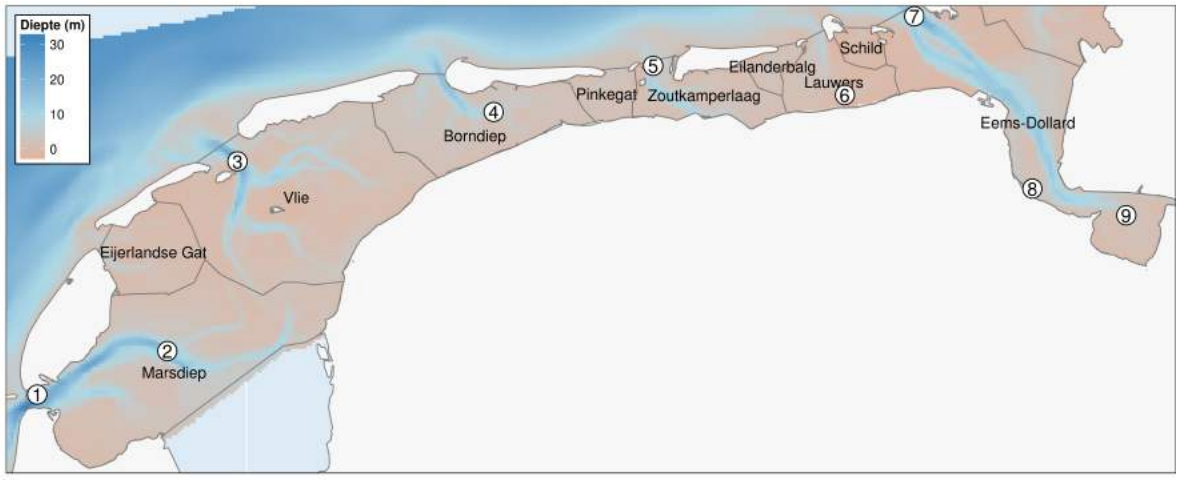

(a) Map of the Dutch Wadden Sea with the stations where chlorophyll-a and nutrient concentrations are monitored. The black lines denote the boundaries of the ten tidal basins.

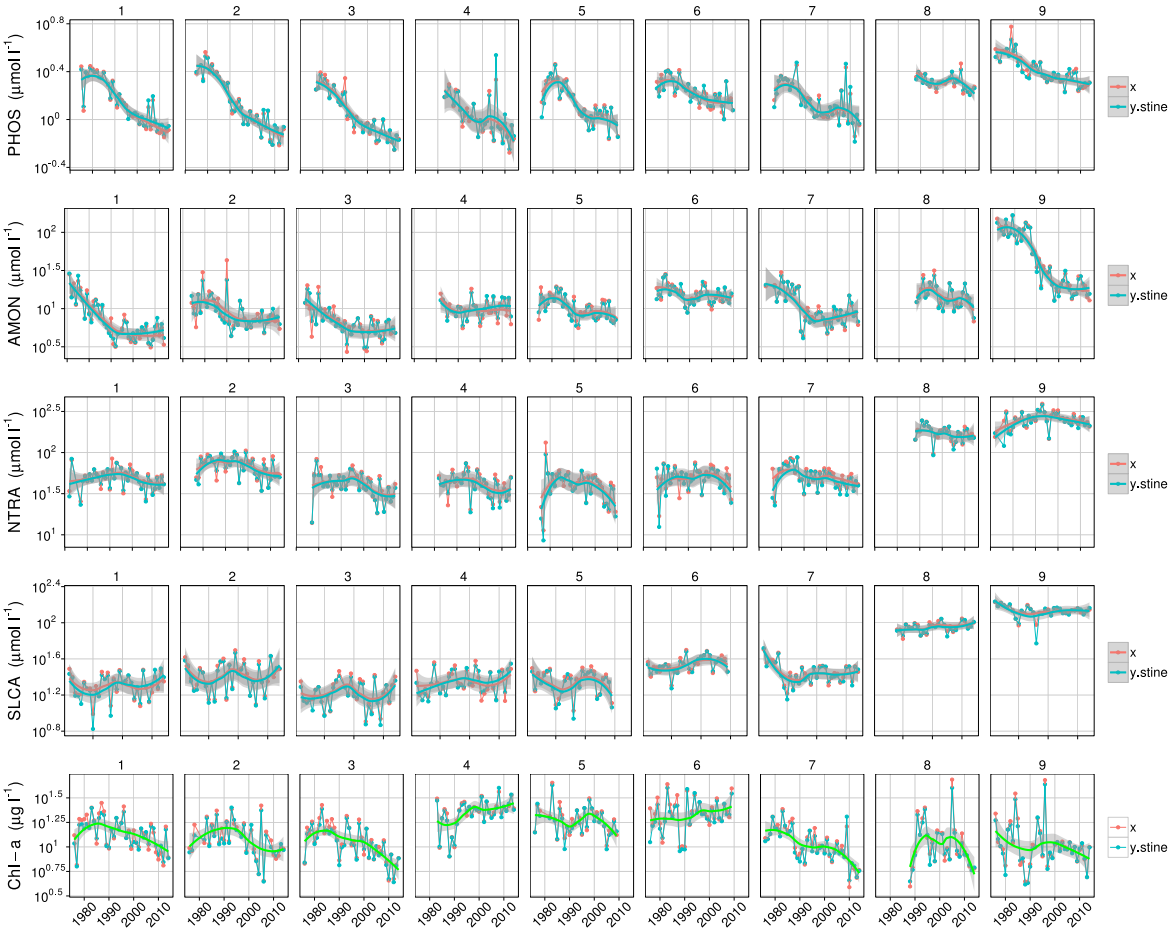

(b) Trends in winter nutrients and summer chlorophyll-a concentrations.

Figure 4: Water quality sampling stations and trends in the Dutch Wadden Sea.

3 Results

3.1 Sediment dynamics

Maps, cumulative distributions and boxplots of yearly *mud* and *mgs* by tidal basin are provided in Appendix C (Figures 21, 22 and 23). The fixed effects of the regression models are presented in Table 1. Because *mud* was logit-transformed, the regression coefficients represent the average intercept and yearly changes on logit scale.

The average yearly increase in *mgs* is 0.89 μm. The yearly change in *mud* is in line with the change in *mgs*; the average mud fraction of the tidal flats has reduced with an average of 0.24% per year[1].

Table 1: Fixed effects of the linear mixed-effects models explaining the variance in median grain size and mud content.

	mgs	mud
Constant	149.004***	−2.312***
	(0.728)	(0.022)
dyear	0.891***	−0.030***
	(0.068)	(0.003)
Observations	18,708	18,708
Log Likelihood	−81,355.940	−21,780.090
Notes:	***Significant at the 1 percent level.	
	**Significant at the 5 percent level.	
	*Significant at the 10 percent level.	

Figure 5 presents maps with the coefficients of the random effects of the mixed models. The top row shows the intercepts for each pixel (because the variable year was centered, the intercept corresponds to the mean *mgs*). The bottom row shows the yearly change in *mgs* and *mud*. The average change in *mgs* ranges between -10 and 15 µm per year and the average yearly in *mud* fraction ranges between -0.04 and 0.02 (-4% and 2%). The spatial changes in *mgs* and *mud* are in line with each other in that the largest increases in *mgs* and the largest decreases of *mud* tend to occur near the main land. The scatterplots in Figure 6 of the yearly changes against the mean *mgs* and *mud* in figure illustrate this phenomenon in more detail.

[1] $logit^{-1}(-2.312 - 0.030) - logit^{-1}(-2.312) = -0.0024 = -0.24\%$

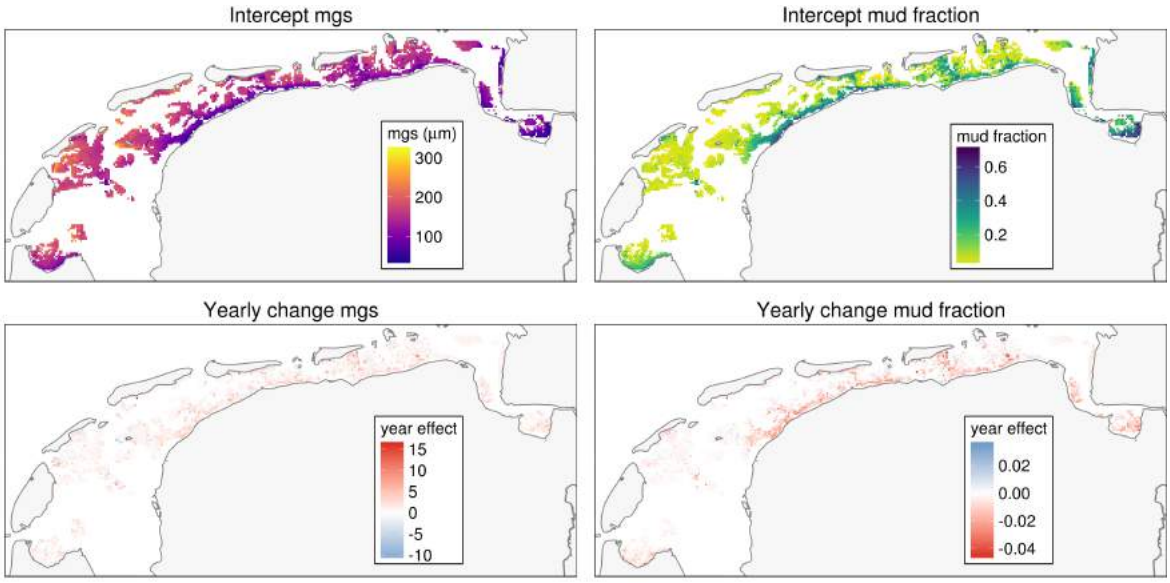

Figure 5: Maps with the coefficients of the random effects of the mixed models for median grain size (*mgs*) and *mud* fraction. The intercept and yearly change in *mud* fraction were back-transformed by means of the inverse logit.

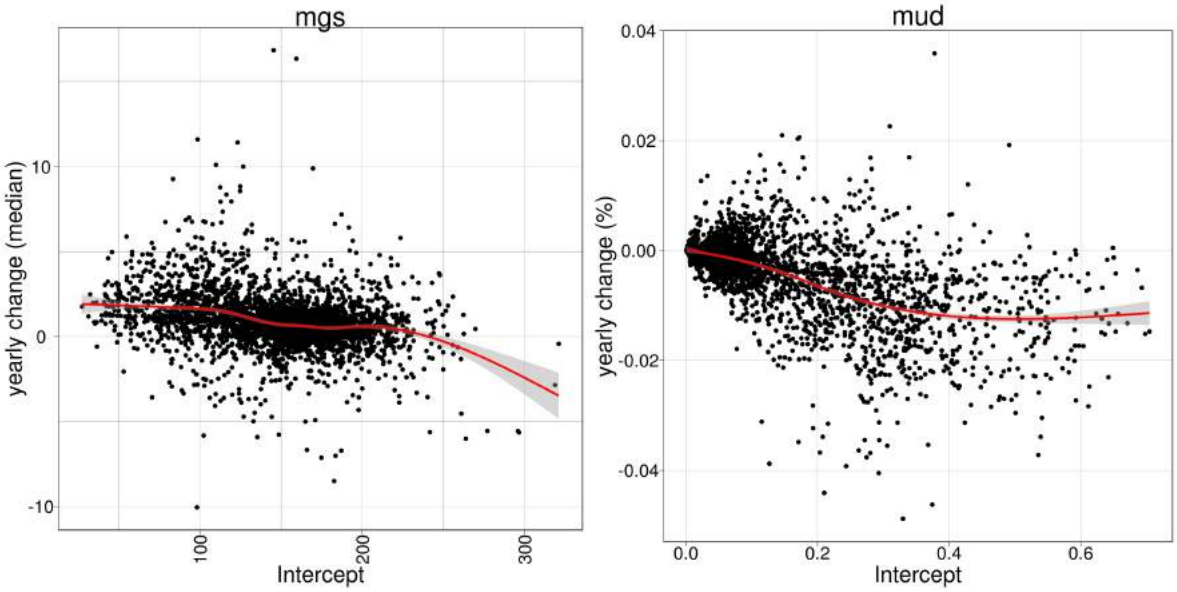

Figure 6: Scatterplots of the yearly changes against the intercepts of *mgs* and *mud*. The data points are the random effects of the mixed models.

3.2 Benthos - general patterns

This section describes some general patterns of the benthos in the Wadden Sea. The species in Table 3, which includes the abreviated species codes, are analysed in this report. Section 3.2.1 describes the yearly biomass, density and occupancy of the most abundant species and timeseries are presented in Appendix E.

code	species	class
Abrten	*Abra tenuis*	Mollusca
Ceredu	*Cerastoderma edule*	Mollusca
Ensdir	*Ensis leei*	Mollusca
Macbal	*Limecola balthica*	Mollusca
Myaare	*Mya arenaria*	Mollusca
Perulv	*Peringia ulvae*	Mollusca
Scrpla	*Scrobicularia plana*	Mollusca
Alivir	*Alitta virens*	Polychaeta
Aphmar	*Aphelochaeta marioni*	Polychaeta
Aremar	*Arenicola marina*	Polychaeta
Capcap	*Capitella capitata*	Polychaeta
Etelon	*Eteone longa*	Polychaeta
Heddiv	*Hediste diversicolor*	Polychaeta
Hetfil	*Heteromastus filiformis*	Polychaeta
Lancon	*Lanice conchilega*	Polychaeta
Marvir	*Marenzelleria viridis*	Polychaeta
Nephom	*Nephtys hombergii*	Polychaeta
Phymuc	*Phyllodoce mucosa*	Polychaeta
Polcor	*Polydora cornuta*	Polychaeta
Pygele	*Pygospio elegans*	Polychaeta
Scoarm	*Scoloplos armiger*	Polychaeta
Spimar	*Spio martinensis*	Polychaeta
Oligoc	*Oligochaeta sp.*	Oligochaeta
Batsar	*Bathyporeia sarsi*	Crustacea
Carmae	*Carcinus maenas*	Crustacea
Corosp	*Corophium sp.*	Crustacea
Uropos	*Urothoe poseidonis*	Crustacea

Table 2: Abreviated code name and scientific name and class of the benthos species.

3.2.1 Biomass, numeric density and occupancy per species

Cockles (*Cerastoderma edule*) are the most important species in terms of biomass per squared meter followed by lugworms (*Arenicola marina*), sand gaper (*Mya arenaria*), razor clam (*Ensis* leei) and baltic tellin (*Limecola balthica*). The yearly average biomass of cockles ranges between

4 and 10 g m^{-2} and of lugworms and sand gaper between 1.5 and 3 g m^{-2}. The numerically most important species are mudsnails (*Peringia ulvae*) and the tubeworm (*Pygospio elegans*). In terms of occupancy (% of sites occupied) the differences between species are less pronounced.

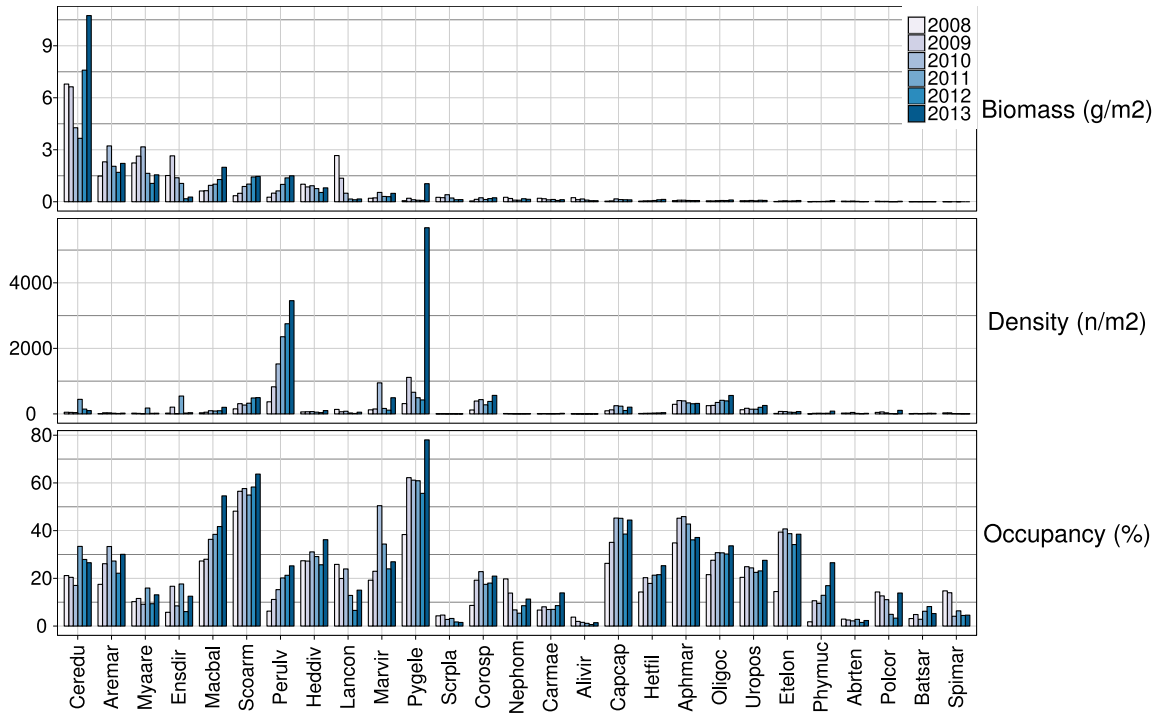

Figure 7: Average biomass (g m^{-2}), numeric density (specimens m^{-2}) and occupancy (%) for the 27 selected most abundant benthos species in the Dutch Wadden Sea.

Maps of yearly distributions of benthos are presented in Figs. 30 - 56 in Appendix F. The following paragraphs highlight some general patterns that are relevant for the SDMs developed in Section 3.4.

Molluscs The general picture that emerges from the mollusc distribution maps in Section F.1 is that the same intertidal flat areas tend to be occupied across years but that the yearly densities vary strongly. There are some interesting exceptions to this general pattern, however. For instance, the density of razor clam (*Ensis leei*) is high on the mudflats south of Griend in 2009 while it is virtually absent in this area in 2010. In 2011, the density of razor clam is exceptionally high south of Vlieland while the densities had been low in the years before. This type of spatially variable boom-and-bust dynamics is exception rather than rule for other bivalve species. *Abra tenuis* has a rather specific spatial distribution in that it is limited to highly elevated areas on distinct tidal flats like Balgzand, between Texel and Vlieland, east of Griend and south of Rottumerplaat (Fig. 36).

Polychaetes The spatial distributions of the different polychaete species are also rather constant in that the same areas tend to be occupied year after year (Section F.2). However, the densities may vary strongly between years (also see Fig. 28). *Lanice conchilega* is somewhat exceptional and shows a rather steep decline over the entire area between 2009 and 2012 after which the densities increase again (Fig. 40).

Crustaceans The spatial distribution of crustaceans is also constant in that the same mudflats tend to be occupied (Section F.3). There are striking differences between species. For instance, *Corophium sp.* tend to occupy the mudflats near the mainland shore (Fig. 53) while *Urothoe poseidonis* tends to occupy the mudflats in the vicinity of the tidal inlets (Fig. 55). The distributions are constant between years. In the following section the relationships between the distribtution of benthos in relation to environmental variables are considered in further detail.

3.2.2 Occupancy environment relationships

Figure 8 shows the relationships between the occupancy of the intertidal flats by bivalves for the different species and the environmental predictors for each year over the period 2008-2013. The relationships are consistent through time which implies that the average densities are systematic and robust representatives of the year-wise relationships. Figs 57 and 58 in Appendix G show the occupancy environment relationships for polychaetes and crustaceans. We also refer to the figures with the yearly spatial distributions of benthos in Appendix F. Because the relationships are systematic we can model the average density of benthos per site as functions of the environmental variables (Section 3.4).

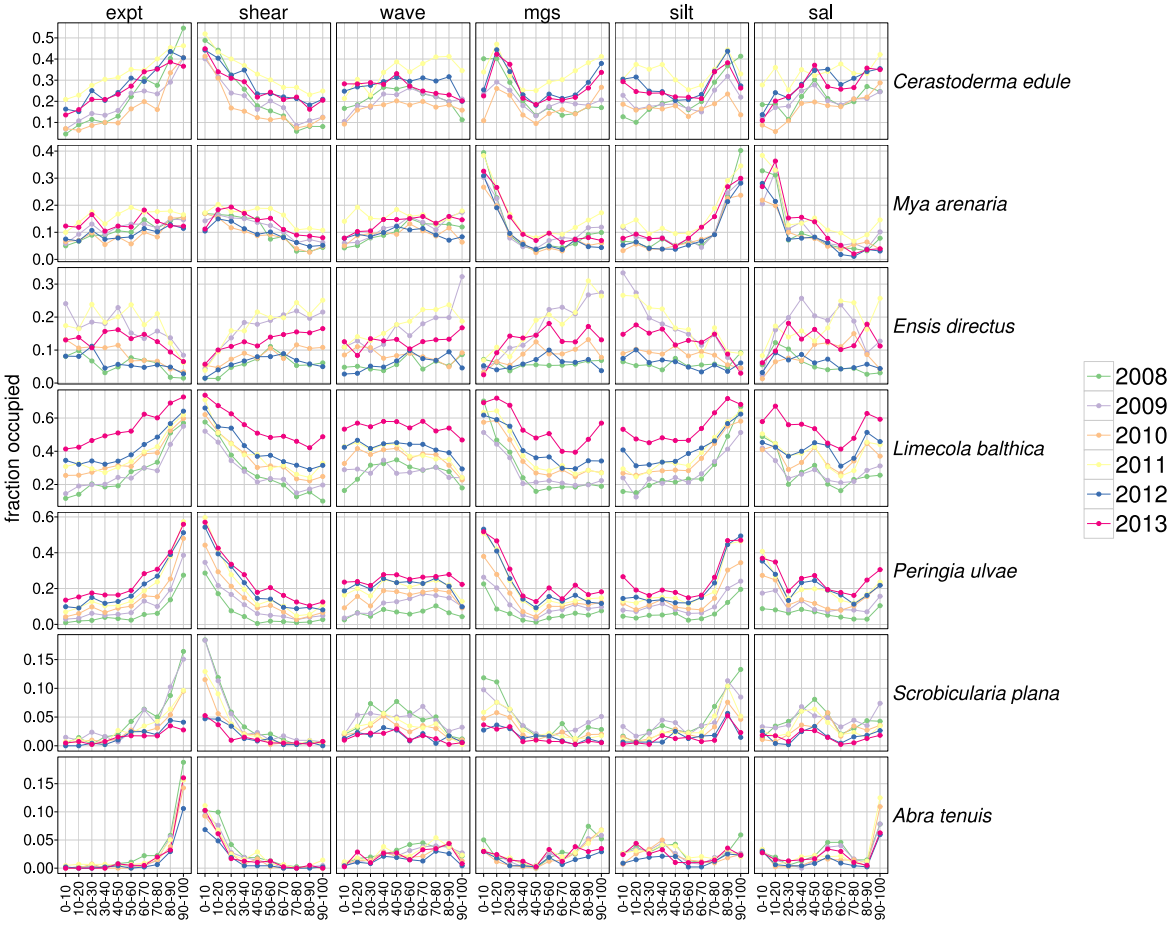

Figure 8: Fraction of benthos sampling sites that are occupied by molluscs against the 10 deciles of the predictor variables.

3.3 Multivariate analyses

The principal component analysis of the predictor variables shows that the first two components describe nearly 72% of the variance in the predictor dataset (Fig. 9). The biplot in Fig. 9 shows that the first principal component, which describes approximately 47% of the variation, is mainly associated with the sediment properties *mgs*, *mud* and *sal*. The second principal component is mainly associated with *expt*, *wave* and *shear*.

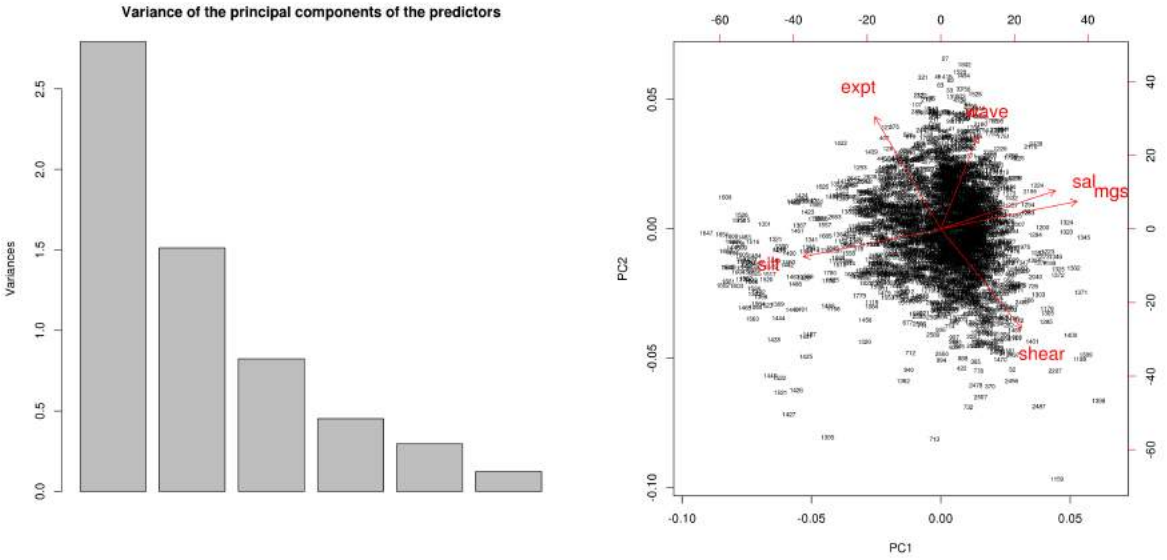

Figure 9: PCA of the environmental predictor variables. The scree plot in the left panel gives the variance against the principal components. The biplot in the right panel shows the loadings of the variables on the first and second principal components.

There were eight sites where none of the 27 benthos species were present in the period 2009-2013; these sites were not included in the correspondence analysis. The correspondence analysis of the benthos community shows the associations between the different species. The biplot in the left panel of Fig. 10 shows that while there are gradients over which the species tend to co-occur, there are no distinct clusters of species. This observation is in line with the distinct spatial distributions presented in Appendix F.

Constrained correspondence analysis provides insight into how variation in the benthos community may be explained by environmental variables. The biplot in the right panel of Fig. 10 shows that species like *Ensis leei*, *Spio martinensis, Nephthys hombergii, Scoloplos armiger* tend to co-occur in areas with course sediment. *Abra tenuis* and *Scrobicularia plana* are species that occur at intertidal flats with high exposure times, i.e. at highly elevated locations.

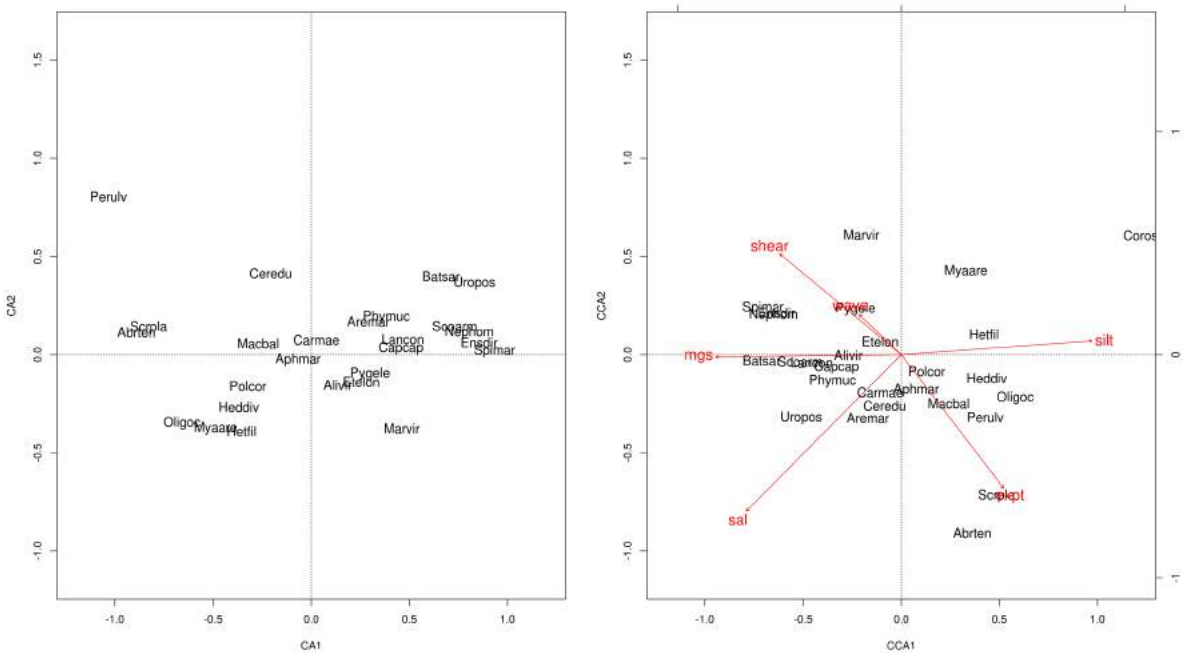

Figure 10: Biplots of the correspondence analysis and the constrained correspondence analysis of the benthos community (number of specimens per meter squared) in the Wadden Sea.

3.4 Spatial distributions and species distribution models

Species specific distributions of all species presented in table 2 over the period 2008-2013 are presented in Appendix F. Here we describe the modelling results for the log-transformed average biomass of *Cerastoderma edule* to illustrate the workflow and interpretation. The modelling results for the other species are presented in Appendix H.

Table 3 presents the prediction errors (RMSE) for the different frameworks. RMSE is relatively high across modelling frameworks for all the holdout sets which implies that none of the models adequately captured the variability of the data. This, however, does not imply that the environmental predictors have little effect on the benthos distributions.

The maps in the left panels in Fig. 11 show the observed cockle biomass (obs), the consensus prediction (wavg) and the residuals (obs - wavg). Although the differences between observed and the consensus predictions are large and the models tend to underpredict high values and overpredict low values (see scatterplot), the models tend to capture the main spatial patterns in the cockle distributions. The consensus SDM has "explained" variability and also reduced the spatial autocorrelation (Fig. 11). However, substantial autocorrelation in the residual terms remains.

holdout	ncells	RF	GBM	MARS	SVM	GAM	CONS
1	3564	5.97	5.96	5.96	6.62	6.31	5.97
2	4644	5.62	5.63	5.68	5.74	5.80	5.54
3	2280	5.66	5.63	5.65	5.60	5.97	5.60
4	1788	5.81	5.79	5.95	6.05	5.86	5.78
5	1794	5.61	5.76	5.78	5.31	6.14	5.57
6	1524	5.43	4.73	4.89	6.82	5.81	4.73
$\overline{RMSE}$ (non-random CV)		5.71	5.65	5.70	6.02	5.99	
$\overline{RMSE}$ (random CV)		5.22	5.27	5.50	5.49	5.54	

Table 3: Ceredu: Transferability assessment of the best tuned models (one for each modeling framework) on the basis of non-random cross validation for the six spatial subsets within the Dutch Wadden Sea. RMSEs are given for RF, GBM, MARS, SVM, GAM predictions and for the consensus prediction (CONS). The row $\overline{RMSE}$ (random CV) gives the average RMSE of the models that were tuned by conventional random cross-validation.

When there is good agreement between the observed and predicted distribution patterns, partial dependence plots may provide insight into the univariate relationships (and the causal relationships) between the benthos density and the predictor variables. Table 4 gives the R^2 values between observed and predicted values for the different species. The R^2 values for *Scoloplos armiger* and *Corophium sp.* are high while the values for *Carcinus maenas*, *Spio martinensis*, *Alitta virens* and *Eteone longa* are very low.

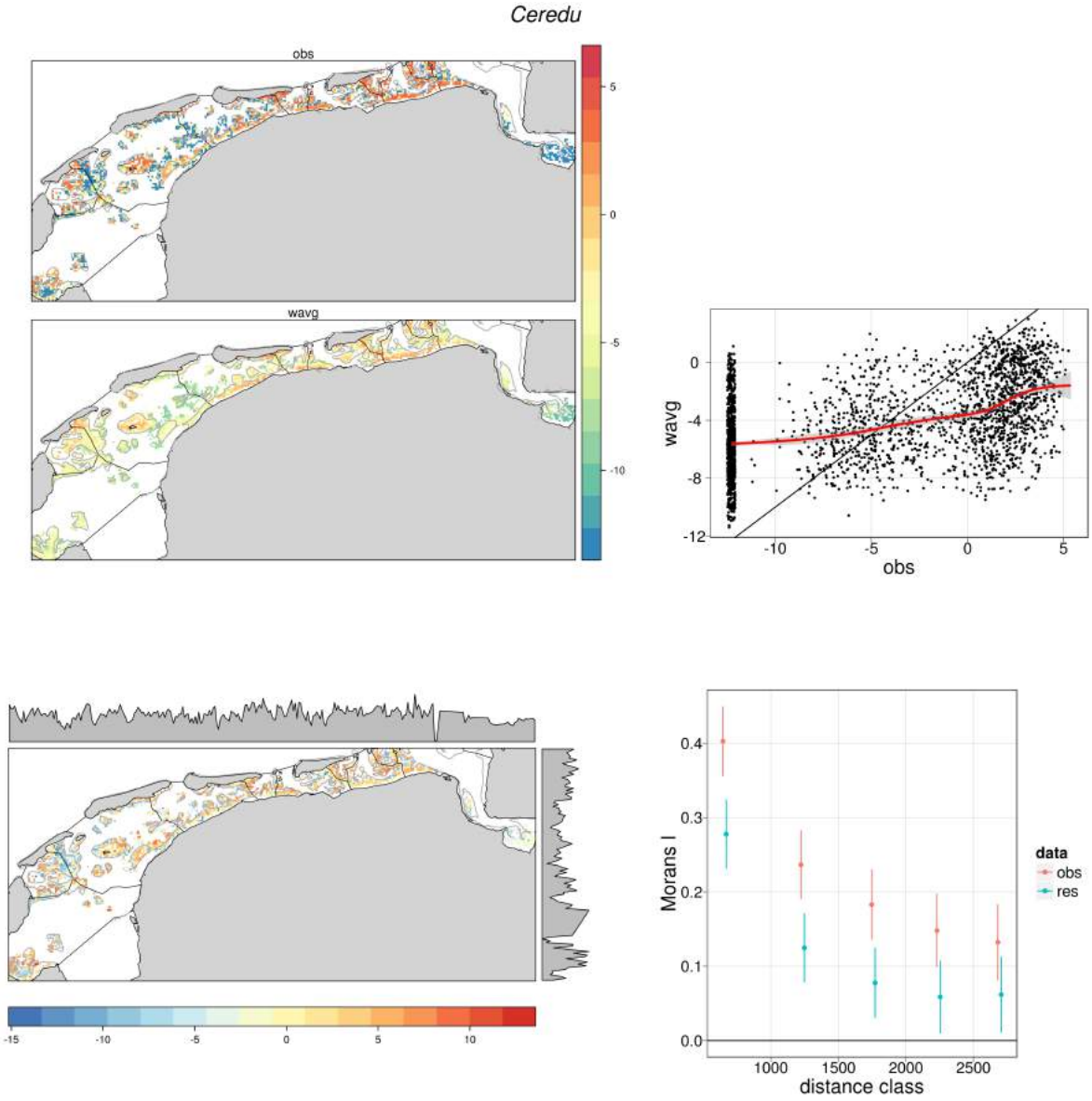

Figure 11: SDM results for cockle biomass distributions. obs: observed response variable (i.e. log-transformed mean biomass over the period 2009-2013); wavg: consensus prediction (weighted average of the predictions of the various machine learning algorithms). The bottom-left panel maps the residuals. The margins of the bottom-left panel represent the mean values of the residual and indicate the spatial trend. The top-right panel shows observed biomass vs the weighted average of the predictions. The red line represents the smooth conditional means; the black line represents the situation where wavg=obs. The right bottom scatterplot shows Moran's I statistic of the observed variable and the residuals.

spec	All	Fold01	Fold02	Fold03	Fold04	Fold05	Fold06
Scoarm	0.59	0.63	0.71	0.45	0.13	0.28	0.72
Corosp	0.46	0.55	0.47	0.19	0.10	0.08	0.82
Uropos	0.36	0.51	0.29	0.31	0.19	0.27	0.41
Heddiv	0.34	0.20	0.46	0.38	0.34	0.22	0.08
Perulv	0.33	0.06	0.37	0.39	0.31	0.23	0.13
Aphmar	0.31	0.12	0.24	0.02	0.31	0.35	0.47
Capcap	0.29	0.21	0.24	0.27	0.02	0.03	0.27
Oligoc	0.28	0.27	0.38	0.24	0.32	0.29	-0.30
Hetfil	0.27	0.32	0.32	0.07	0.16	0.02	0.30
Marvir	0.26	0.10	0.21	0.20	-0.31	-0.04	-0.18
Nephom	0.24	0.16	0.24	0.31	0.15	0.23	0.30
Scrpla	0.23	0.14	0.13	0.29	0.15	0.20	-0.24
Ceredu	0.22	-0.02	0.14	0.27	0.08	0.08	0.46
Aremar	0.21	0.14	0.17	0.05	0.02	0.06	0.49
Myaare	0.19	0.09	0.24	0.21	0.02	0.16	0.17
Batsar	0.16	0.07	0.24	0.16	0.10	0.17	0.11
Phymuc	0.15	0.07	0.18	0.11	-0.08	-0.08	0.42
Polcor	0.13	-0.04	0.01	0.14	0.21	0.13	0.21
Pygele	0.11	0.08	0.16	0.06	-0.06	0.04	-1.01
Ensdir	0.10	0.07	0.01	0.14	0.04	-0.02	0.10
Lancon	0.10	0.04	0.04	0.07	0.02	0.04	0.25
Macbal	0.04	-0.24	0.04	0.03	-0.09	-0.37	-0.19
Abrten	0.04	0.14	0.03	-0.05	-0.10	0.12	-7.18
Carmae	0.03	-0.02	0.04	0.02	0.03	-0.05	-0.12
Spimar	0.03	0.02	0.03	-0.02	0.02	0.00	-0.01
Alivir	0.01	0.00	0.01	-0.01	-0.01	0.03	-0.34
Etelon	-0.01	-0.26	0.06	0.04	-0.08	0.01	-0.85

Table 4: R-squared of the consensus model constructed on the basis of non-random cross validation for the six spatial subsets within the Dutch Wadden Sea. The species are ordered by decreasing R-squared.

3.4.1 Partial dependence plots

Figures 12-15 present the predicted relationships between biomass per species and the predictor variables by means of partial dependence plots. The points in the figures represent the raw data which help to interpret the predicted relationships and develop expectations when the environmental conditions change. We consider a number of distinct bivalves, polychaetes and crustaceans to highlight some striking relationships and to illustrate the interpretation of the partial dependence plots.

Bivalves ***Cerastoderma edule*** The top row of panels in Fig. 12 shows that mean exposure time (*expt*) is an important determinant of *Cerastoderma* density. Particularly, the biomass

tends to increase between exposure time 0 and 0.6 after which it levels off. The effect of waves is monotonically negative. The effect of the sediment properties is remarkable in that high biomass tends to occur at low and high values of *mgs* but that biomass is lower at intermediate values. In addition, the impact of *mud* is negative at very low values but becomes positive at levels greater that 10%.

Mya arenaria The biomass of *Mya* shows non-linear relationships with median grain size and mud fraction and a positive linear relationship with wave forcing. Also in these cases the models seem to be in line with each other, though GAM predicts notably lower biomasses at high mud fractions that the other modelling frameworks.

Abra tenuis The bottom row of panels in Fig. 12 shows that mainly the mean exposure time (*expt*) affects the biomass of *Abra*. The predictions of the different models correspond relatively well although the MARS model predicts lower abundances at high exposure times. *Abra* is only observed at locations where exposure time is greater than 0.50. The other variables have seemingly little impact on *Abra*. It should be noted, however, that the spatial range over which *Abra* occurs is limited which limits the ranges of the other predictor variables. If the exposure times at the intertidal flats with high exposure times would decrease, the density and biomass of *Abra* is expected to be reduced.

Polychaetes The polychaete species were split into two groups on the basis of the canonical correspondence analysis (Fig. 10). The partial dependence plots of the polychaetes which were associated with coarse sediments are presented in figure 13 and the polychaete species that were associated with sediments with high mud fraction are presented in figure 14.

Arenicola marina The biomass of the lugworms tends to increase between exposure time 0 and 0.4 after which it levels off and even decreases slightly. The impacts of shear stress, waves and brackish water are negative.

Nephthys hombergii The biomass of *Nephtys* tends to decrease with increasing exposure time. The biomass increases with wave impact and shear stress up to a level after which the impact of shear becomes negative. *Nephtys* does not occur at locations salinity where the mean salinity levels are below 20 psu.

Hediste diversicolor The biomass of *Hediste* tends to increase between exposure time 0 and 0.5 after which it levels off. The impacts of shear stress and wave forcing are negative, though not very strong.

Crustaceans The four main crustaceans and their relationships with the environmental variables are presented in figure 15. The relationships of all species with exposure time are similar in that biomass tends to increase with exposure time, though the density of *Urothoe poseidonis* shows a hump-shaped curve. The other relationships are more variable.

The partial dependence plots provide insight into the effects of the environmental variables on the benthos species. They can be used model spatial distributions under future conditions. It is important to note, however, that nearly all species occur over a wide range of environmental conditions. This implies that drastic shifts are not expected under slightly changing

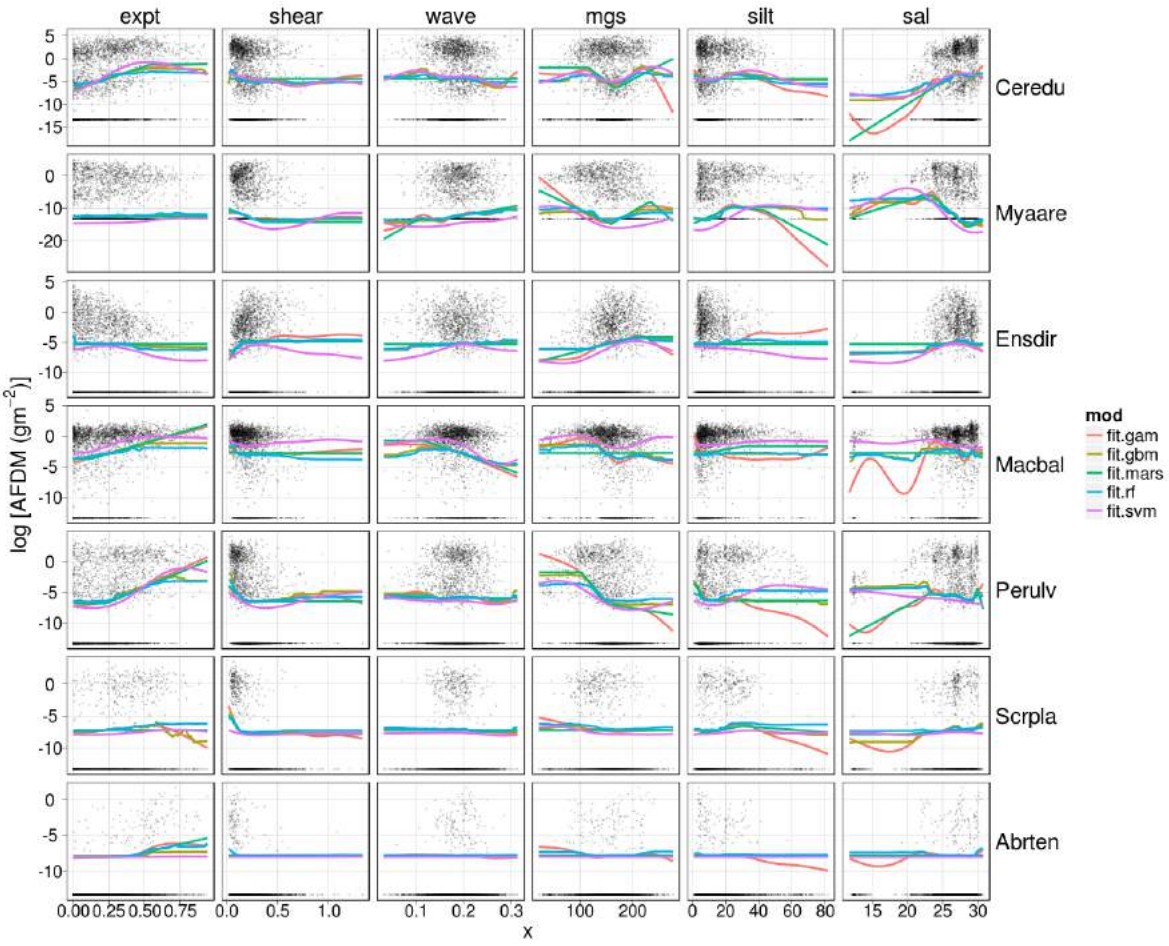

Figure 12: Partial dependence plots for the modelled relationships between (log-transformed) biomass of the bivalve species and predictor variables. The different curves within panels represent partial dependence plots for the different modelling algorithms.

abiotic conditions on the short term. On the long term, however, changes in morphology and hydrodynamics are expected to induce spatial redistributions of benthos.

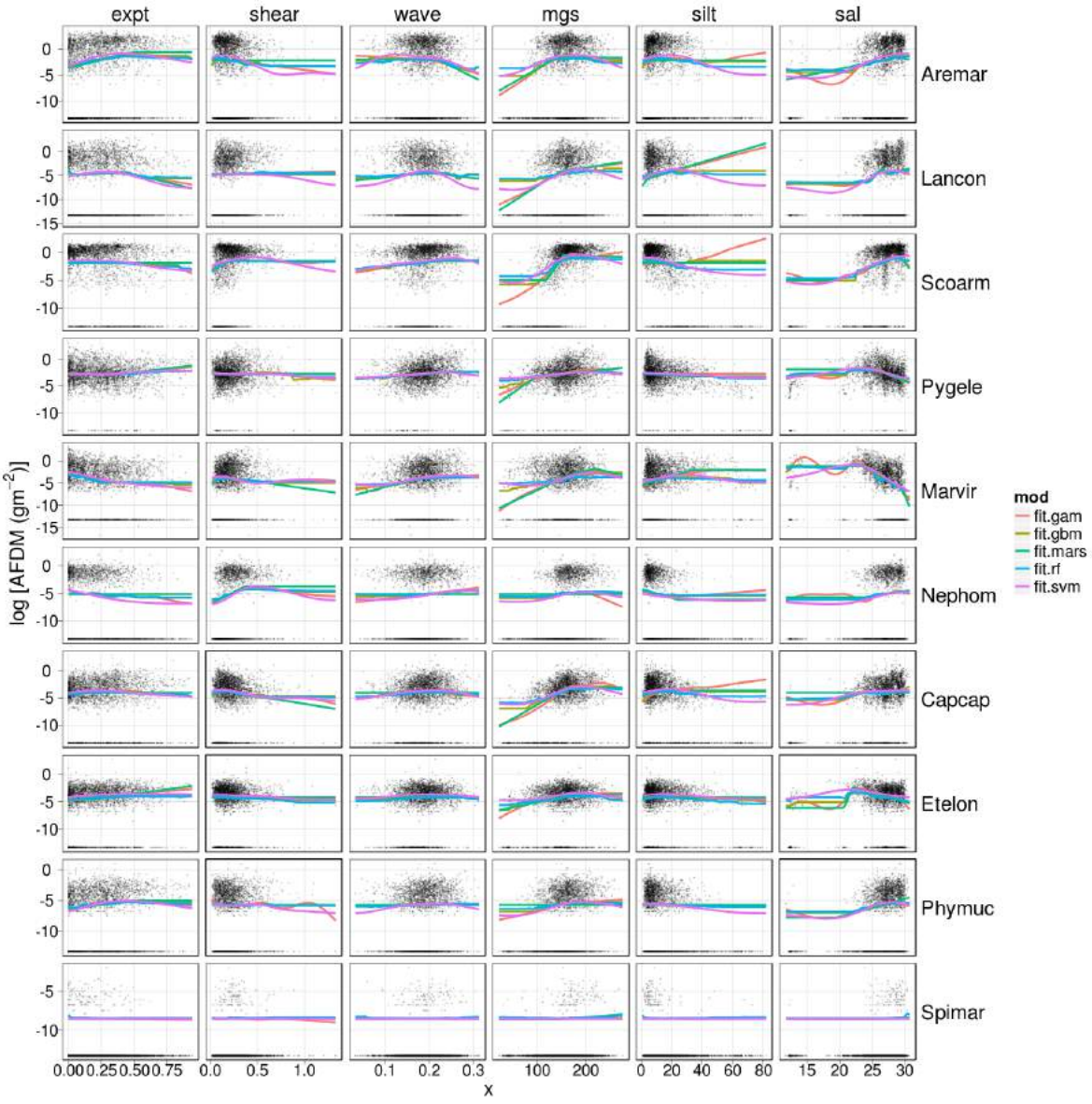

Figure 13: Partial dependence plots for the modelled relationships between (log-transformed) biomass and the predictor variables of the polychaete species that are associated with coarse sediment. The different curves within panels represent partial dependence plots for the different modelling algorithms.

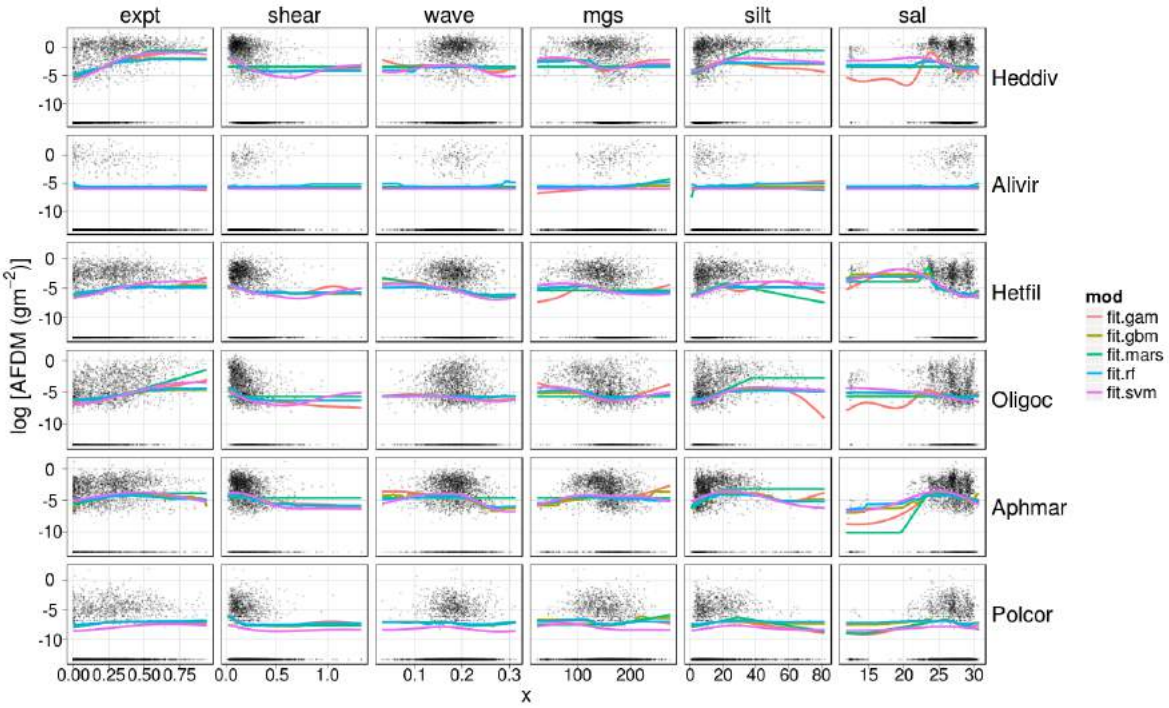

Figure 14: Partial dependence plots for the modelled relationships between (log-transformed) biomass of the polychaete species that are associated with fine sediment and the predictor variables. The different curves within panels represent partial dependence plots for the different modelling algorithms.

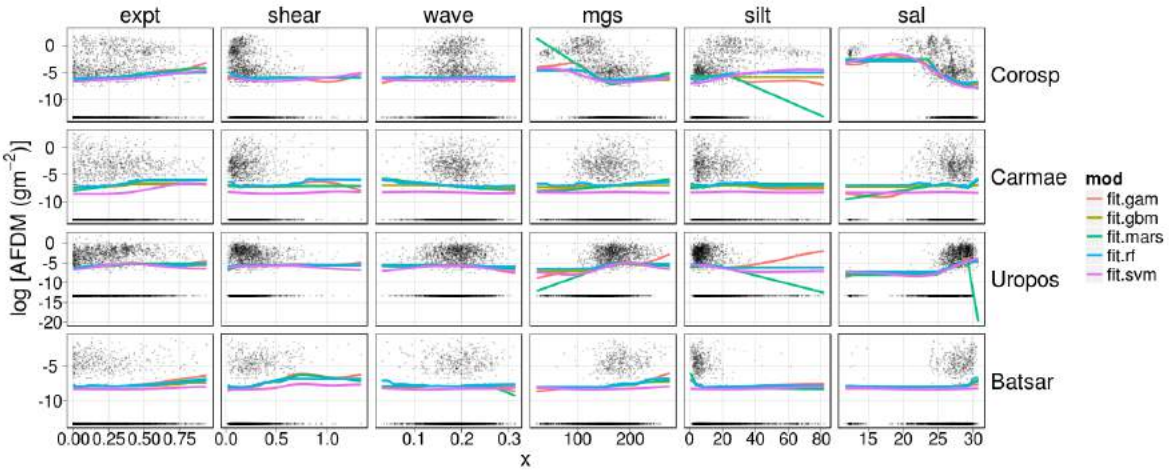

Figure 15: Partial dependence plots for the modelled relationships between (log-transformed) biomass of the crustacean species and predictor variables. The different curves within panels represent partial dependence plots for the different modelling algorithms.

3.5 Benthos biomass - productivity relationships

Figure 4b shows that the average chlorophyll-a concentrations and their trends differ significantly within the Dutch Wadden Sea. Particularly, chlorophyll-a concentrations are relatively high and constant in the tidal basins Borndiep, Zoutkamperlaag and Lauwers while they are decreasing in the western tidal basins and in the Eems-Dollard region. Figure 16 presents the average biomass per tidal basin for the years 2008-2013 for four bivalve species (*Cerastoderma edule, Mya arenaria, Limecola balthica, Peringia ulvae*) with relatively high average biomasses and relatively consistent distributions[1]. In the areas with high chlorophyll-a concentrations the average biomass of cockles, Baltic tellins and periwinkles also are relatively high, though variable between years (Fig. 16). It is possible that the tidal basins with relatively high chlorophyll-a concentrations are systematically different in terms of one or more physical predictors. Therefore, the analysis below considers the relationship between the residual biomass (i.e. obs - wavg) and chlorophyll-a concentration.

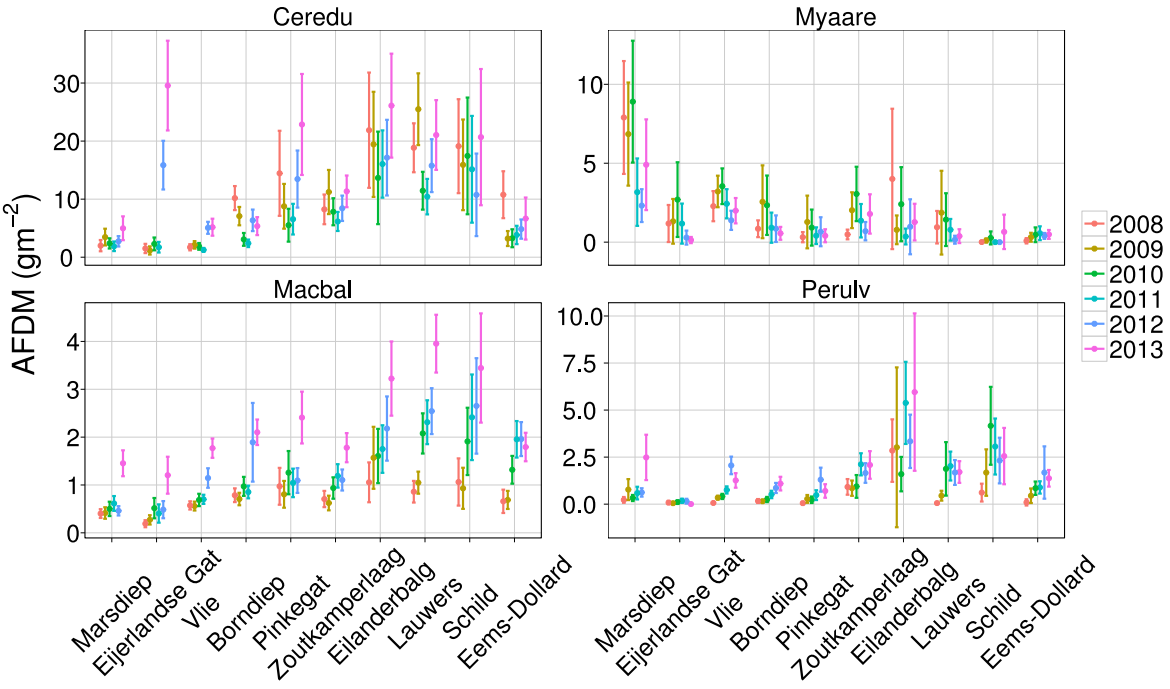

Figure 16: Average biomass and standard error of a number of selected benthos species for the years 2008-2013 in the tidal basins of the Dutch Wadden Sea.

Figure 17 and Table 5 show that there are positive associations between chlorophyll-a concentrations and the biomass residuals of cockles, Baltic tellins and periwinkles. The regression coefficient for the effect of chlorophyll-a on the residual biomass of *Mya arenaria* is negative. It is important to note that the analyses are incomplete in that spatial autocorrelation in

[1]Species with temporally variable distributions are unlikely to show systematic relationships with chlorophyll-a concentrations (because chlorophyll-a concentrations show less variable dynamics).

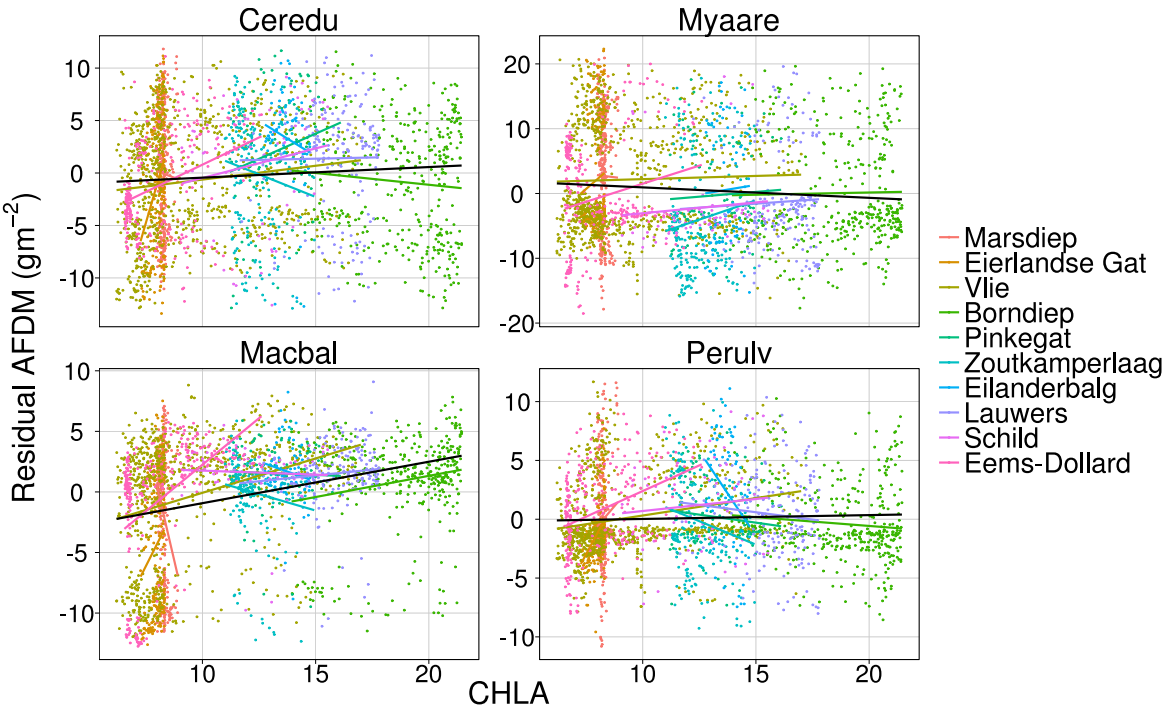

Figure 17: Relationships between chlorophyll-a concentrations and residual biomass of the four selected bivalve species. The coloured lines show the relationships within tidal basins and the black lines show the relationships across all data .

the regression errors is not accounted for which leads underestimation of the standard errors. Furthermore, it should be noted that the explanatory power of the effect of chlorophyll-a concentration is extremely low which is due to the high variability in the residual biomass.

Figure 17 also shows linear regression lines for within tidal basin relationships. Obviously, the ranges of chlorophyll-a concentrations are much lower that the range across the tidal basins. Systematic within tidal basin relationships do not show up.

3.6 Impacts of changing environmental conditions on shorebirds

In this section we consider the impact of changing environmental conditions on the abundance and distribution of a number of shorebirds. Particularly, based on the notion that the environmental conditions affect shorebird densities via the densities of benthos, we interpret the partial dependence plots in figures 12 - 15. We focus on the most prominent relationships of the most important prey species.

Red knot

- *Limecola balthica*: There is a positive relationship between the biomass of *Limecola* and exposure time. If relative sea level rise is positive, the exposure time is expected to

Table 5: Regression table for the models estimating the effects of chlorophyll-a concentration on the residuals of benthos biomass for a selection of bivalve species.

	Ceredu	Myaare	Macbal	Perulv
Constant	−1.452***	2.552***	−4.350***	−0.302
	(0.319)	(0.488)	(0.266)	(0.205)
CHLA	0.101***	−0.161***	0.342***	0.033*
	(0.026)	(0.040)	(0.022)	(0.017)
Observations	2,599	2,599	2,599	2,599
R^2	0.006	0.006	0.086	0.001
Adjusted R^2	0.005	0.006	0.086	0.001
Residual Std. Error (df = 2597)	5.587	8.564	4.658	3.587
F Statistic (df = 1; 2597)	14.842***	16.093***	245.202***	3.774*
Notes:	***Significant at the 1 percent level.			
	**Significant at the 5 percent level.			
	*Significant at the 10 percent level.			

decrease which would lead to decrease of *Limecola* and thus Red knots. On the other hand, if sedimentation rates are high enough to compensate or overcompensate then *Limecola* is expected to maintain its levels or even increase, *ceteris paribus*. There is a clear negative relationship between the biomass of *Limecola* and wave forcing which implies that if wave forcing increases the biomass of *Limecola* and the foraging conditions for red knots would deteriorate.

- *Cerastoderma edule:* As noted above, there is a positive relationship between mean exposure time (*expt*) and cockle biomass. If the the highly elevated and exposed intertidal flats would sink and become less exposed, this would lead to a reduction in the biomass of cockles. On the other hand, if the area of highly elevated intertidal flats would increase, an increase in cockle abundance may be expected which would improve the foraging conditions for red knots. If the median grain size distribution would become more uniform (i.e. the extremes would be reduced) the biomass is expected to decrease.

- *Peringia ulvae:* There is a positive relationship between the biomass of *Peringia* and exposure time which implies that if the area of highly elevated intertidal flats would be reduced the density of *Peringia* and the foraging conditions for red knots would be reduced. If the mud fraction of the highly elevated intertidal were to be reduced *Peringia* would likely decrease in biomass. Note that this finding corresponds with the knowledge that Peringia forages on diatoms which tend to occur in high densities on mudy sediments.

The three main prey species of red knot show similar strong responses to changing exposure time. Therefore, if the total area of high and exposed flats were to be reduced all the important prey species of red knot are expected to decline.

Oystercatcher

- *Cerastoderma edule* and *Limecola balthica* are important prey species; they are discussed above.

- *Ensis leei:* The relationship with shear stress is initially positive but levels off at values greater than 0.5 Nm^{-2}. There is also a positive impact of *mgs* on the biomass of *Ensis*. Thus, *Ensis* is expected to benefit from a more dynamic system with course sediment.
- *Hediste diversicolor:* As noted above, the biomass of *Hediste* increases between exposure time 0 and 0.5 after which it levels off. The impacts of shear stress and wave forcing are negative, though not very strong.

The oystercatcher's main prey items (*Cerastoderma, Limecola* and *Hediste*) will decrease if the exposure time decreases. If the areas with relatively high shear stress expand, the biomass of *Hediste diversicolor* will be reduced while *Ensis leei* might increase. The impact of these environmental changes may lead to a different diet composition of oystercatchers.

Bar-tailed godwit

- *Arenicola marina:* The relationship with exposure time (*expt*) is hump-shaped. The impacts of shear stress and and wave forcing are mainly negative.
- *Hediste diversicolor:* As noted above, the biomass of *Hediste* increases between exposure time 0 and 0.5 after which it levels off. The impacts of shear stress and wave forcing are negative, though not very strong.
- *Scoloplos armiger* and *Nephtys hombergii:* The responses of *Scoloplos* and *Nephtys* are similar and therefore considered simultaneously. The impact of exposure time is slightly negative. The effect of shear is initially positive after which it levels off. The effect of increasing waves and median grain size are positive. The density and biomass of *Nephthys* is expected to increase if disturbance by currents and waves increase.
- *Lanice conchilega: Lanice* occurs over a wide range of exposure time conditions though there is a slight negative effect when exposure time the levels exceed 0.5. There is a clear positive relationship with *mgs*.
- *Limecola balthica:* As noted above there is a positive relationship between the biomass of *Limecola* and exposure time. There is a clear negative relationship between the biomass of *Limecola* and wave forcing which implies that if wave forcing increases the biomass of *Limecola* would decrease.
- *Carcinus maenas:* The relationship with exposure time is positive while the relationship with wave impact is negative. The abundance and biomass of *Carcinus* is expected to decrease if the available mudflats with high exposure times are reduced and if wave forcing increases.

The main prey items of bar-tailed godwits (*Arenicola, Hediste)* are expected to decrease when exposure time decreases and when shear and wave forcing increase. However, alternative prey species such as *Scoloplos* and *Nephtys* are expected to increase if the area of intertidal flats

with low exposure times, high wave forcing and coarse sediments increase. Overall, the broad diet and the diverging responses of the benthos prey to changing conditions suggests that the bar-tailed godwit will continue to have ample foraging possibilities under changing physical conditions.

4 Discussion

Models capturing the dependencies between the density and distribution of organisms and the abiotic environment are a prerequisite to assess ecological impacts of changes in the abiotic environment. In this report we developed species distribution models to be able to forecast possible shifts in the abundance and distribution of intertidal benthos in response to future RSLR and sediment nourishments. To guard against overfitting, the models were tuned on the basis of transferability performance. We developed habitat suitability maps by combining the predictions from five SDMs and we constructed partial dependence plots to assess the response of benthos to changing physical variables univariately. On the basis of the possible shifts in abiotic conditions and benthos distributions we considered the possible consequences for shorebirds foraging on benthos.

The abundance of benthos in terms of biomass, number of specimens and occupancy varies widely between years and over a broad range of environmental conditions. However, as far as was analysed, the relationships between occupancy and the environmental variables were relatively constant between years for most species. This finding justified the use of the average biomass per sampling site to analyse the relationships with the environmental variables. Though averaging across years smoothed the data to a certain extent, they remained zero-inflated. This was one of the motivations for using machine learning algorithms to develop SDMs.

Overall, the SDMs captured the main distribution patterns of the benthos species although they tended to overfit low biomass observations and underfit high biomass observations. Zero-inflation is a common phenomenon, especially across long environmental gradients. The reason is that under unfavourable conditions a species may be absent while favourable conditions promote growth and the development of high densities of organisms. Despite this shortcoming the SDMs were used to assess the response of benthos biomass to possible changes in physical variables by means of partial dependence plots.

The partial dependence plots show that exposure time (*expt*) is crucial to many molluscs (mainly *Cerastoderma edule, Limecola balthica, Peringia ulvae, Abra tenuis*), polychaetes (mainly *Arenicola marina, Lanice conchilega, Marenzelleria viridis*, *Hediste diversicolor, Heteromastus filiformis*) and crustaceans (mainly *Corophium sp.*). Furthermore, changes in shear stress are expected to have strong influence on *Ensis leei, Scrobicularia plana, Arenicola marina, Scoloplos armiger, Nephthys hombergii* and *Hediste diversicolor*. Waves are expected to have strong influence on *Cerastoderma edule, Limecola balthica, Arenicola marina, Scoloplos armiger, Marenzelleria viridis, Heteromastus filiformis* and *Aphelochaeta marioni*. Finally, the variables *mgs* and *mud* are expected to affect the distribution and density of amongst others *Cerastoderma edule, Ensis leei, Peringia ulvae, Arenicola marina, Scoloplos armiger, Marenzelleria viridis, Capitella capitata* and *Phyllodoce mucosa*.

We also considered the impact of changing abiotic conditions on the benthic prey of red knot (*Calidris canutus*), oystercatcher (*Haematopus ostralegus*) and bar-tailed godwit (*Limosa lapponica*). The three main prey species of red knot (i.e. *Limecola balthica, Cerastoderma edule* and *Peringia ulvae*) show similar responses to changing exposure time. Hence, if the total

area of elevated and exposed flats were to be reduced, the important prey species of red knot are expected to decline. The oystercatcher's main prey items (*Cerastoderma, Limecola* and *Hediste*) will decrease if exposure time decreases. If the areas with relatively high shear stress expand, the biomass of *Hediste* will be reduced while *Ensis* might increase. If environmental change would cause benthos distributions to shift, oystercatchers might be able to anticipate by changing the composition of their diet. It should be noted that the blue mussel (*Mytilus edulis*) is an important prey species for oystercatchers but is not considered in this report because mussels are not adequately captured in the SIBES monitoring program. The main prey items of bar-tailed godwits (*Arenicola, Hediste*) are expected to decrease when exposure time decreases and when shear stress and wave forcing increase. However, alternative prey species such as *Scoloplos* and *Nephtys* are expected to increase if there is an increase in the area of intertidal flats with low exposure times, high wave forcing and coarse sediments. Overall, the broad diet and the diverging responses of the benthos prey suggests that bar-tailed godwits will maintain foraging possibilities under changing physical conditions. It is important to note, however, that if changes in the physical drivers are substantial and the benthos community shifts accordingly, shorebirds will require time to respond to changing species compositions and distributions. The systematic changes in benthos should be considered in the perspective of a benthos community that is already highly dynamic, also without systematic changes in the morphodynamic drivers.

4.1 Suggestions for further research

This section describes research that can help to provide more accurate insight into future development of benthos and shorebird communities in response to changing environmental conditions. Suggestions 1-3 require substantial research projects including morphodynamic modelling, ecosystem models and shorebird data and foraging models; suggestions 4-6 are relatively easy to carry out.

1. The finding that most benthos species occur over broad ranges of environmental conditions and that the temporal variabilities are relatively large suggests that the benthos communities are relatively irrepressible to moderate changes in the environmental variables on short timescales. However, the dependence relationships suggest that if there are significant and permanent changes in the abiotic variables, changes in the benthos community are to be expected in the long run. The variability of the benthos densities under relatively constant abiotic conditions (i.e. the conditions considered in this report) suggests that it will take long time and many observations to detect systematic shifts in benthos distributions related to changes in the physical variables. Models simulating the physical environment may provide more detailed insight into possible future scenario's. On the basis of such scenario's more detailed prognoses about the benthos and shorebird communities can be developed which can be used to support decision making with regards to sediment nourishments in a more tangible manner. An advantage of using a realistic scenario approach is that the impact of changing abiotic variables can be modelled simultaneously instead of considering univariate relationships in isolation. Specific

scenario's can also be helpful to assess regional differences in the change of foraging conditions and bird distributions. The constrained correspondence analysis in Section 3.3 suggests that to model shifts in the entire benthos community all physical predictor variables would need to be modelled.

2. Our SDMs performed reasonably well for a large number of species in that they captured the main benthos distribution patterns. However, the SDMs incorporate uncertainties and they are static and incomplete. For instance, possible data errors in the bathymetry will cause errors in the modelled hydrodynamics which affects the SDMs. More importantly our SDMs do not incorporate ecological interactions such as consumption, predation, diseases and facilitation. We have tried to investigate the role of primary production on benthos density by correlating pelagic chlorophyll-a concentrations to the residual biomass of four important benthos species. Even though we found plausible correlations between the residuals of the biomass of *Cerastoderma* and *Limecola* and chlorophyll-a concentrations, the correlations did not account for much of the unexplained variation. One important reason is that chlorophyll-a concentrations are only measured at a small number of stations located in subtidal areas. We linked the residual biomasses to chlorophyll-a concentrations using a weighted (by inverse distance squared) average of measurements at the stations. This crude approach ignores microphytobenthos as food resources for benthos (except for possible resuspension of microphytobenthos) and local processes related to the production and consumption of phytoplankton. Future analyses may benefit from data obtained by means of remote sensing or from ecosystem models where phytoplankton and microphytobenthos production and consumption are modelled in a realistic manner. This would also open possibilities to model growth of benthos dynamically.

3. We assessed the effect of changing abiotic conditions on shorebirds via benthos in a crude qualitative manner; i.e. we merely considered the changes in (known) benthic prey qualitatively. A more adequate and quantitative way would involve statistical testing of the relationships between the spatial distributions of shorebirds and benthos. For instance, there are data available resulting from high tide roost counts that can be used for such analyses (e.g. Blew & Südbeck, 2005; van der Hut *et al.*, 2014). This method requires that the number of birds at high tide roost reflect the local foraging opportunities. More elaborate ways would involve simulation and measurement of foraging behaviour (by means of tagging and following individual birds) in response to "resource landscapes" and possibly "intake rate landscapes" and the depletion of resources. Furthermore, animals are known to be able to shift their diet when there is a shift in the abundance of potential prey. Which shifts are likely to occur under future conditions is an important research question.

4. One practical modelling difficulty concerns zero-inflation. Particularly, histograms of biomass (or number of individuals) of individual species showed asymmetric distributions. This is a common phenomenon because data sampled along a long environmental gradient contain many zero values because species generally have unimodal distributions along environmental gradients and are absent from sites that are far from their optimal

living conditions. This difficulty might be overcome to some extent by aggregating the data on a coarser spatial scale. Another benefit of aggregating observations is that the data set is reduced which speeds up model tuning.

5. A complete assessment of the impact of changing environmental conditions on benthos and bird communities in the Wadden Sea should ideally include blue mussels *(Mytilus edulis)* and Pacific oysters (*Crasostrea gigas*). These species are important in terms of biomass and - especially blue mussels - is an important prey species for oystercatchers. These reef-forming species are not adequately assessed in the SIBES monitoring program. But, yearly monitoring of mussel beds is carried out by Wageningen Marine Research (WMR); we recommend to extend the current research by including SDMs for these species.

6. We found that the average median grain size increased by 0.89 μm per year and that the average mud fraction of the tidal flats had reduced with an average of 0.24% per year over the period 2009-2015. The trends are largely due to changes in 2014 and 2015. From a RSLR and sediment nourishments management point of view it would be interesting to have more detailed insight into the causes underlying the changes.

Acknowledgements

We thank the crew of the RV Navicula, volunteers and collegues for supporting the SIBES program. We thank Jasper Donker for providing the wave data and Tanya Compton, Peter Herman, Theo Prins and Petra Damsma for discussion and useful suggestions.

References

Barry, S. & Elith, J. (2006) Error and uncertainty in habitat models. *Journal of Applied Ecology* **43**, 413–423.

Bates, D., Maechler, M. & Bolker, B. (2012) lme4: Linear mixed-effects models using S4 classes.

Bijleveld, A.I., van Gils, J.A., van der Meer, J., Dekinga, A., Kraan, C., van der Veer, H.W. & Piersma, T. (2012) Designing a benthic monitoring programme with multiple conflicting objectives. *Methods in Ecology and Evolution* **3**, 526–536.

Blew, J. & Südbeck, P. (2005) *Migratory Waterbirds in the Wadden Sea 1980-2000*. Common Wadden Sea Secretariat, Trilateral Monitoring ans Assessment Group, Joint Monitoring Group of Migratory Birds in the Wadden Sea, Wilhelmshaven, Germany.

Breiman, L. (2001) Random Forests. *Machine Learning* **45**, 5–32.

Burchard, H. & Bolding, K. (2002) GETM - a General Estuarine Transport Model. Scientific documentation. Technical Report EUR 20253 EN.

Buuren, S.v. & Groothuis-Oudshoorn, K. (2011) mice: Multivariate Imputation by Chained Equations in R. *Journal of Statistical Software* **45**, 1–67.

Compton, T.J., Holthuijsen, S., Koolhaas, A., Dekinga, A., ten Horn, J., Smith, J., Galama, Y., Brugge, M., van der Wal, D., van der Meer, J., van der Veer, H.W. & Piersma, T. (2013a) Distinctly variable mudscapes: Distribution gradients of intertidal macrofauna across the Dutch Wadden Sea. *Journal of Sea Research* **82**, 103–116.

Compton, T.J., van der Meer, J., Holthuijsen, S., Koolhaas, A., Dekinga, A., ten Horn, J., Klunder, L., McSweeney, N., Brugge, M. & van der Veer, H.W. (2013b) Synoptic Intertidal Benthic Surveys Across the Dutch Wadden Sea 2008 to 2011. Tech. Rep. NIOZ 2013-1, NIOZ, Texel.

Cutler, D.R., Edwards, T.C., Beard, K.H., Cutler, A., Hess, K.T., Gibson, J. & Lawler, J.J. (2007) Random Forests for Classification in Ecology. *Ecology* **88**, 2783–2792.

Donker, J.J.A. (2015) *Hydrodynamic processes and the stability of intertidal mussel beds in the Dutch Wadden Sea*.

Drake, J.M., Randin, C. & Guisan, A. (2006) Modelling ecological niches with support vector machines. *Journal of Applied Ecology* **43**, 424–432.

Elith, J. & Leathwick, J.R. (2009) Species Distribution Models: Ecological Explanation and Prediction Across Space and Time. *Annual Review of Ecology, Evolution, and Systematics* **40**, 677–697.

Elith, J., Leathwick, J.R. & Hastie, T. (2008) A working guide to boosted regression trees. *Journal of Animal Ecology* **77**, 802–813.

Folmer, E.O., Olff, H. & Piersma, T. (2010) How well do food distributions predict spatial distributions of shorebirds with different degrees of self-organization? *Journal of Animal Ecology* **79**, 747–756.

Folmer, E.O., Van Beusekom, J.E.E., Dolch, T., Gräwe, U., Katwijk, M.M., Kolbe, K. & Philippart, C.J.M. (2016) Consensus forecasting of intertidal seagrass habitat in the Wadden Sea. *Journal of Applied Ecology* **53**, 1800–1813.

Friedman, J.H. (1991) Multivariate adaptive regression splines. *The annals of statistics* pp. 1–67.

Gräwe, U., Flöser, G., Gerkema, T., Duran-Matute, M., Badewien, T.H., Schulz, E. & Burchard, H. (2016) A numerical model for the entire Wadden Sea: Skill assessment and analysis of hydrodynamics. *J. Geophys. Res. Oceans* **121**, 5231–5251.

Gräwe, U., Holtermann, P., Klingbeil, K. & Burchard, H. (2015) Advantages of vertically adaptive coordinates in numerical models of stratified shelf seas. *Ocean Modelling* **92**, 56–68.

Guisan, A., Tingley, R., Baumgartner, J.B., Naujokaitis-Lewis, I., Sutcliffe, P.R., Tulloch, A.I., Regan, T.J., Brotons, L., McDonald-Madden, E., Mantyka-Pringle, C. & others (2013) Predicting species distributions for conservation decisions. *Ecology letters* **16**, 1424–1435.

Hastie, T., Tibshirani, R. & Friedman, J.H. (2009) *The elements of statistical learning. Data mining, inference, and prediction*. Springer, New York.

Heip, C.H.R., Goosen, N.K., Herman, P.M.J., Kromkamp, J., Middelburg, J.J. & Soetaert, K. (1995) Production and consumption of biological particles in temperate tidal estuaries. *Oceanography and Marine Biology - an Annual Review, Vol 33* (eds. A.D. Ansell, R.N. Gibson & M. Barnes), vol. 33, pp. 1–149, U C L Press Ltd, London, wOS:A1995BE76V00001.

Herman, P., Middelburg, J., van de Koppel, J. & Heip, C. (1999) Ecology of estuarine macrobenthos. *Advances in Ecological Research, Vol 29: Estuaries* (eds. D. Nedwell & D. Raffaelli), vol. 29, pp. 195–240, Elsevier Academic Press Inc, San Diego, wOS:000084726400005.

Kabat, P., Jacobs, C.M.J., Hutjes, R.W.A., Hazeleger, W. & Engelmoer, M. (2009) *Klimaatverandering en het Waddengebied*. 2009-06, De Waddenacademie KNAW.

Karatzoglou, A., Smola, A., Hornik, K. & Zeileis, A. (2004) kernlab – An S4 Package for Kernel Methods in R. *Journal of Statistical Software* **11**, 1–20.

Kraan, C., Aarts, G., van der Meer, J. & Piersma, T. (2010) The role of environmental variables in structuring landscape-scale species distributions in seafloor habitats. *Ecology* **91**, 1583–1590.

Kuhn, M. (2014) caret: Classification and Regression Training. R package version 6.0-37.

Kuhn, M. & Johnson, K. (2013) *Applied Predictive Modeling*. Springer, New York, NY.

Legendre, P. & Legendre, L. (1998) *Numerical ecology*. Elsevier.

Liaw, A. & Wiener, M. (2002) Classification and Regression by randomForest. *R News* **2**, 18–22.

Lyashevska, O., Brus, D.J. & van der Meer, J. (2016) Mapping species abundance by a spatial zero-inflated Poisson model: a case study in the Wadden Sea, the Netherlands. *Ecol Evol* **6**, 532–543.

Marra, G. & Wood, S.N. (2011) Practical variable selection for generalized additive models. *Computational Statistics & Data Analysis* **55**, 2372–2387.

McCue, A.J., McGrath, M.J. & Wiersma, Y.F. (2014) Benefits and drawbacks of two modelling approaches for a generalist carnivore: can models predict where Wile E. Coyote will turn up next? *International Journal of Geographical Information Science* **28**, 1590–1609.

Milborrow, S. (2015) earth: Multivariate Adaptive Regression Splines.

Oksanen, J., Kindt, R., Legendre, P., O'Hara, B., Simpson, G.L., Solymos, P., Stevens, M.H. & Wagner, H. (2007) Vegan: community ecology package. *R package version* **1**.

Prasad, A.M., Iverson, L.R. & Liaw, A. (2006) Newer Classification and Regression Tree Techniques: Bagging and Random Forests for Ecological Prediction. *Ecosystems* **9**, 181–199.

Ridgeway, G. (2013) gbm: Generalized Boosted Regression Models. R package version 2.1.

Smola, A.J. & Schölkopf, B. (2004) A tutorial on support vector regression. *Statistics and Computing* **14**, 199–222.

Stineman, R. (1980) A Consistently Well Behaved Method of Interpolation. *Creative Computing* **6**, 54–57.

van der Hut, R., Folmer, E., Koffijberg, K., Roomen, M., van der Zee, E., Stahl, J. & Boudewijn, T. (2014) Vogels langs de randen van het wad. Verkenning van knelpunten en kansen op broedlocaties en hoogwatervluchtplaatsen. A&W rapport 1982.

van der Meer, J., Beukema, J.J. & Dekker, R. (2001) Long-term variability in secondary production of an intertidal bivalve population is primarily a matter of recruitment variability. *Journal of Animal Ecology* **70**, 159–169.

Vapnik, V.N. (1998) *Statistical Learning Theory*. Wiley-Interscience, New York.

Venables, W.N. & Ripley, B.D. (2002) *Modern Applied Statistics with S*. Springer New York.

Wenger, S.J. & Olden, J.D. (2012) Assessing transferability of ecological models: an underappreciated aspect of statistical validation. *Methods in Ecology and Evolution* **3**, 260–267.

Wood, S. (2006) *Generalized Additive Models: An Introduction with R*. Chapman & Hall/CRC, 1 edn.

Wood, S. (2015) mgcv: Mixed GAM Computation Vehicle with GCV/AIC/REML Smoothness Estimation.

Zhao, Q. & Hastie, T. (2017) Causal interpretations of black-box models. *Journal of Business & Economic Statistics, to appear* .

A Depth and exposure time

Depth measurements are done part by part in the Dutch Wadden Sea and completion of a cycle takes 6 years. Because there are continuous morphological changes, the bathymetry data that are used for hydrodynamic modelling might not accurately represent the actual depths at the moment of benthos sampling. An potential improvement could be to make use of the measurements with a time stamp ("vaklodingen") instead of the bathymetry (which is a construction of measurements over a time span of 6 years) of the entire Wadden Sea. Since the distribution of benthos is affected by inundation time rather than actual depth it is important to know the relationship between depth and inundation time before depth can be used as a "substitute". The scatterplot in Fig. 18 shows the relationship between depth and inundation time. The correlation between the two variables is too low to justify the use of depth as a predictor variable instead of inundation time.

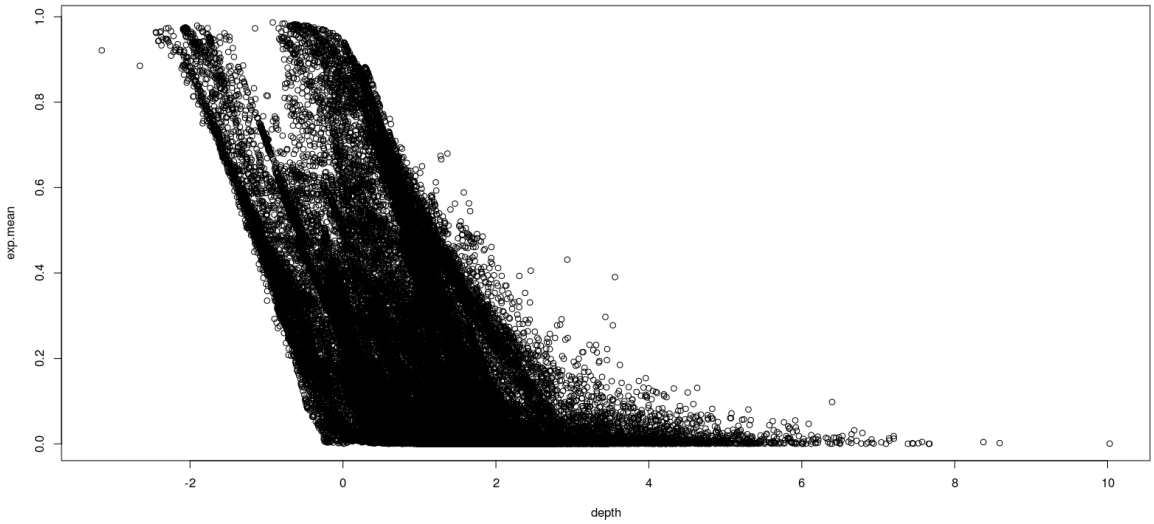

Figure 18: Scatterplot of depth (m) against exposure time (fraction).

B Wave dynamics

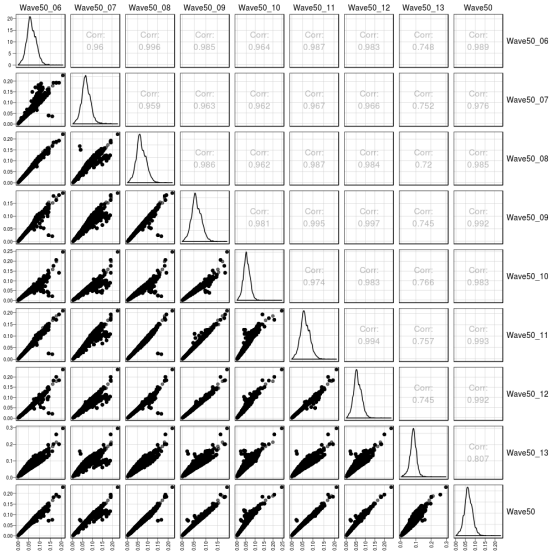

Figure 19: Correlation between the yearly medians of wave forcing on the SIBES benthos sampling locations for the period 2006-2013.

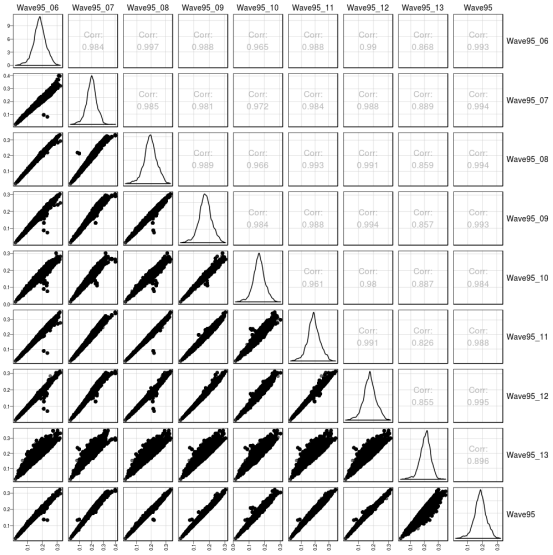

Figure 20: Correlation between the yearly 95th percentiles of wave forcing on the SIBES benthos sampling locations for the period 2006-2013.

C Sediment dynamics

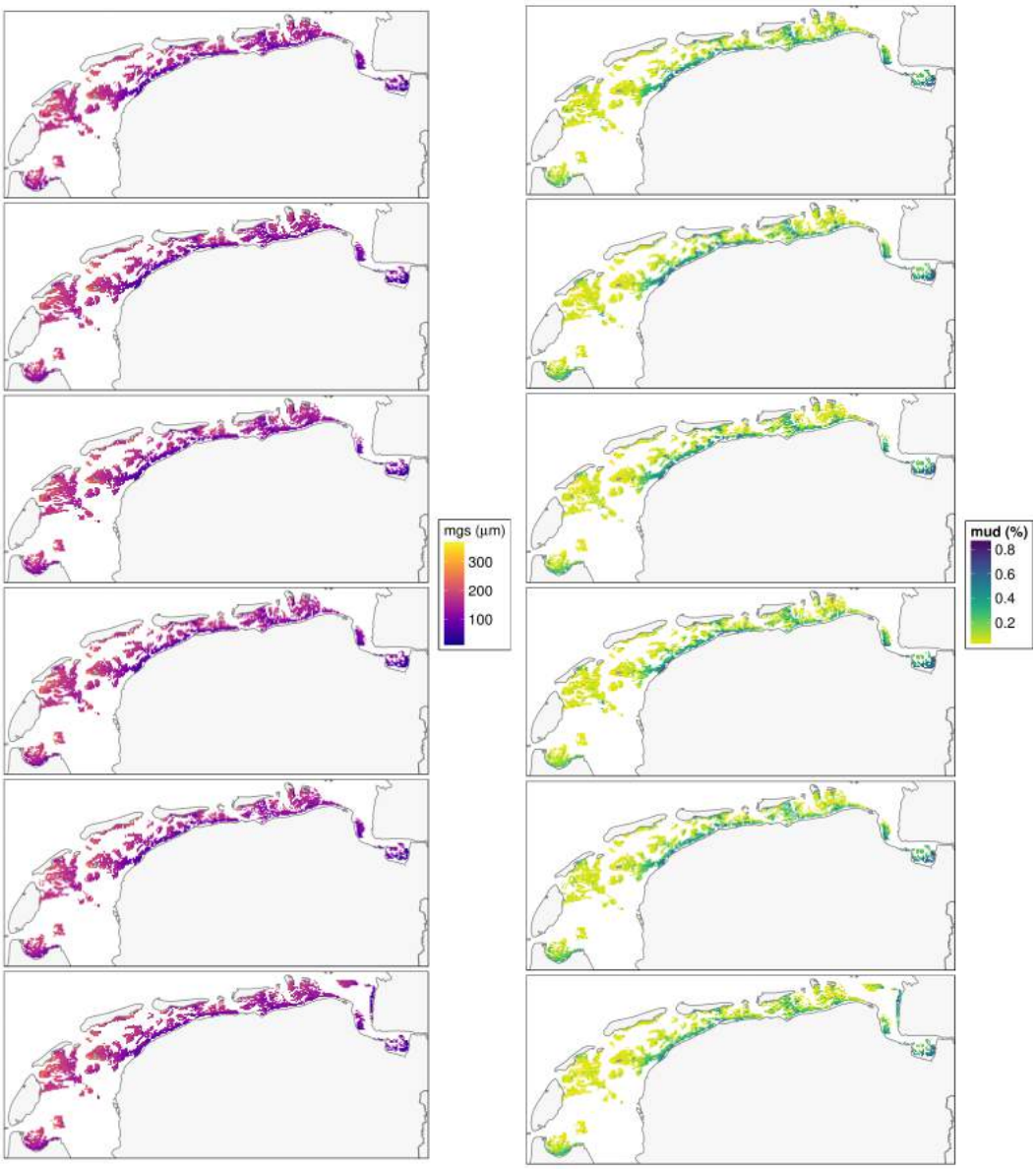

Figure 21: Yearly maps of the median grain size and mud fraction of the intertidal flats in the Wadden Sea for the period 2009 - 2014.

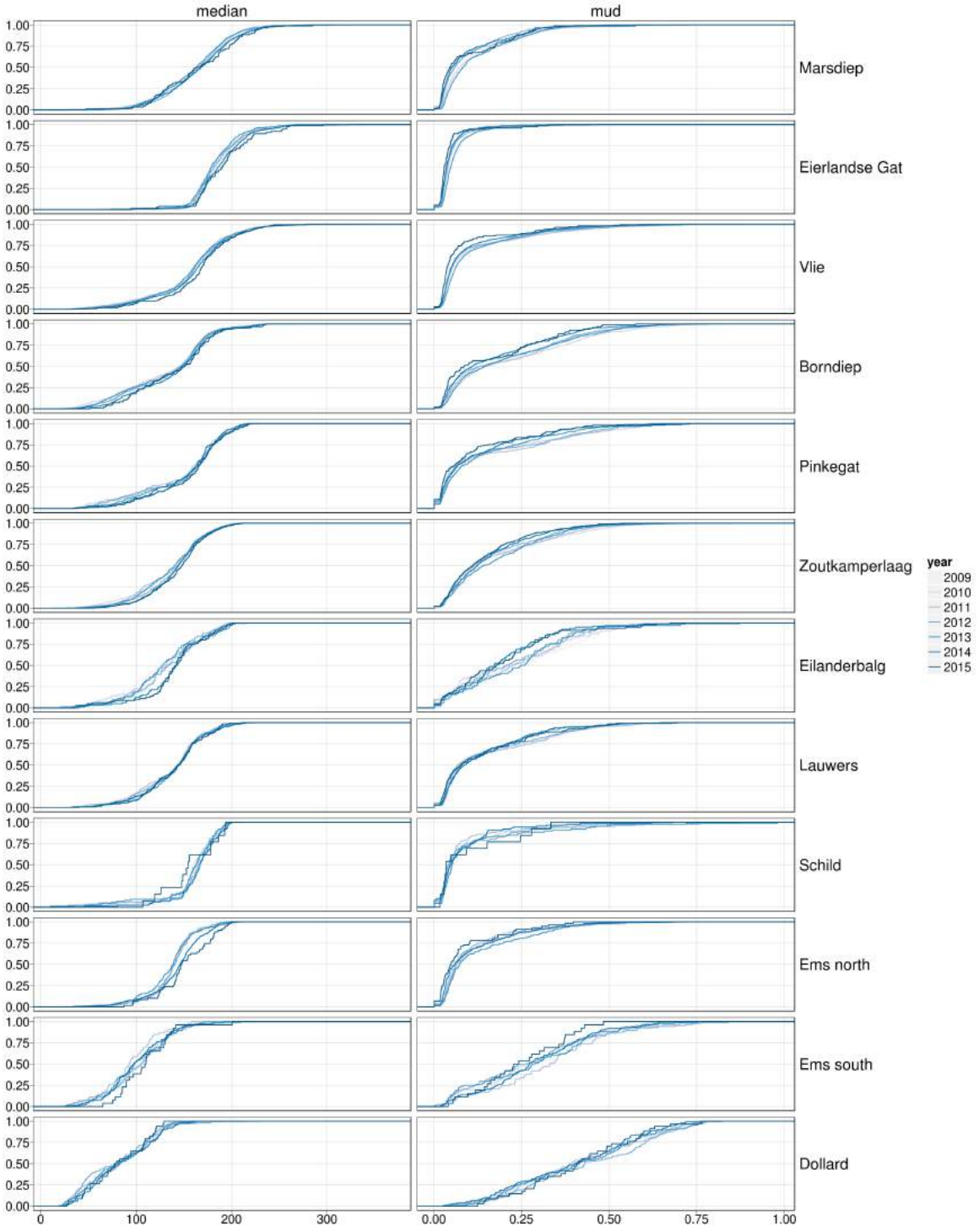

Figure 22: Empirical cumulative distributions of the yearly mud fraction and median grain size distributions per tidal basin for the period 2009 - 2015.

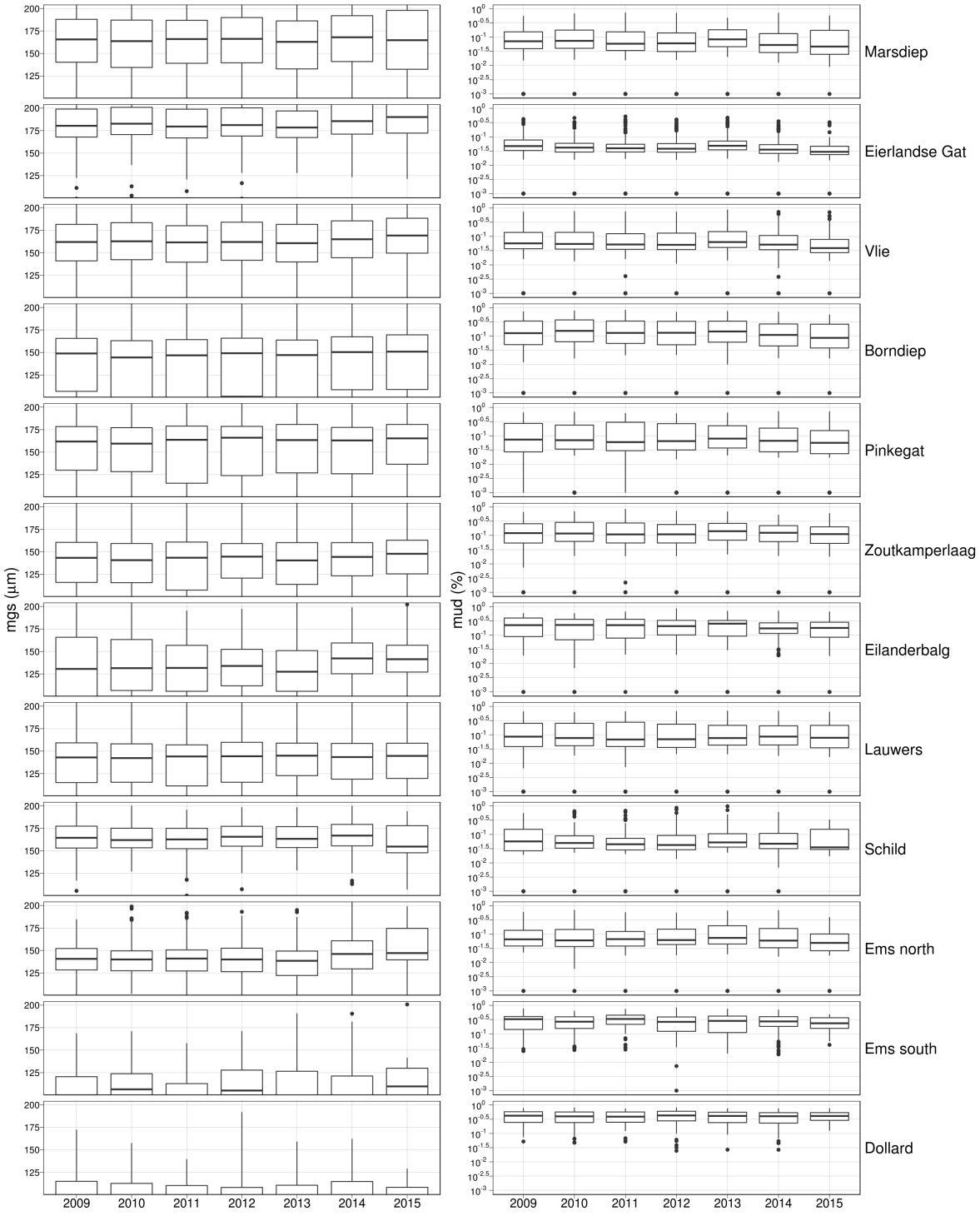

Figure 23: Boxplots of the mud fraction and median grain size distributions per tidal basin for the period 2009 - 2015.

D Benthos imputation

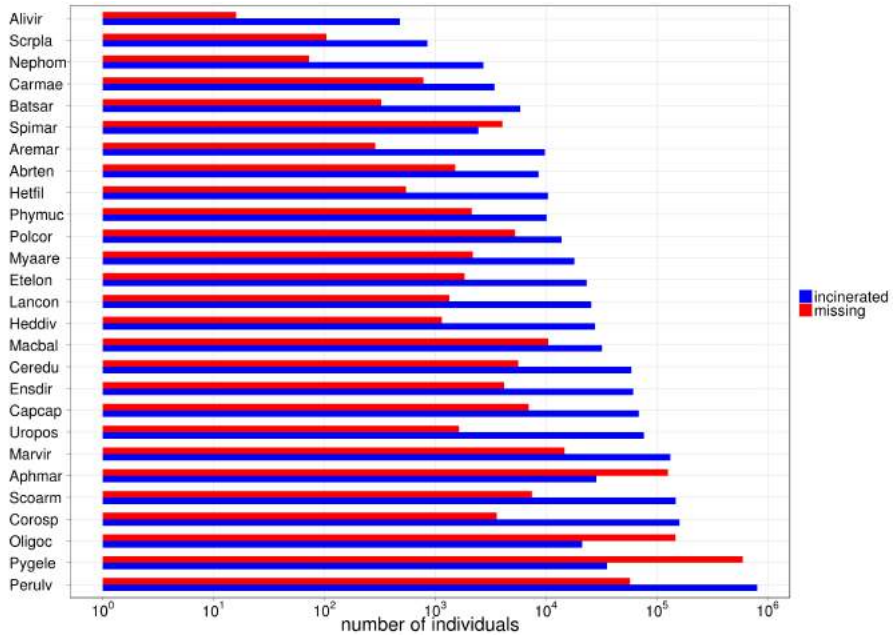

Figure 24: The number of individuals that were incinerated and the number of missing data per species. The reason for the large number of missing biomass data is that small polychaetes (which may be numerically abundant) are not longer incinerated since 2012/2013 because the biomass of the small polychaetes are relatively constant.

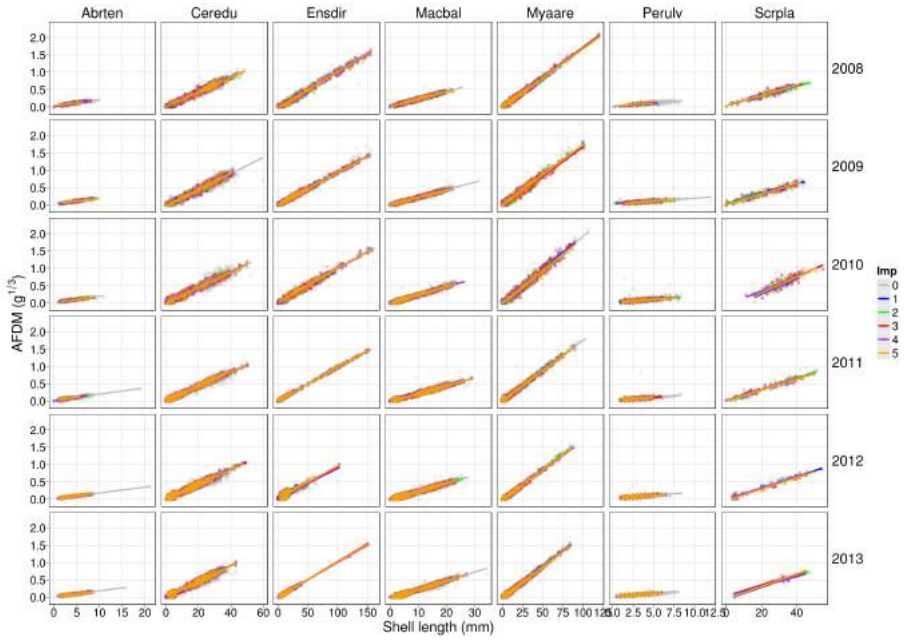

Figure 25: Imputation results for bivalves. Scatterplot of length against the cubic root of AFDM. The different colours denote the original data and the regression lines (Imp = 0) and the imputed values and regression lines on the basis of the imputed data (Imp 1-5).

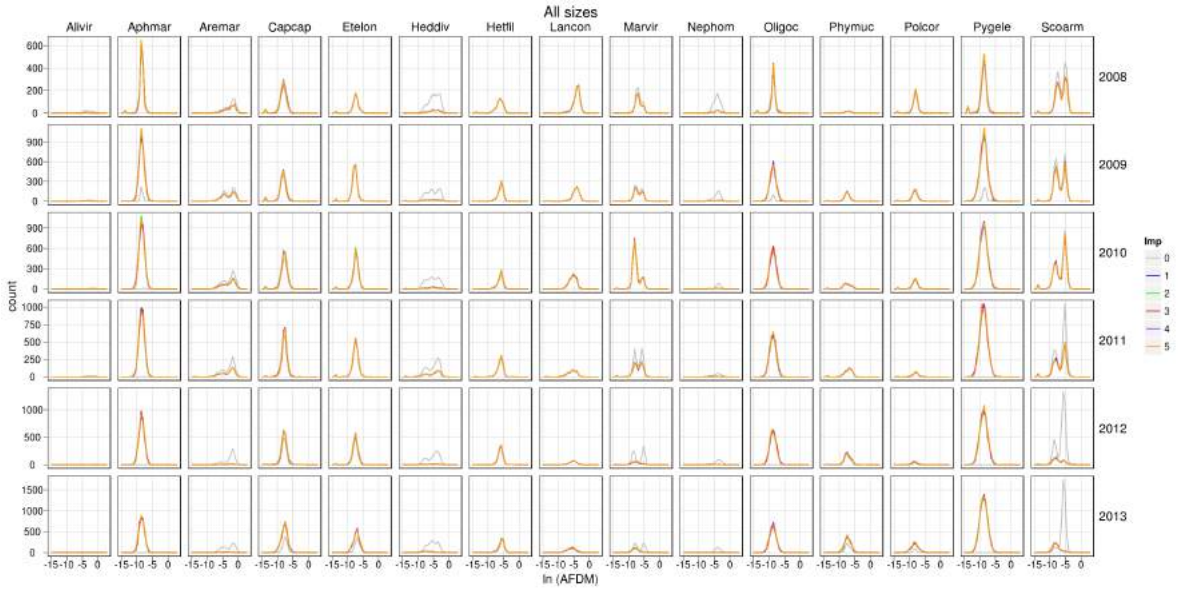

Figure 26: Imputation results for polychaetes. Density distributions of original (Imp=0) and imputed (Imp=1-5) data for the polychaetes.

E Benthos time series by tidal basin

Figures 27, 28, 29 show the average benthos densities per tidal basin for the entire Dutch Wadden Sea for the period 2008-2013.

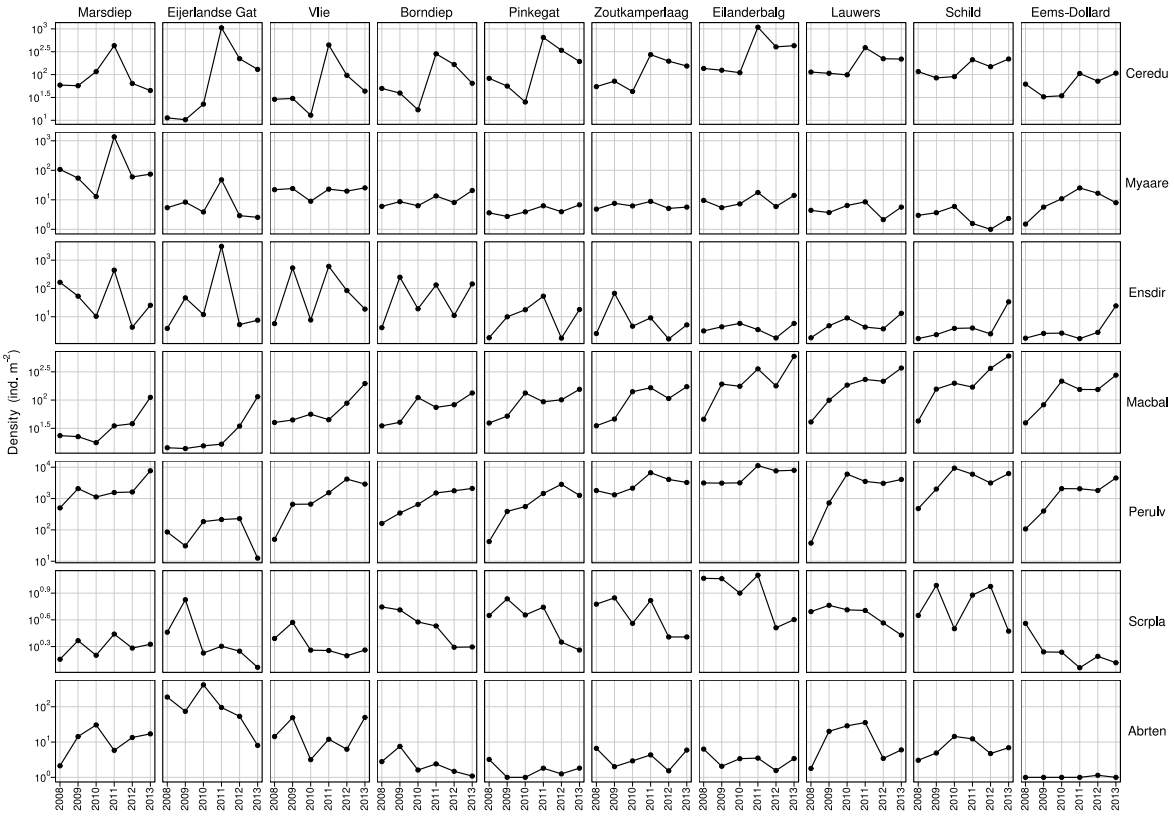

Figure 27: Average yearly mollusc densities for the period 2008-2013 per tidal basin.

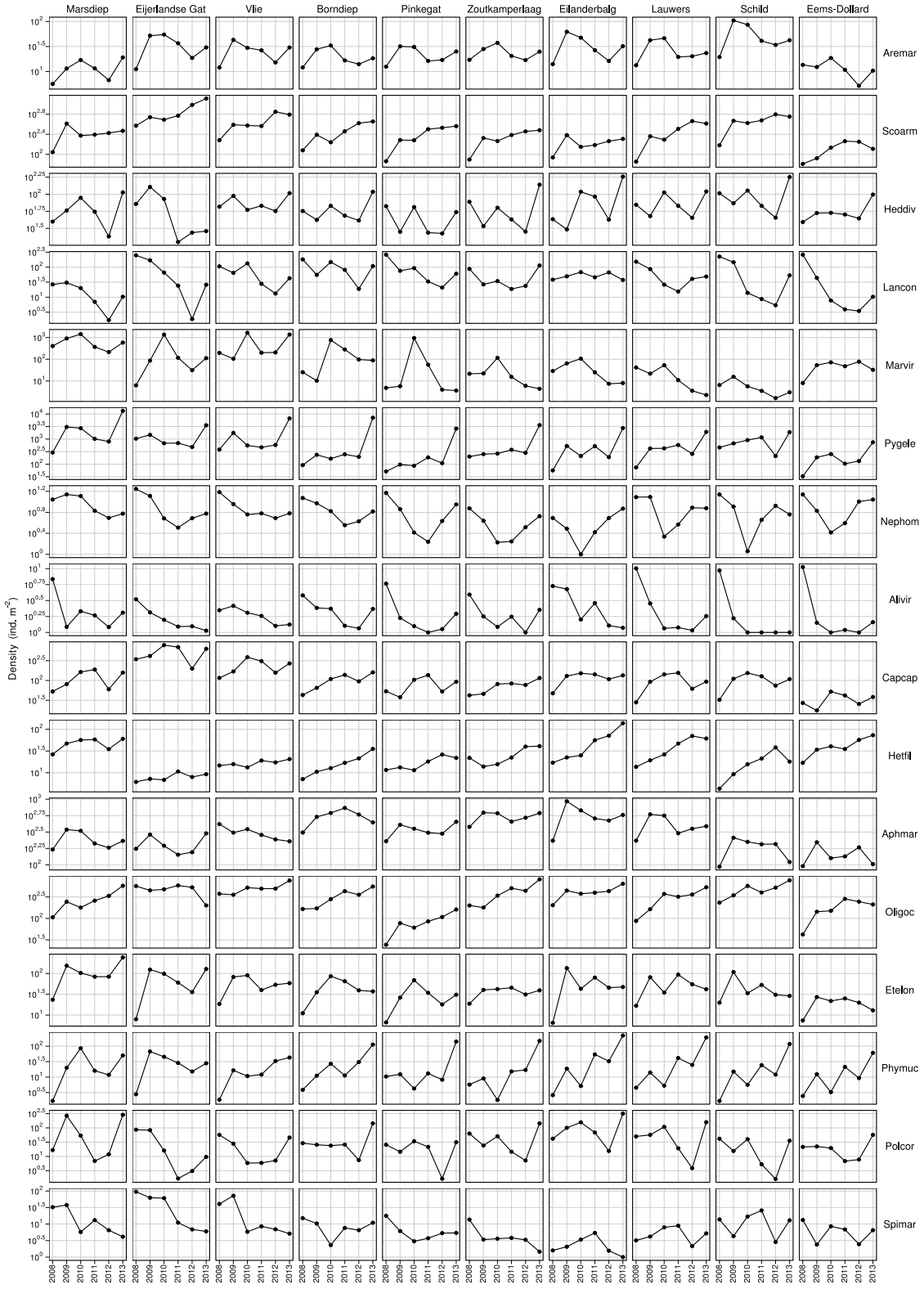

Figure 28: Average polychaete and oligochaete densities in the period 2008-2013 per tidal basin.

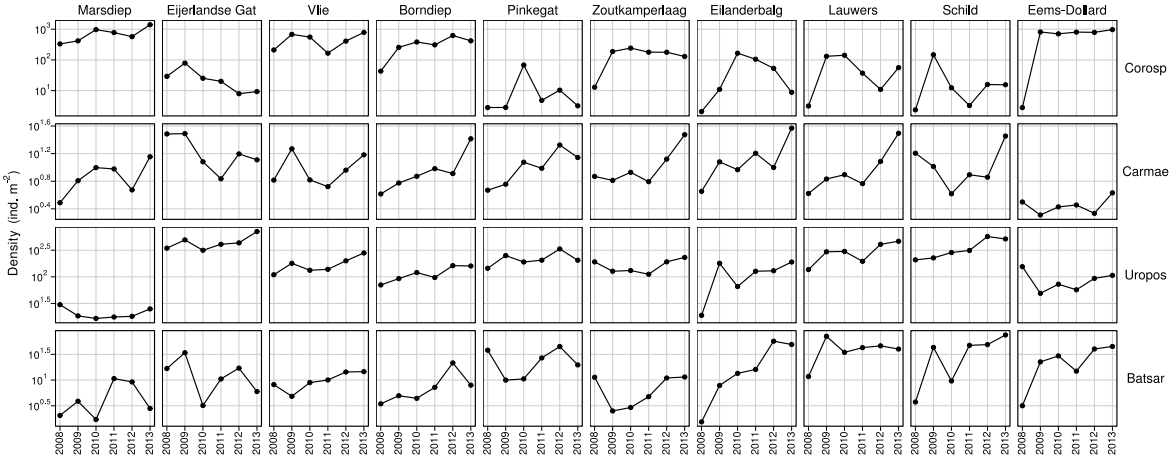

Figure 29: Average densities of crustaceans in the period 2008-2013 per tidal basin.

F Benthos maps

F.1 Molluscs (bivalves & gastropods)

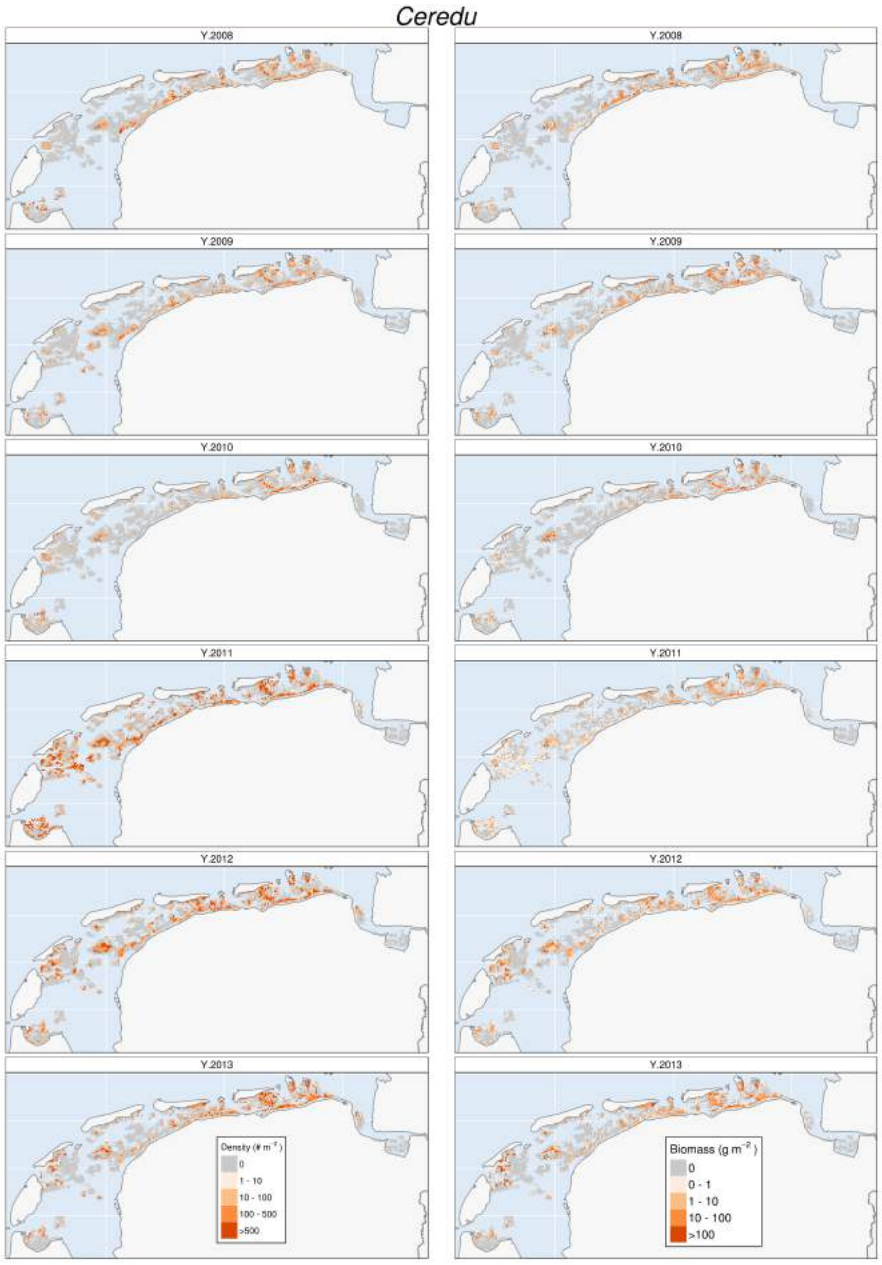

Figure 30: Spatial distributions of *Cerastoderma edule* between 2008 and 2013 in the Dutch Wadden Sea.

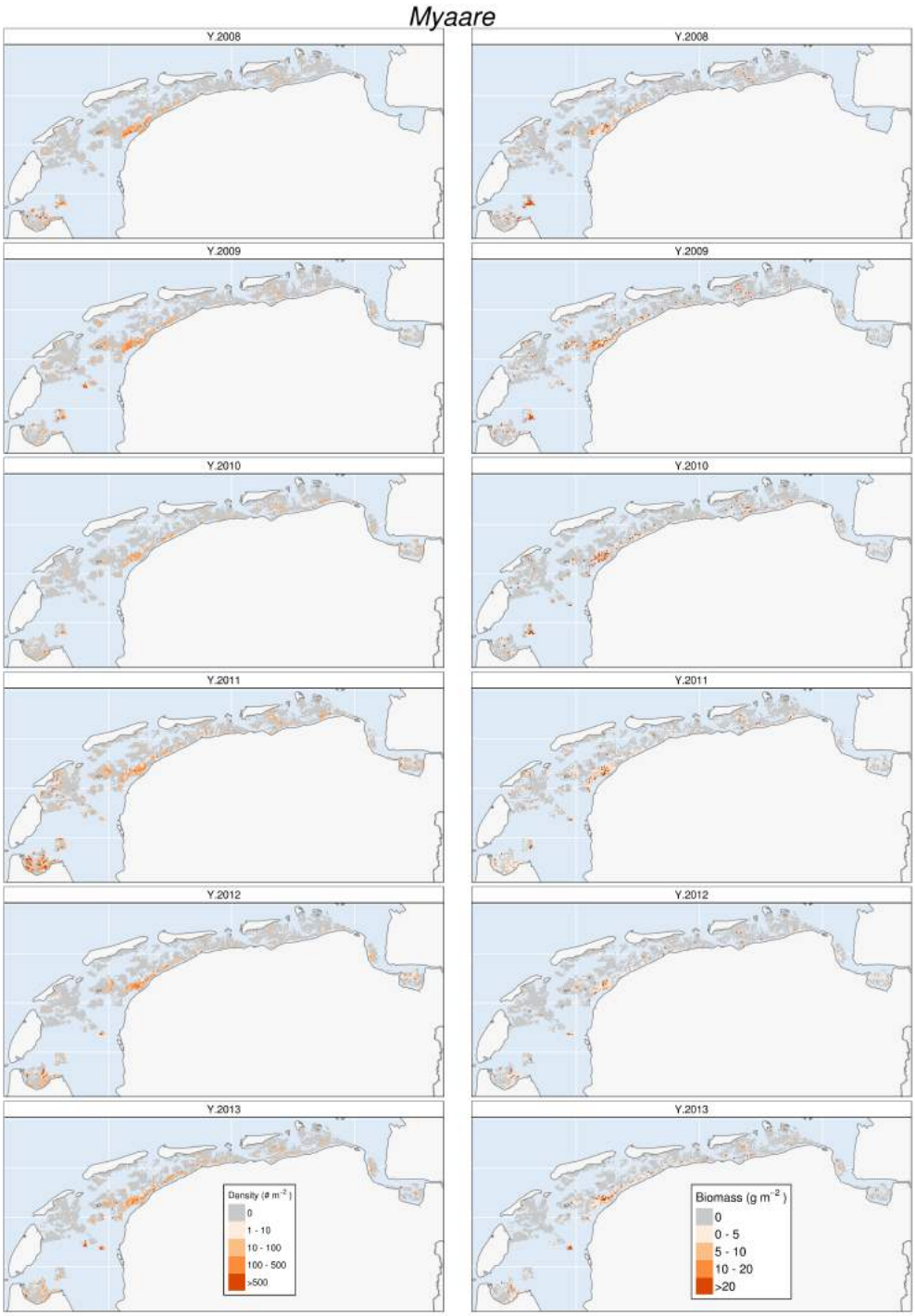

Figure 31: Spatial distributions of *Mya arenaria* between 2008 and 2013 in the Dutch Wadden Sea.

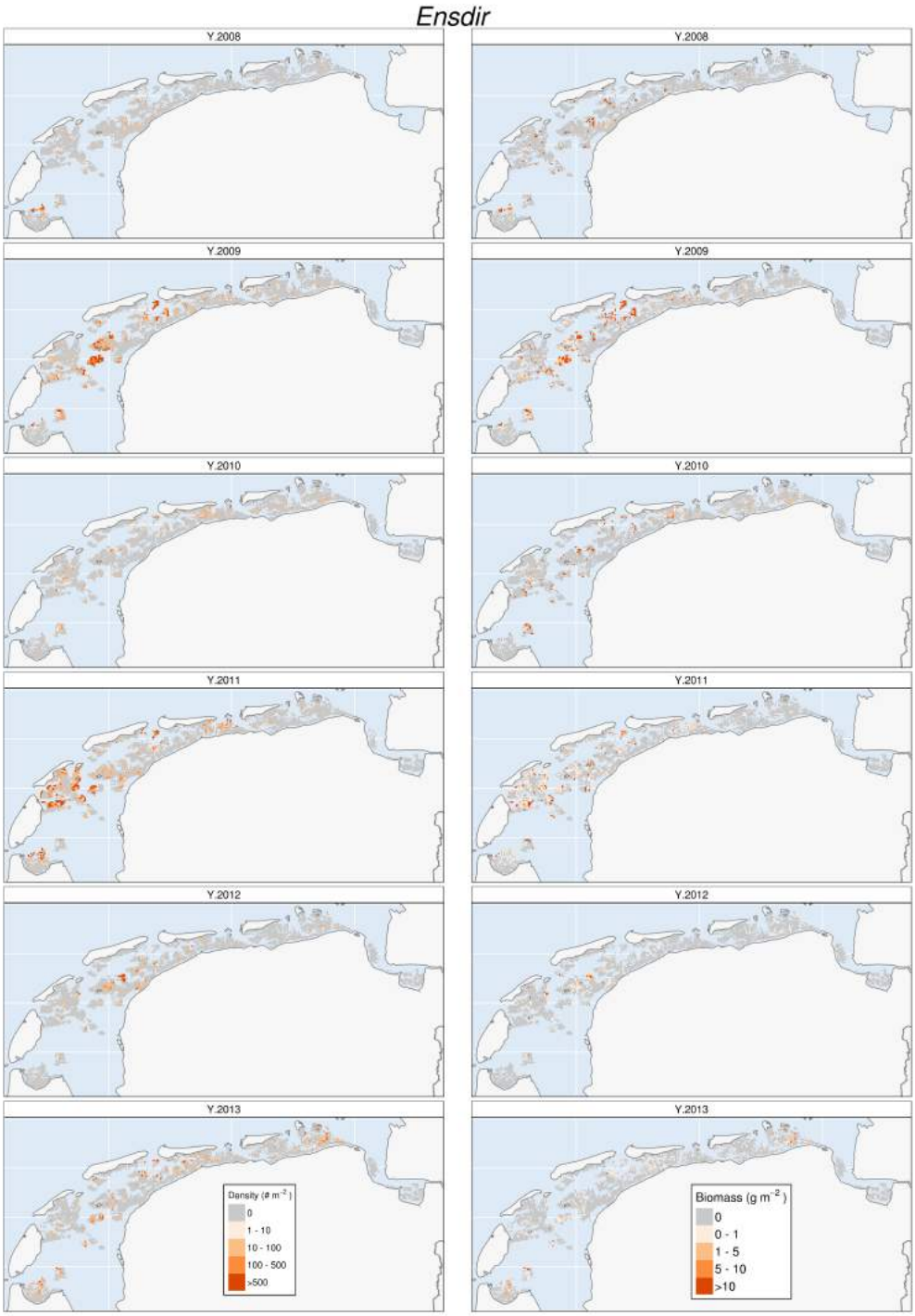

Figure 32: Spatial distributions of *Ensis leei* between 2008 and 2013 in the Dutch Wadden Sea.

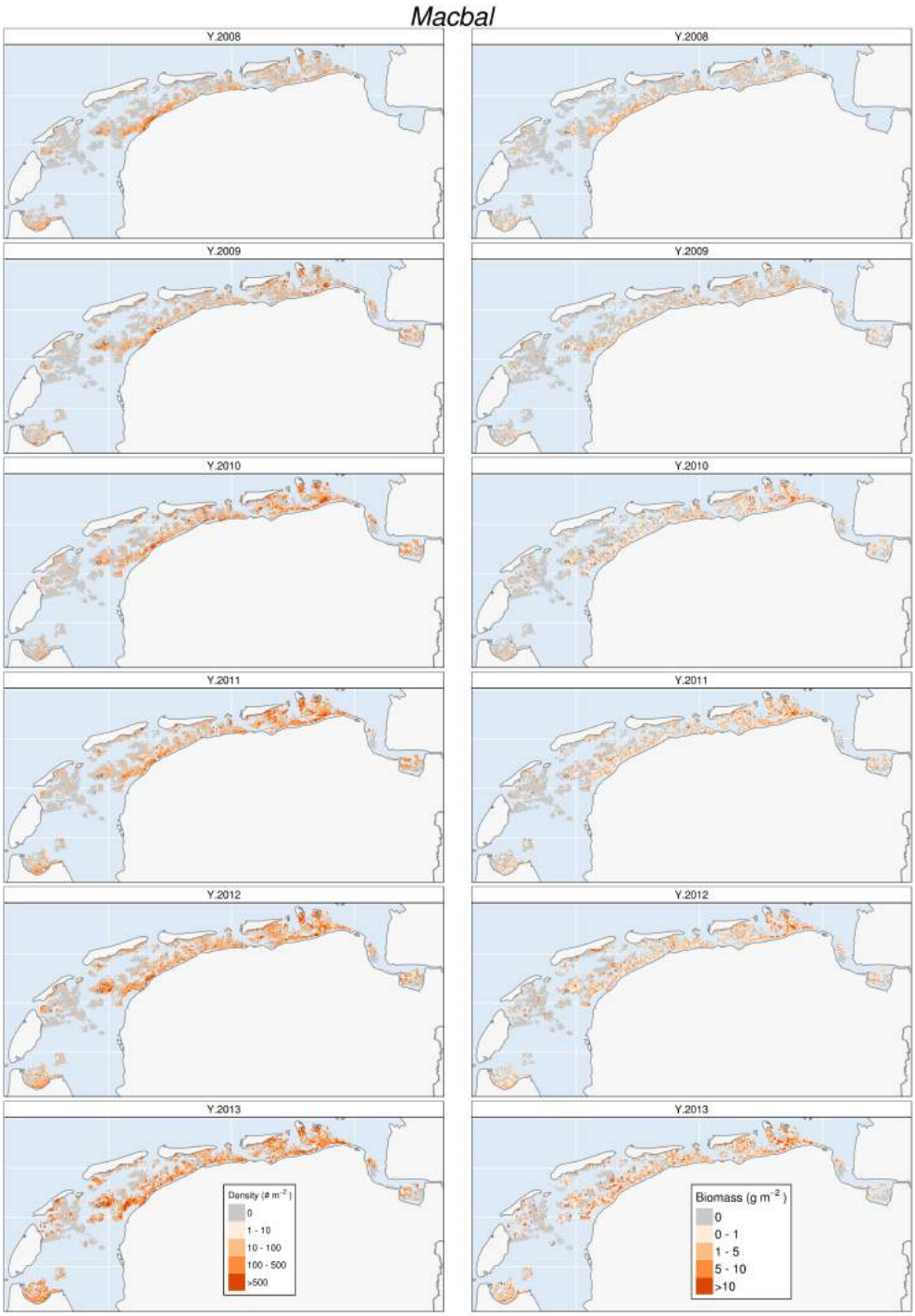

Figure 33: Spatial distributions of *Limecola balthica* between 2008 and 2013 in the Dutch Wadden Sea.

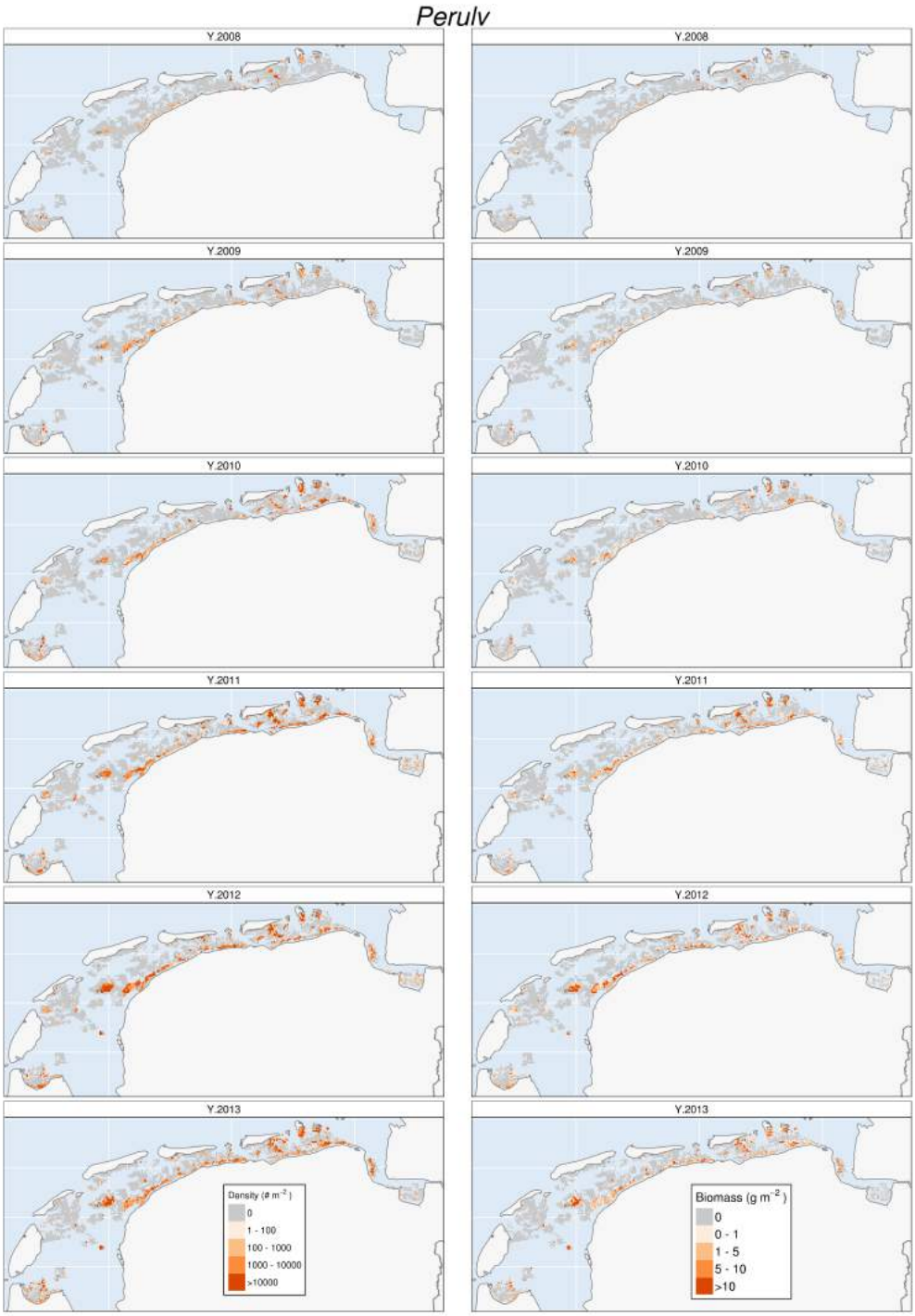

Figure 34: Spatial distributions of *Peringia ulvae* between 2008 and 2013 in the Dutch Wadden Sea.

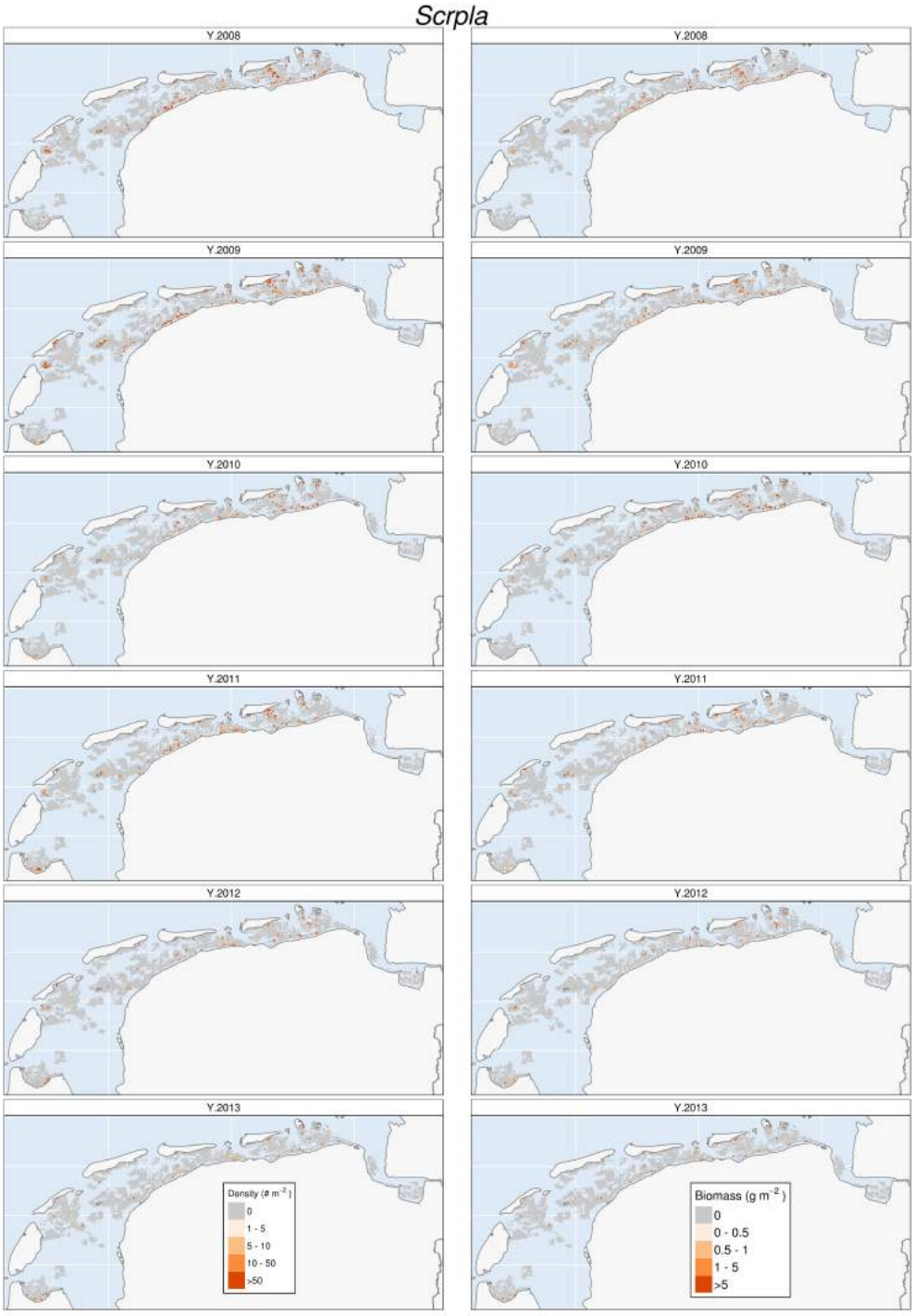

Figure 35: Spatial distributions of *Scrobicularia plana* between 2008 and 2013 in the Dutch Wadden Sea.

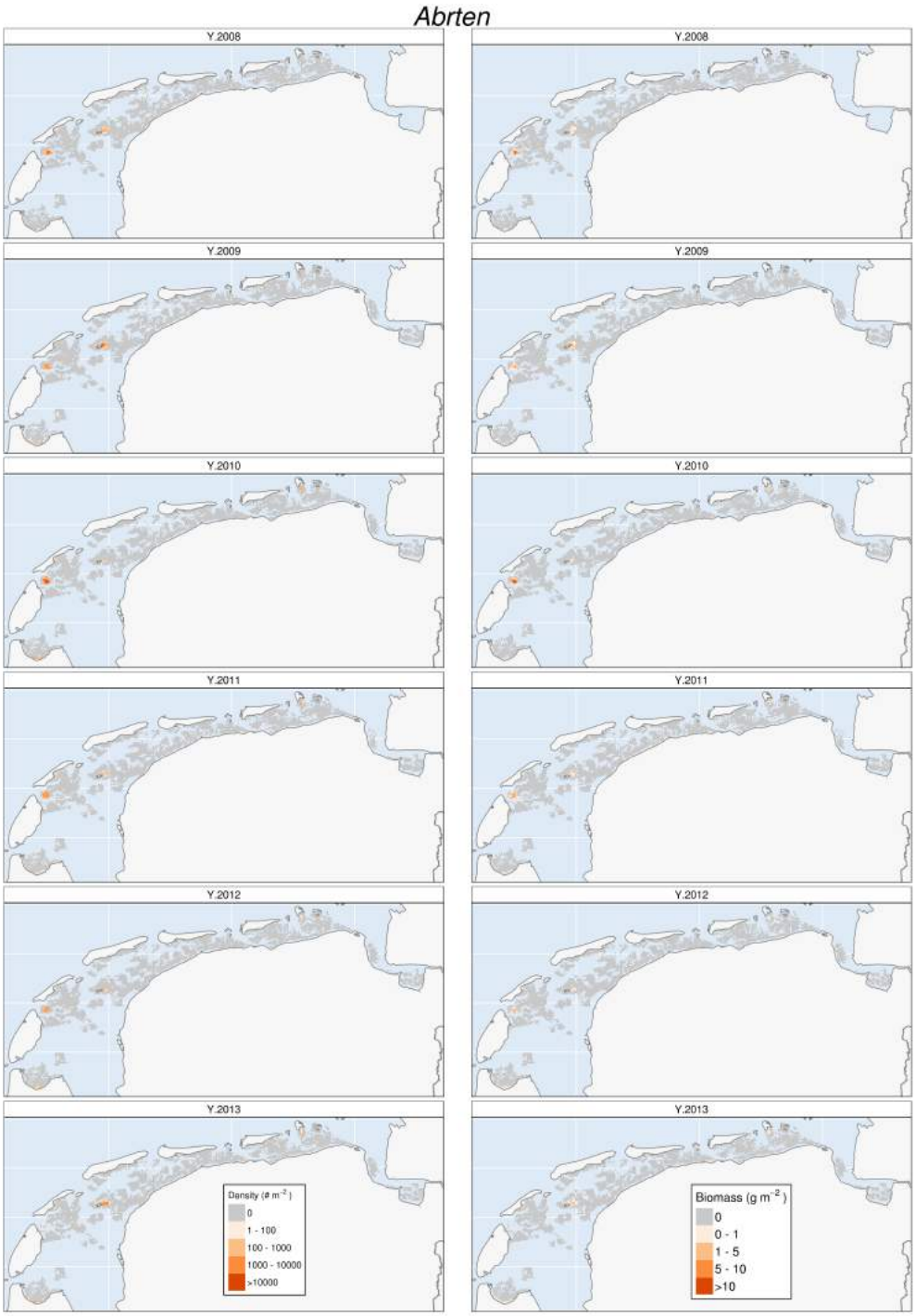

Figure 36: Spatial distributions of *Abra tenuis* between 2008 and 2013 in the Dutch Wadden Sea.

F.2 Polychaetes

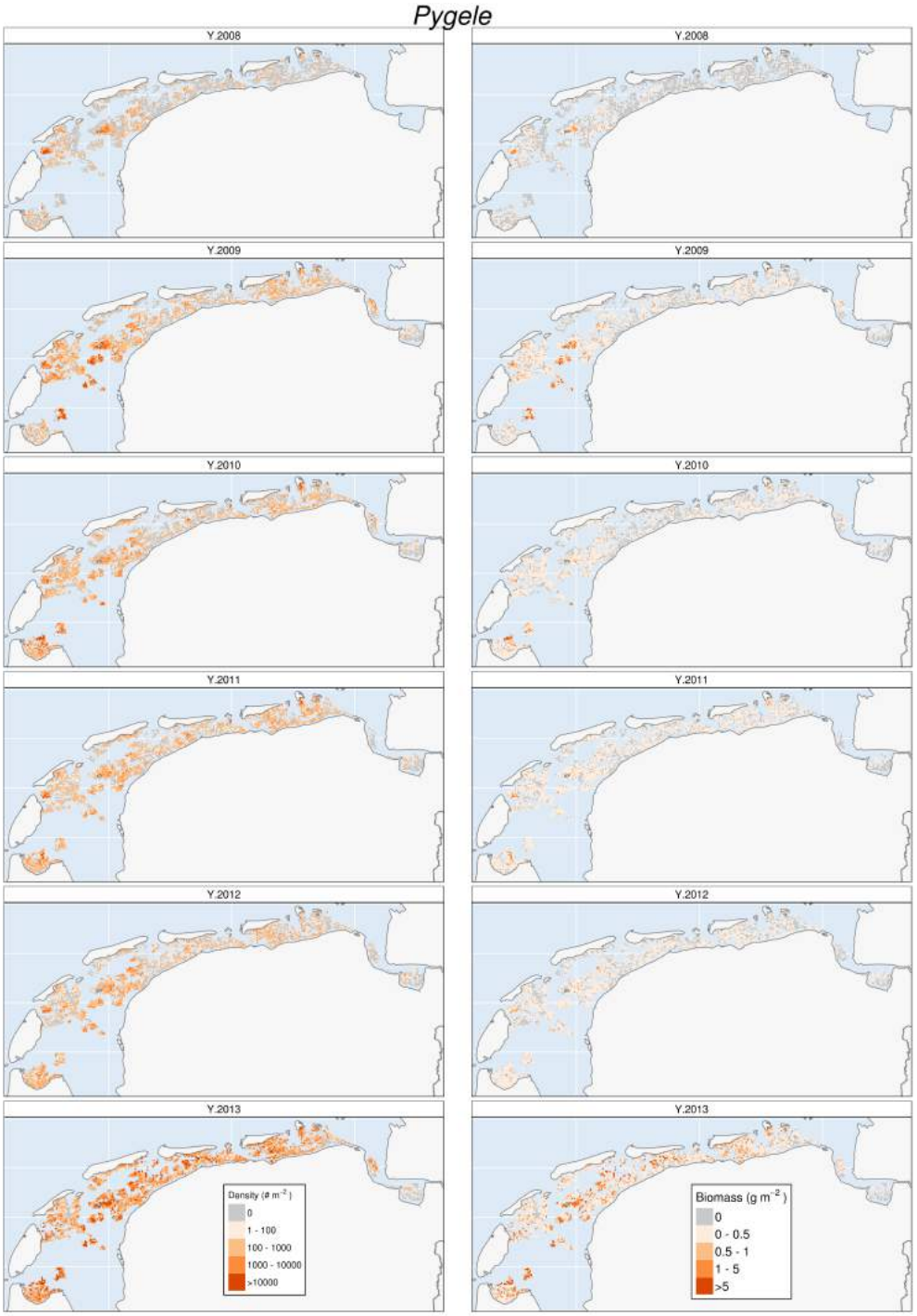

Figure 42: Spatial distributions of *Pygospio elegans* between 2008 and 2013 in the Dutch Wadden Sea.

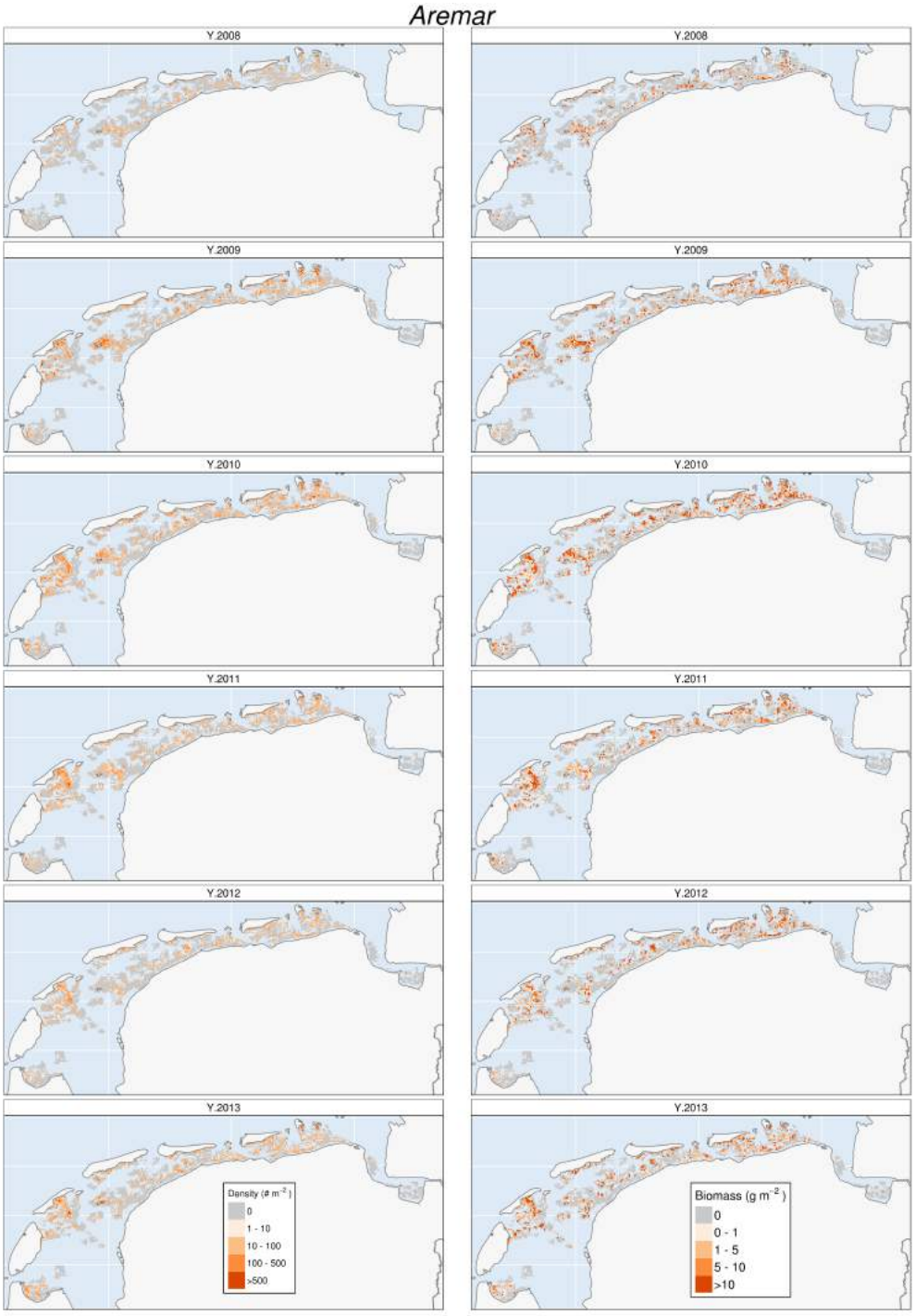

Figure 37: Spatial distributions of *Arenicola marina* between 2008 and 2013 in the Dutch Wadden Sea.

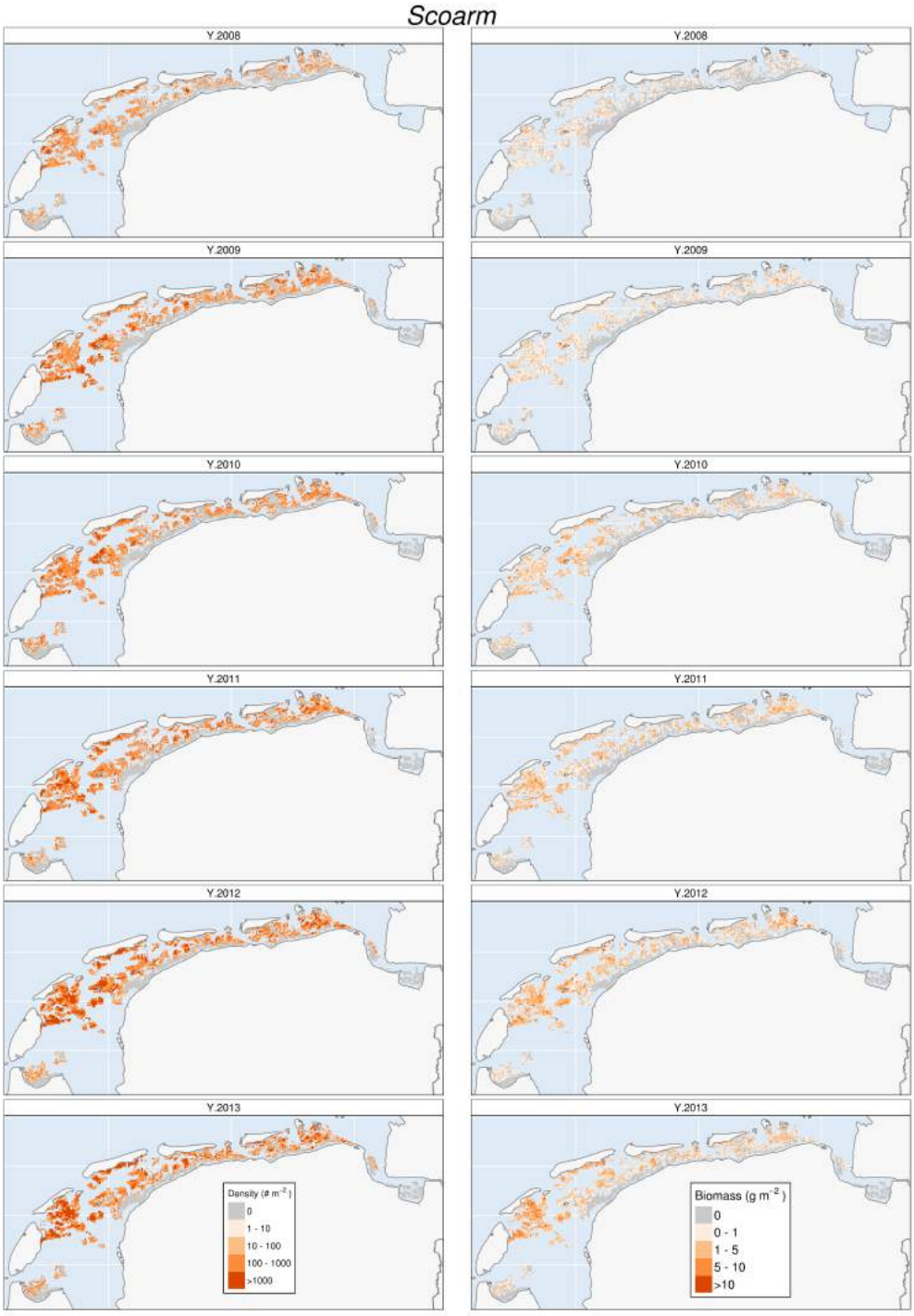

Figure 38: Spatial distributions of *Scoloplos armiger* between 2008 and 2013 in the Dutch Wadden Sea.

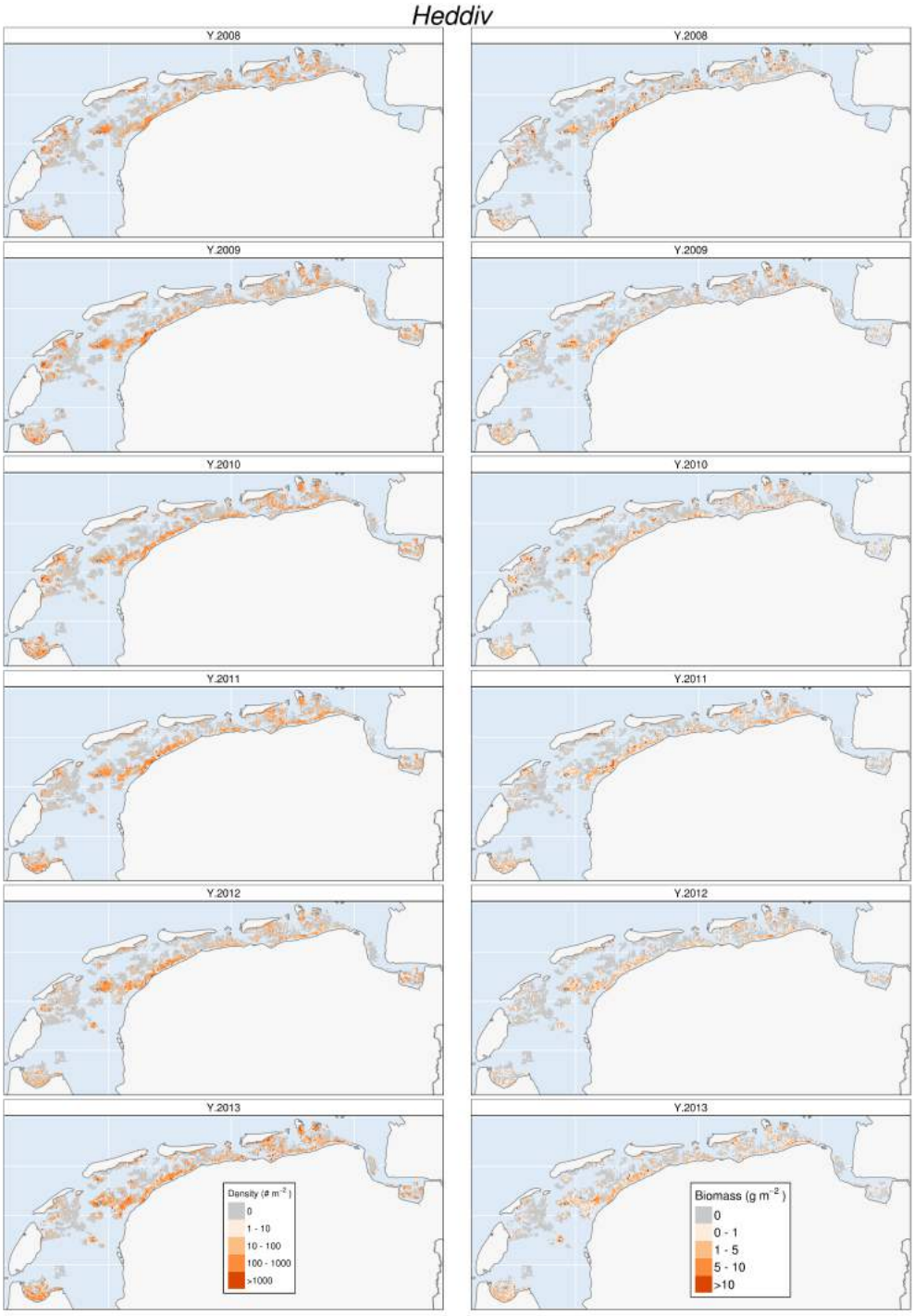

Figure 39: Spatial distributions of *Hediste diversicolor* between 2008 and 2013 in the Dutch Wadden Sea.

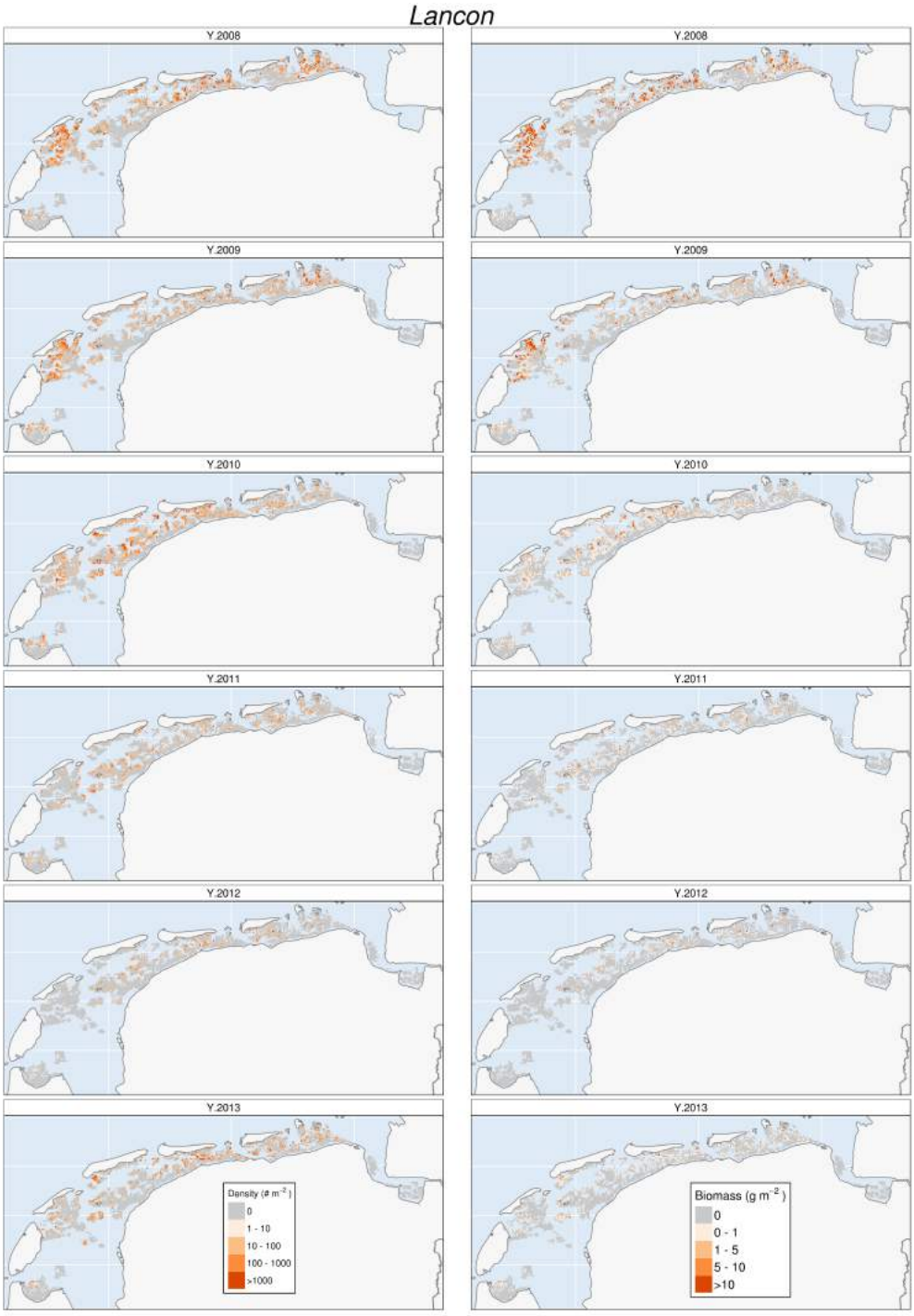

Figure 40: Spatial distributions of *Lanice conchilega* between 2008 and 2013 in the Dutch Wadden Sea.

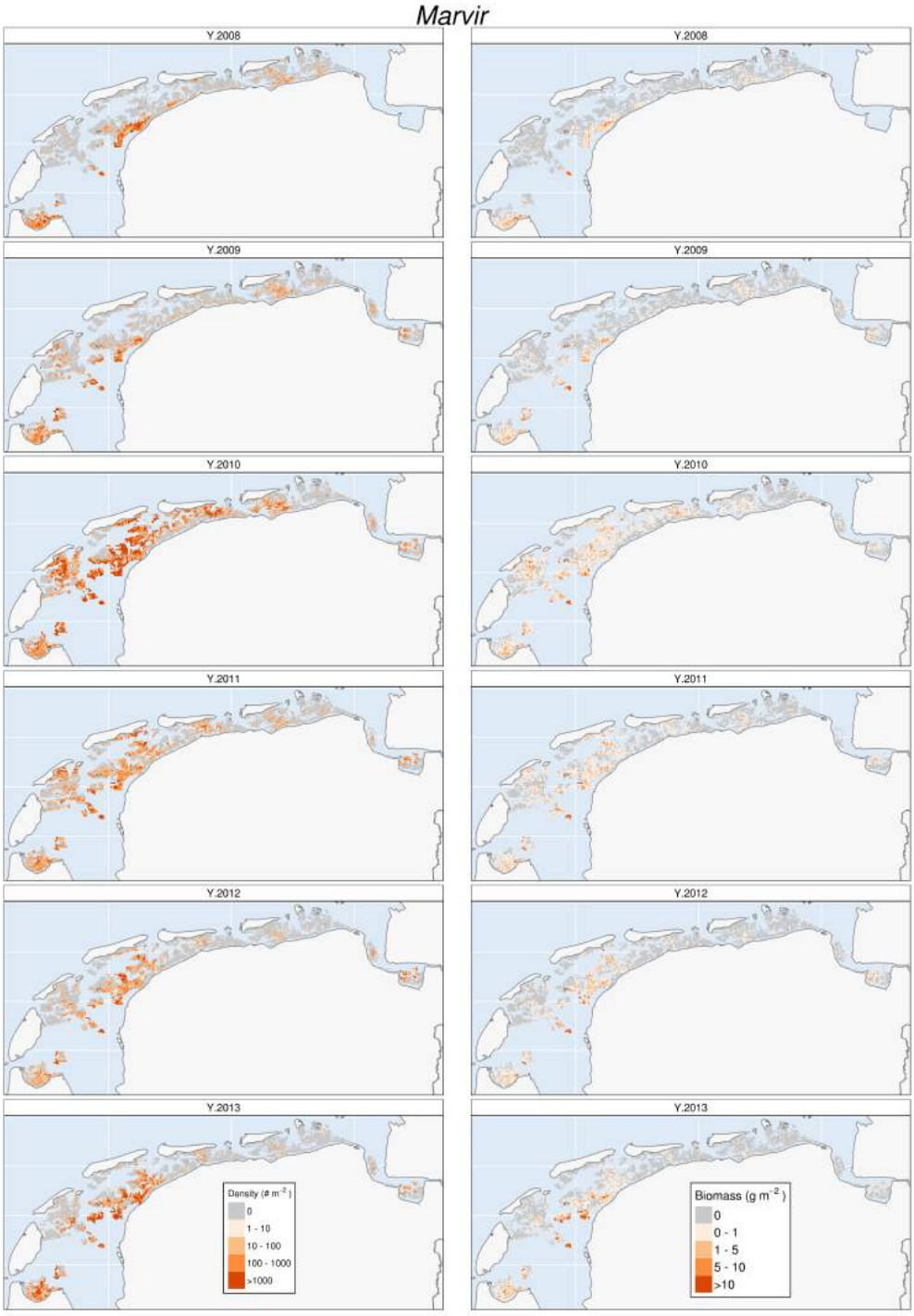

Figure 41: Spatial distributions of *Marenzelleria viridis* between 2008 and 2013 in the Dutch Wadden Sea.

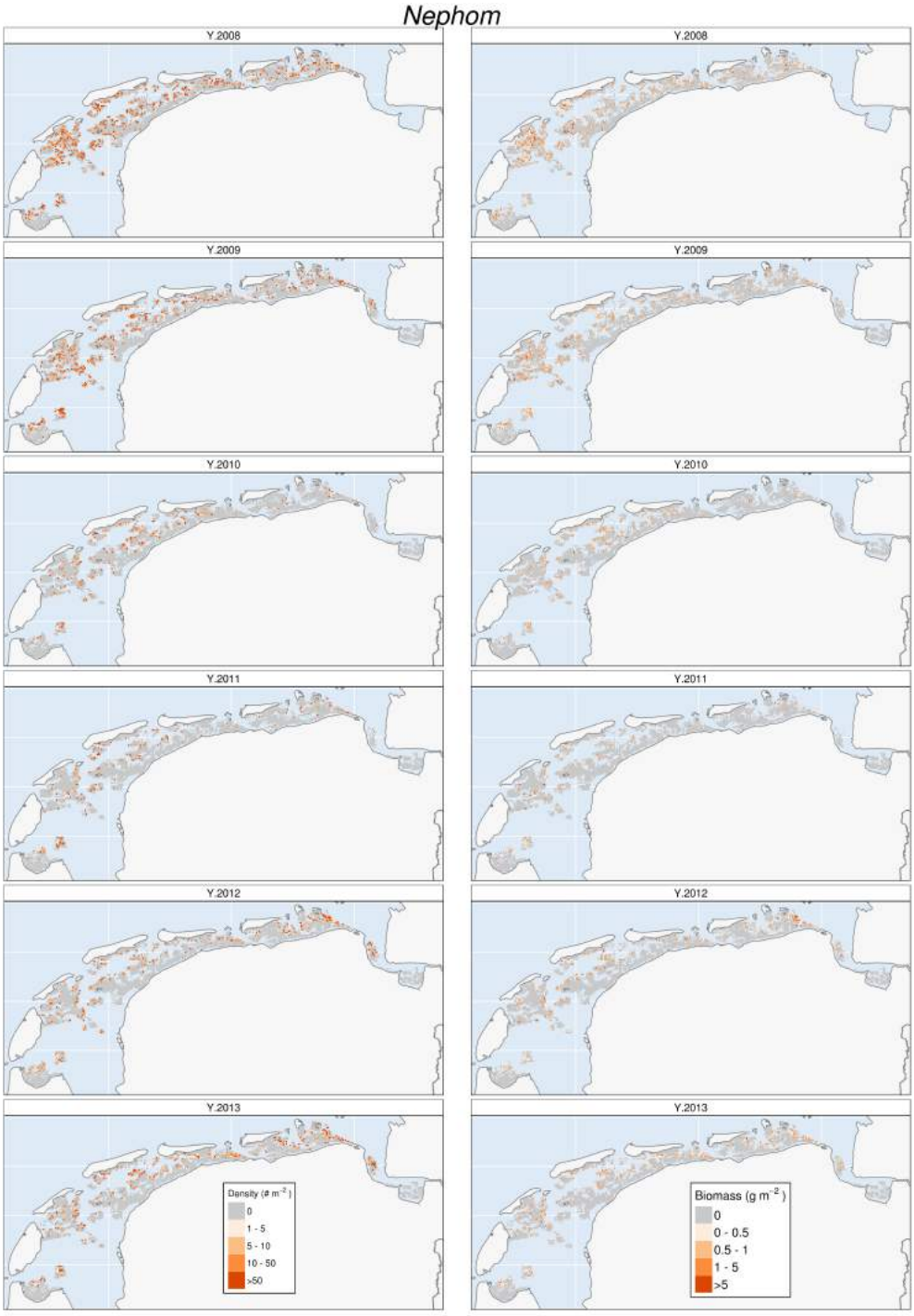

Figure 43: Spatial distributions of *Nephtys hombergii* between 2008 and 2013 in the Dutch Wadden Sea.

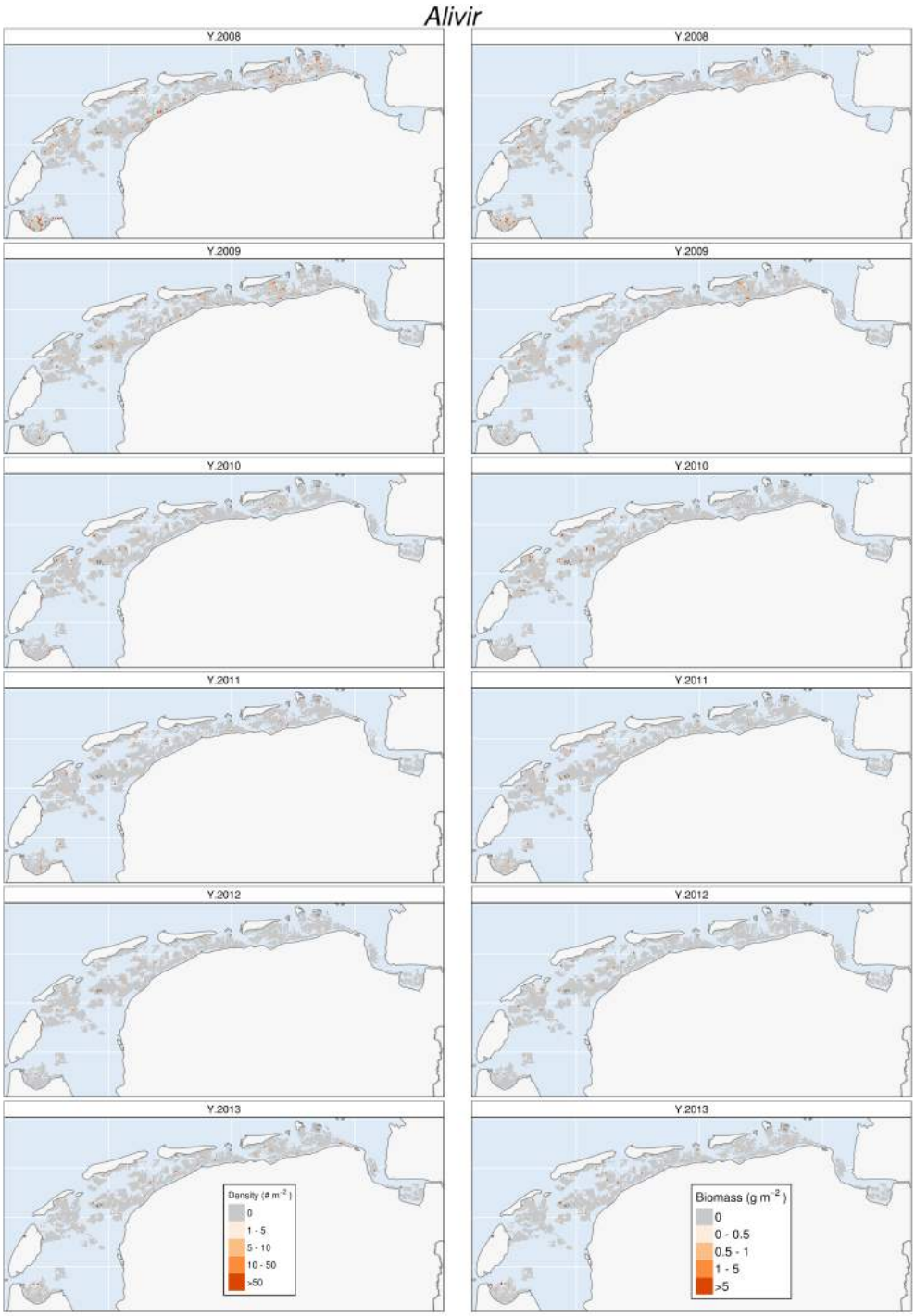

Figure 44: Spatial distributions of *Alitta virens* between 2008 and 2013 in the Dutch Wadden Sea.

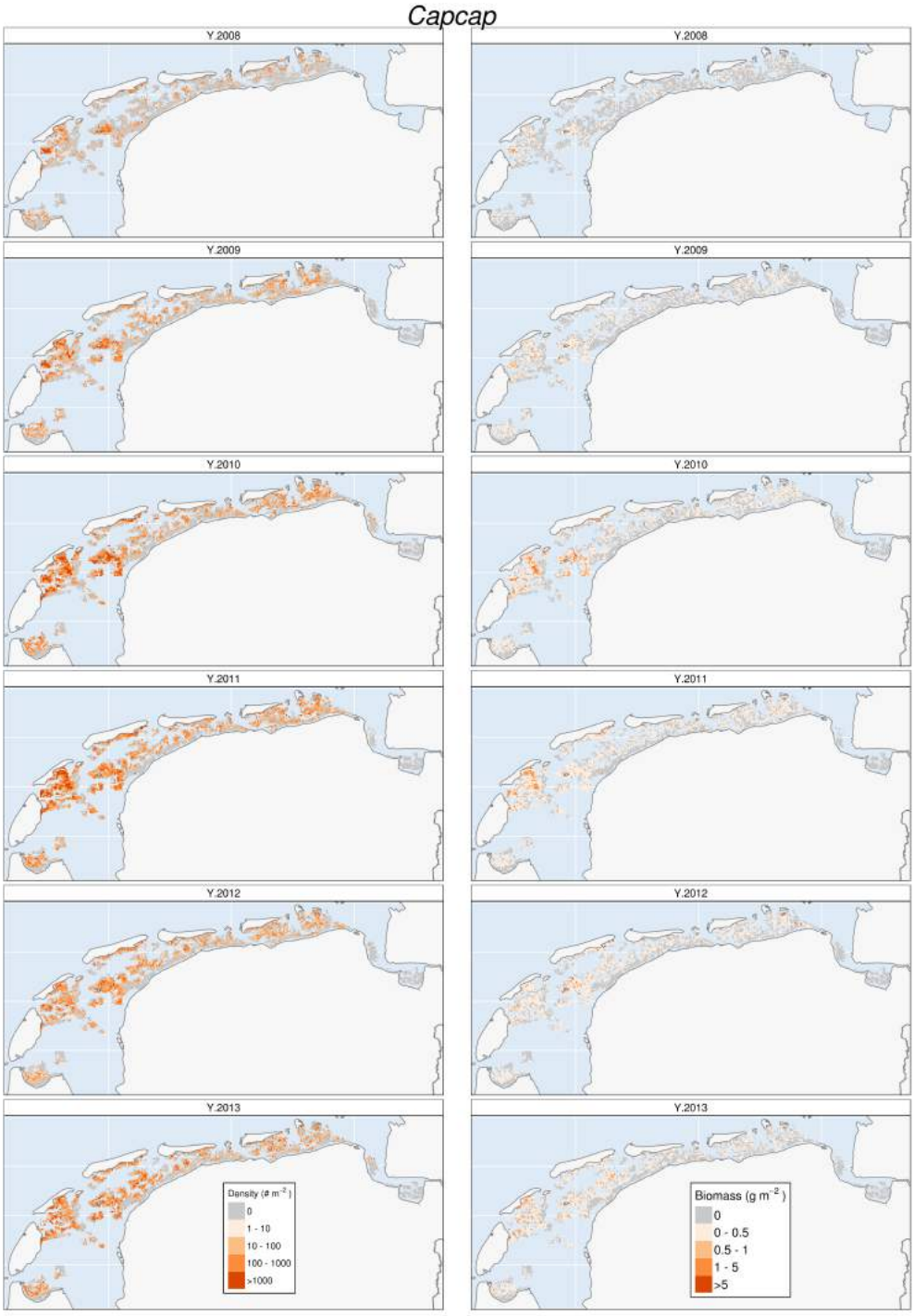

Figure 45: Spatial distributions of *Capitella capitata* between 2008 and 2013 in the Dutch Wadden Sea.

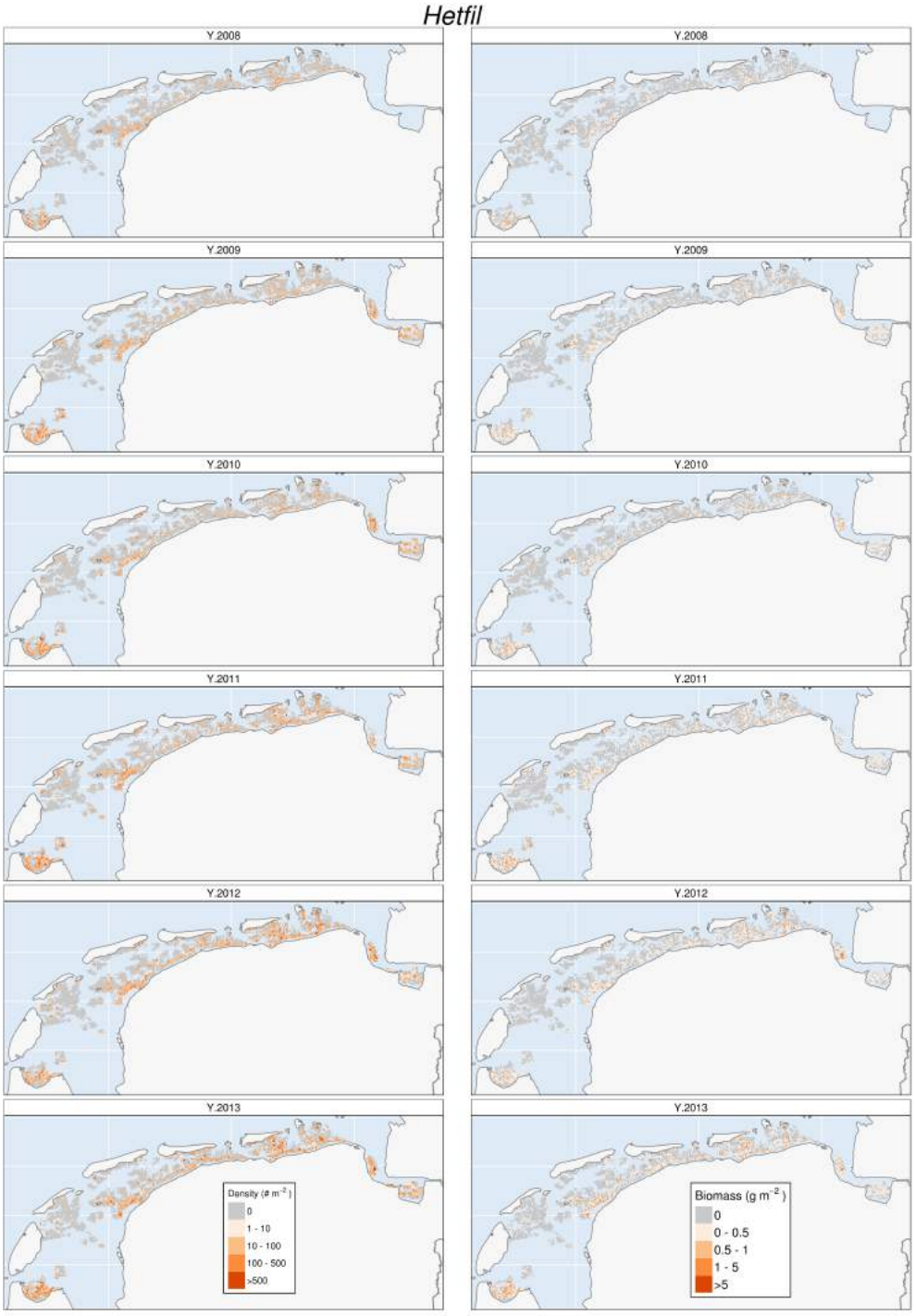

Figure 46: Spatial distributions of *Heteromastus filiformis* between 2008 and 2013 in the Dutch Wadden Sea.

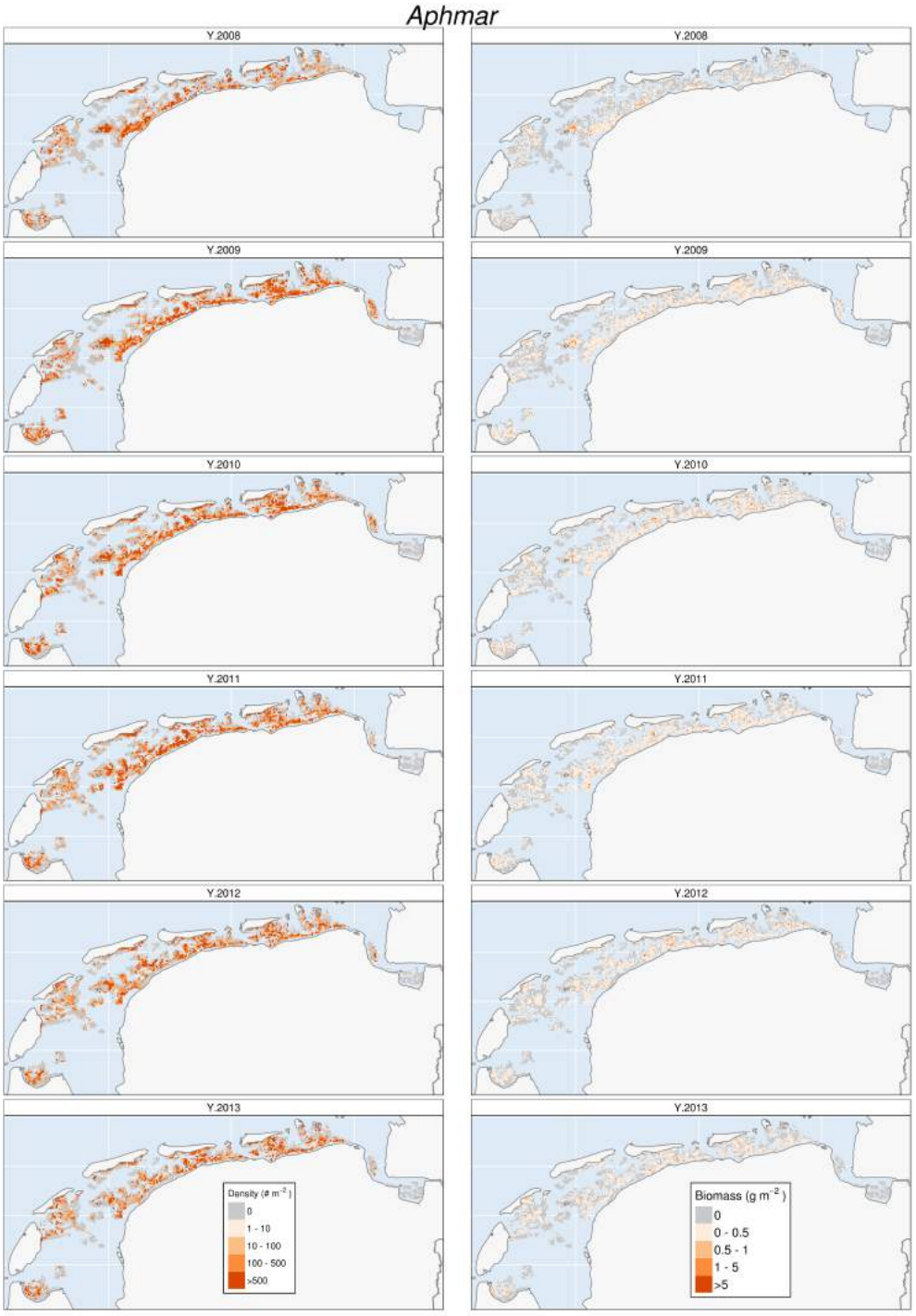

Figure 47: Spatial distributions of *Aphelochaeta marioni* between 2008 and 2013 in the Dutch Wadden Sea.

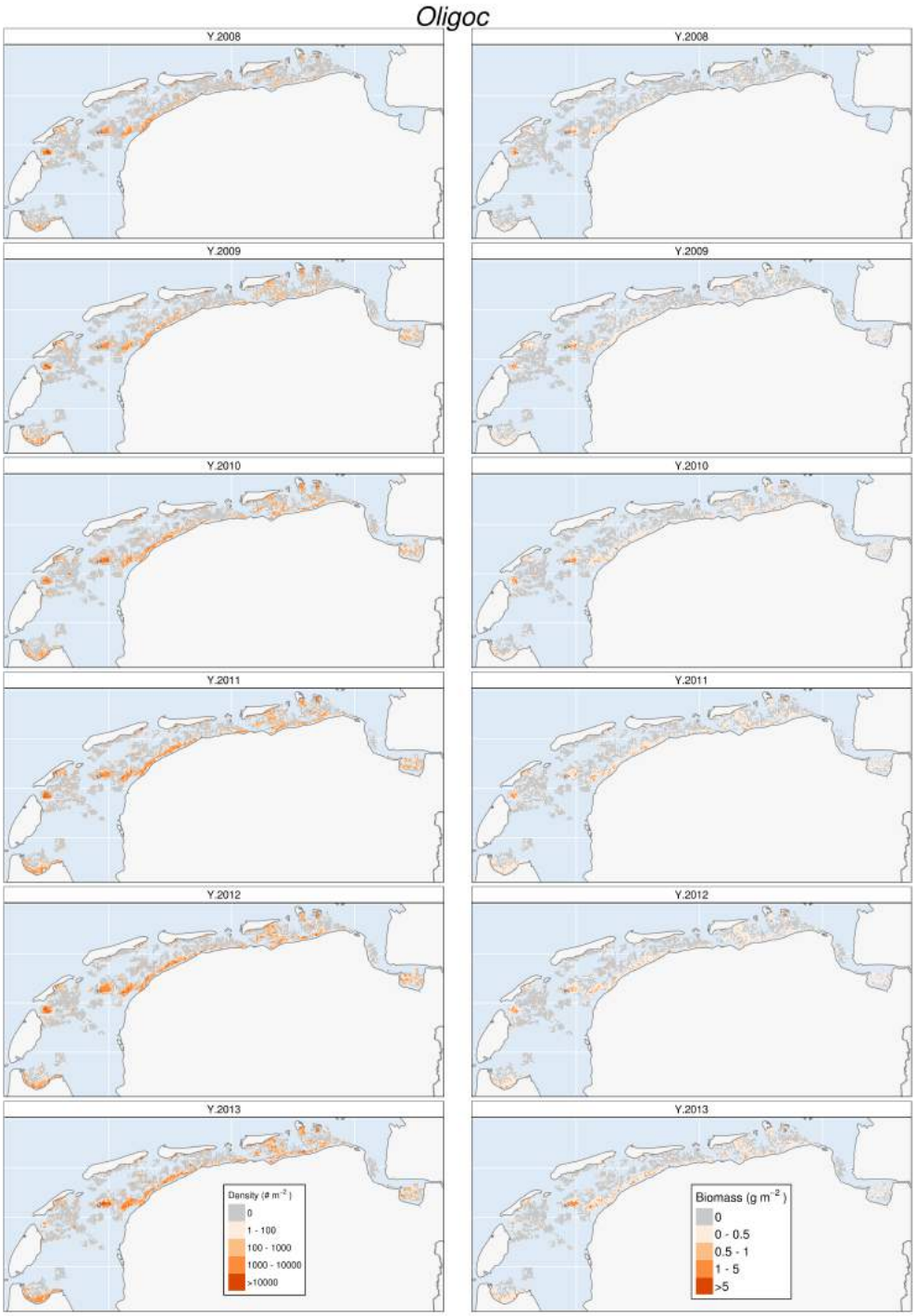

Figure 48: Spatial distributions of *Oligochaeta sp* between 2008 and 2013 in the Dutch Wadden Sea.

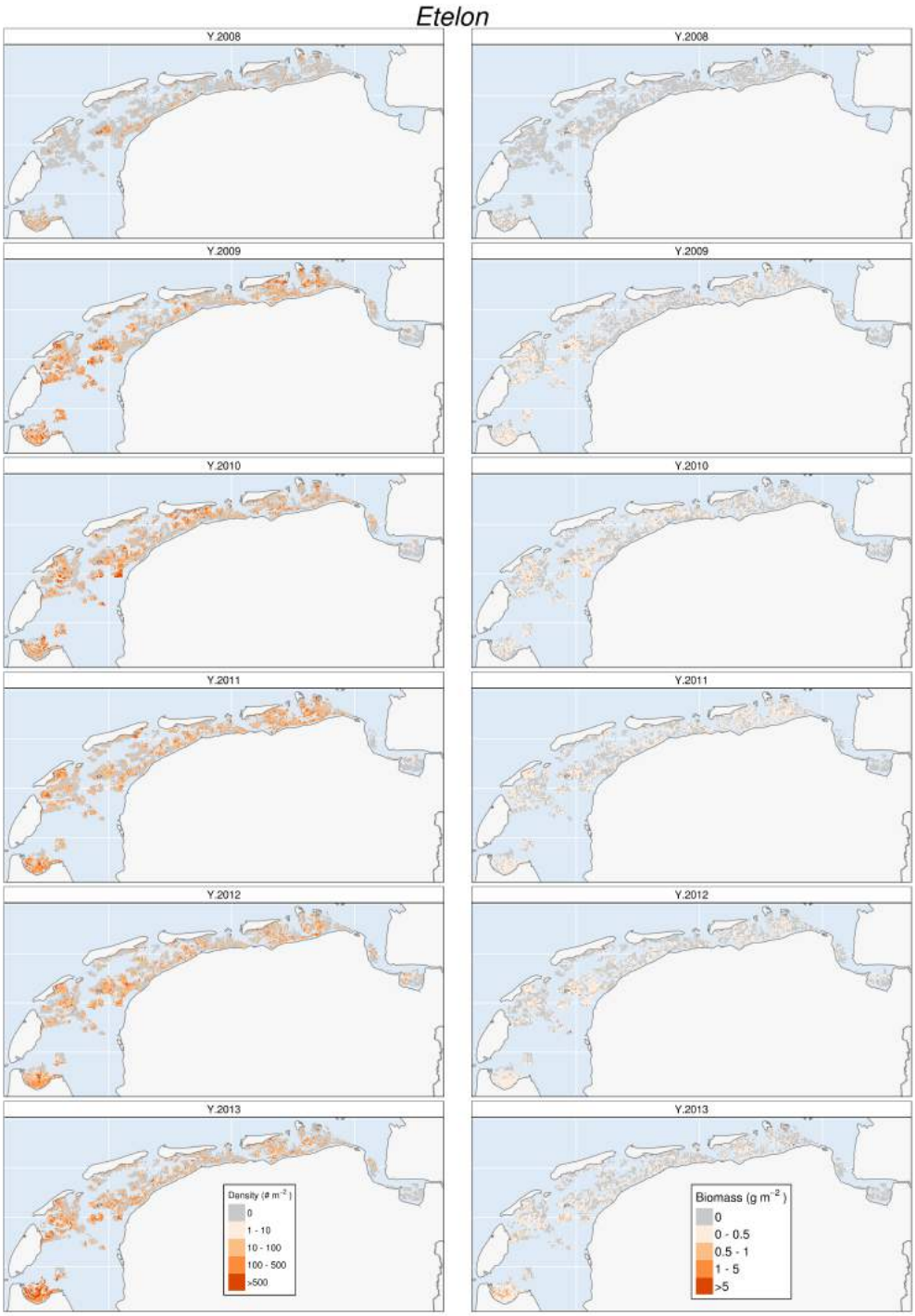

Figure 49: Spatial distributions of *Eteone longa* between 2008 and 2013 in the Dutch Wadden Sea.

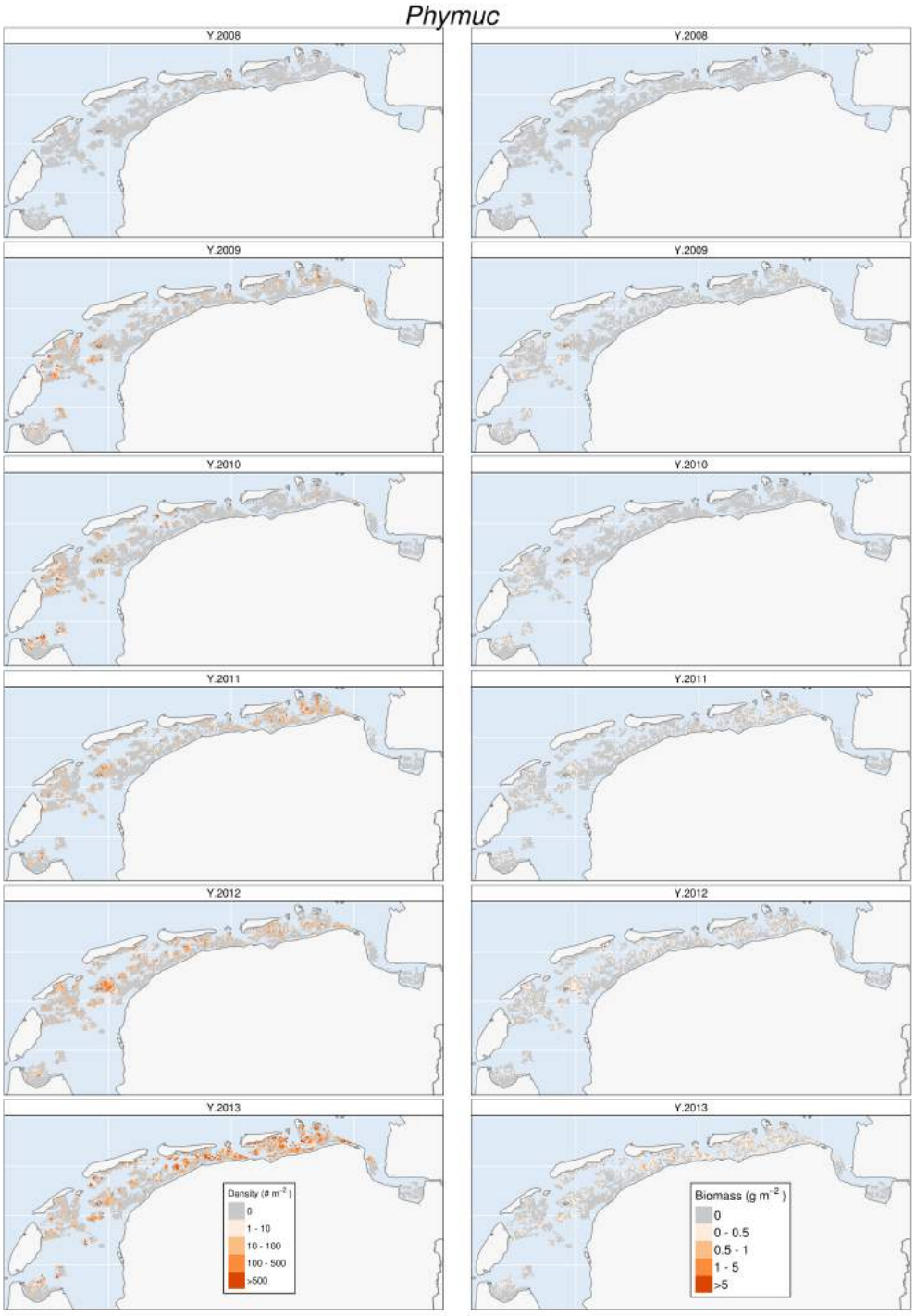

Figure 50: Spatial distributions of *Phyllodoce mucosa* between 2008 and 2013 in the Dutch Wadden Sea.

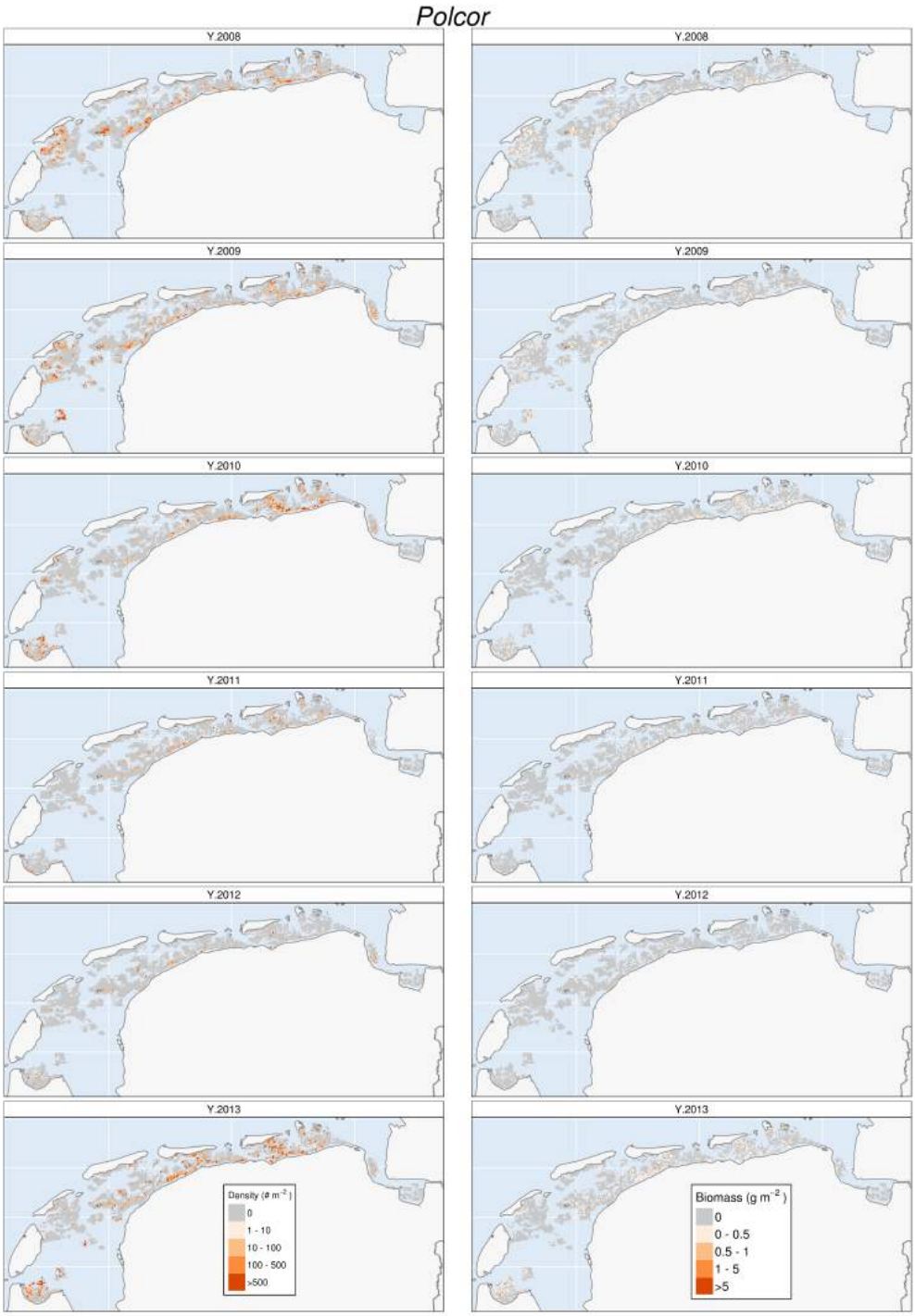

Figure 51: Spatial distributions of *Polydora cornuta* between 2008 and 2013 in the Dutch Wadden Sea.

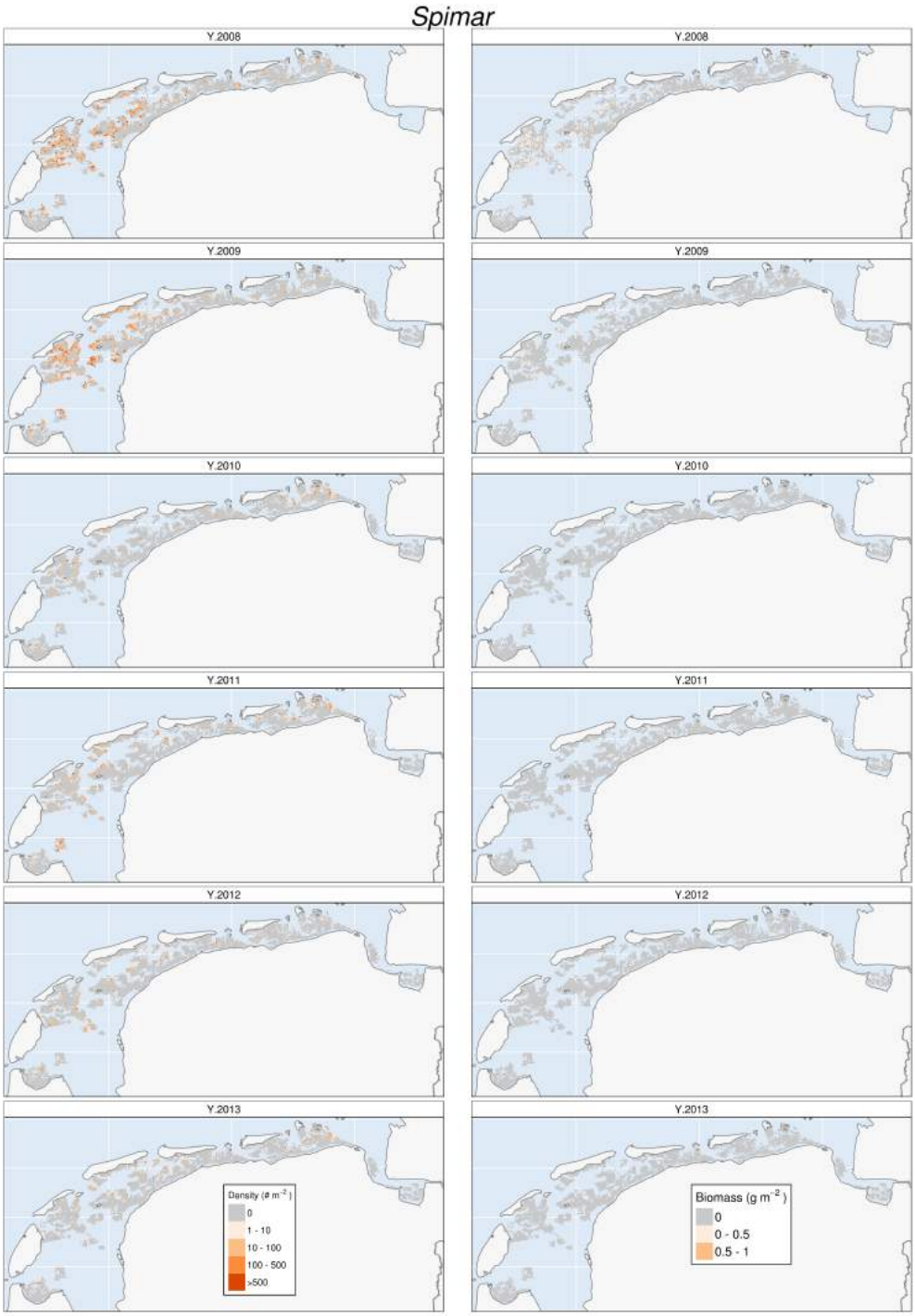

Figure 52: Spatial distributions of *Spio martinensis* between 2008 and 2013 in the Dutch Wadden Sea.

F.3 Crustaceans

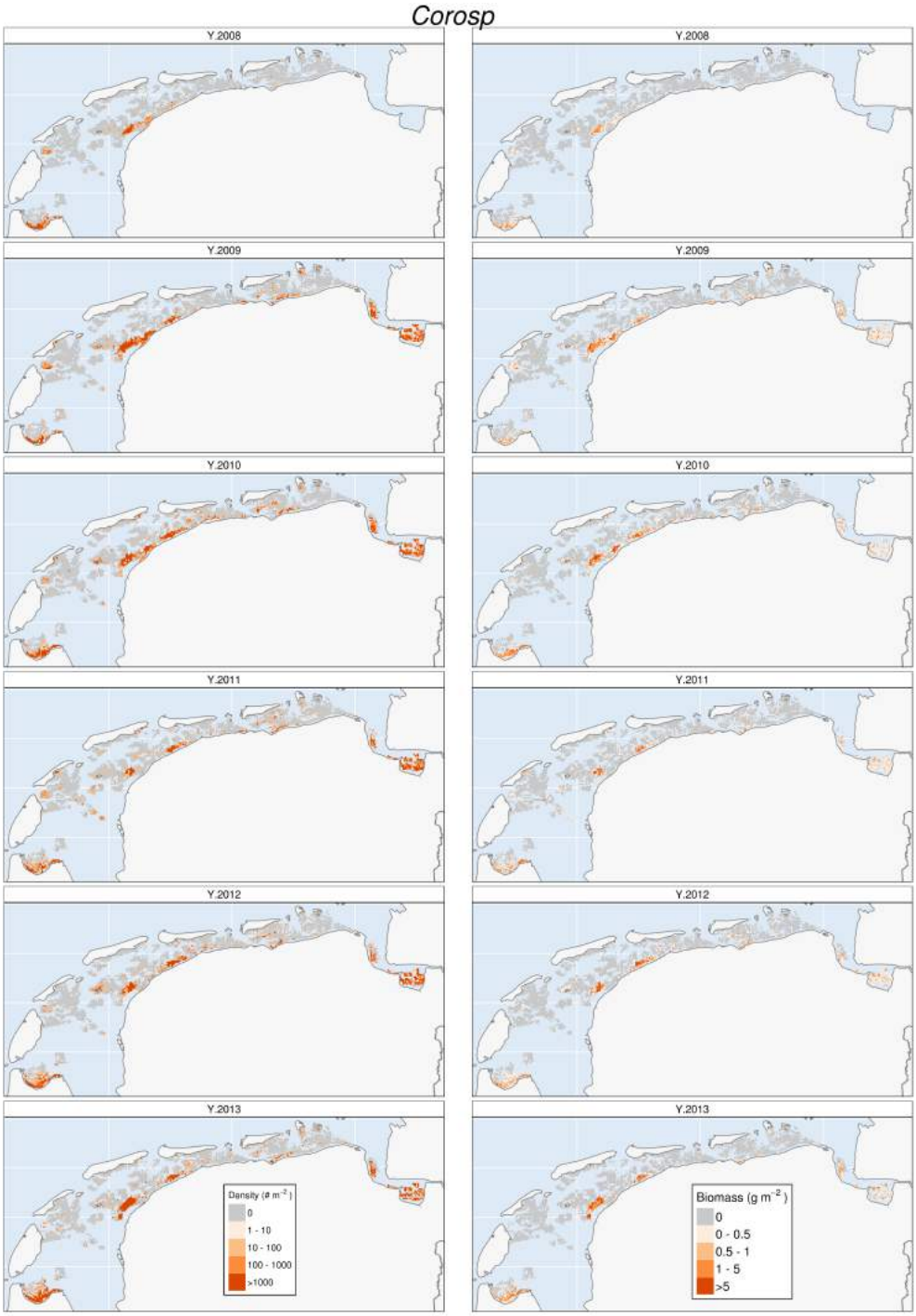

Figure 53: Spatial distributions of *Corophium sp.* between 2008 and 2013 in the Dutch Wadden Sea.

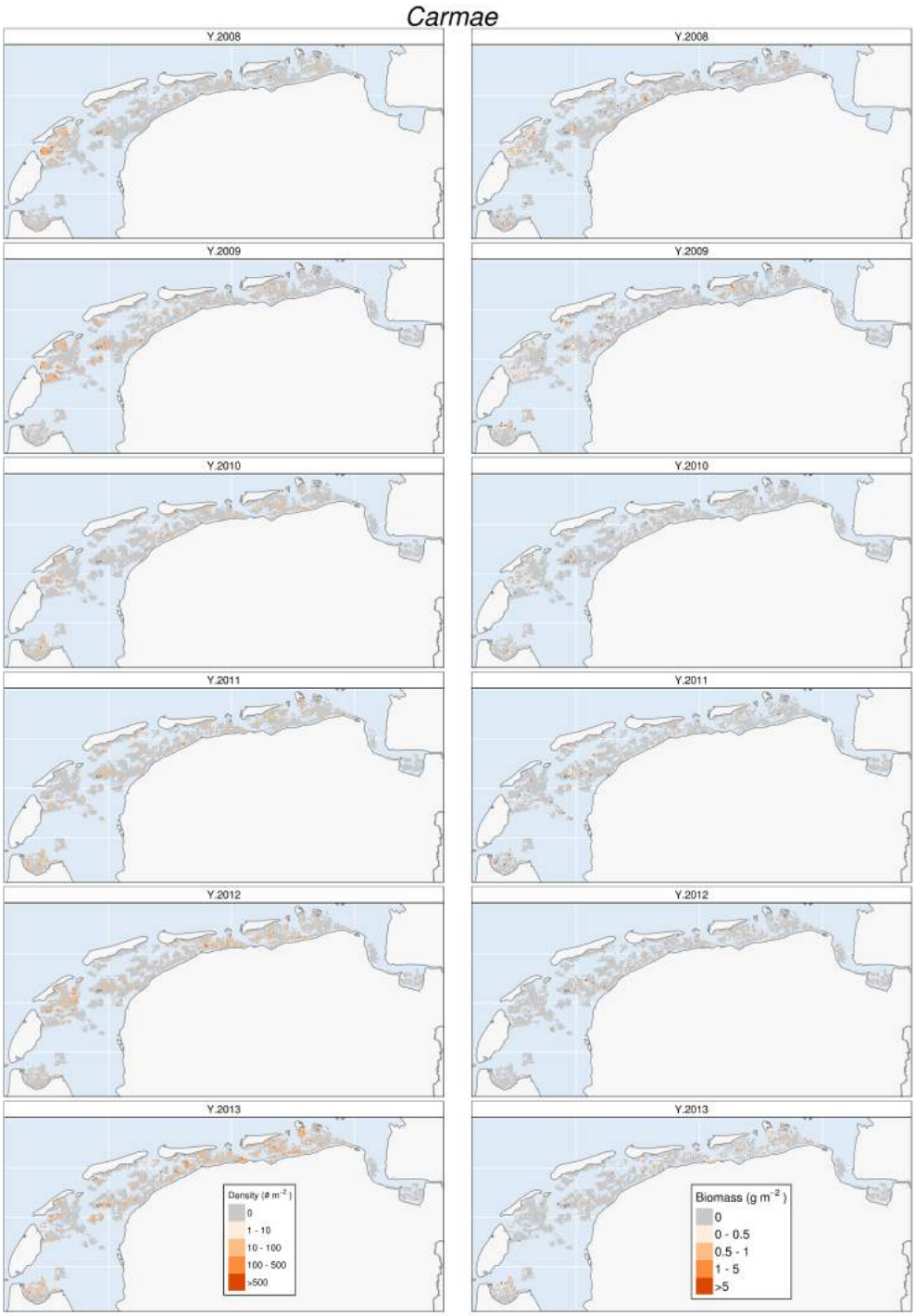

Figure 54: Spatial distributions of *Carcinus maenas* between 2008 and 2013 in the Dutch Wadden Sea.

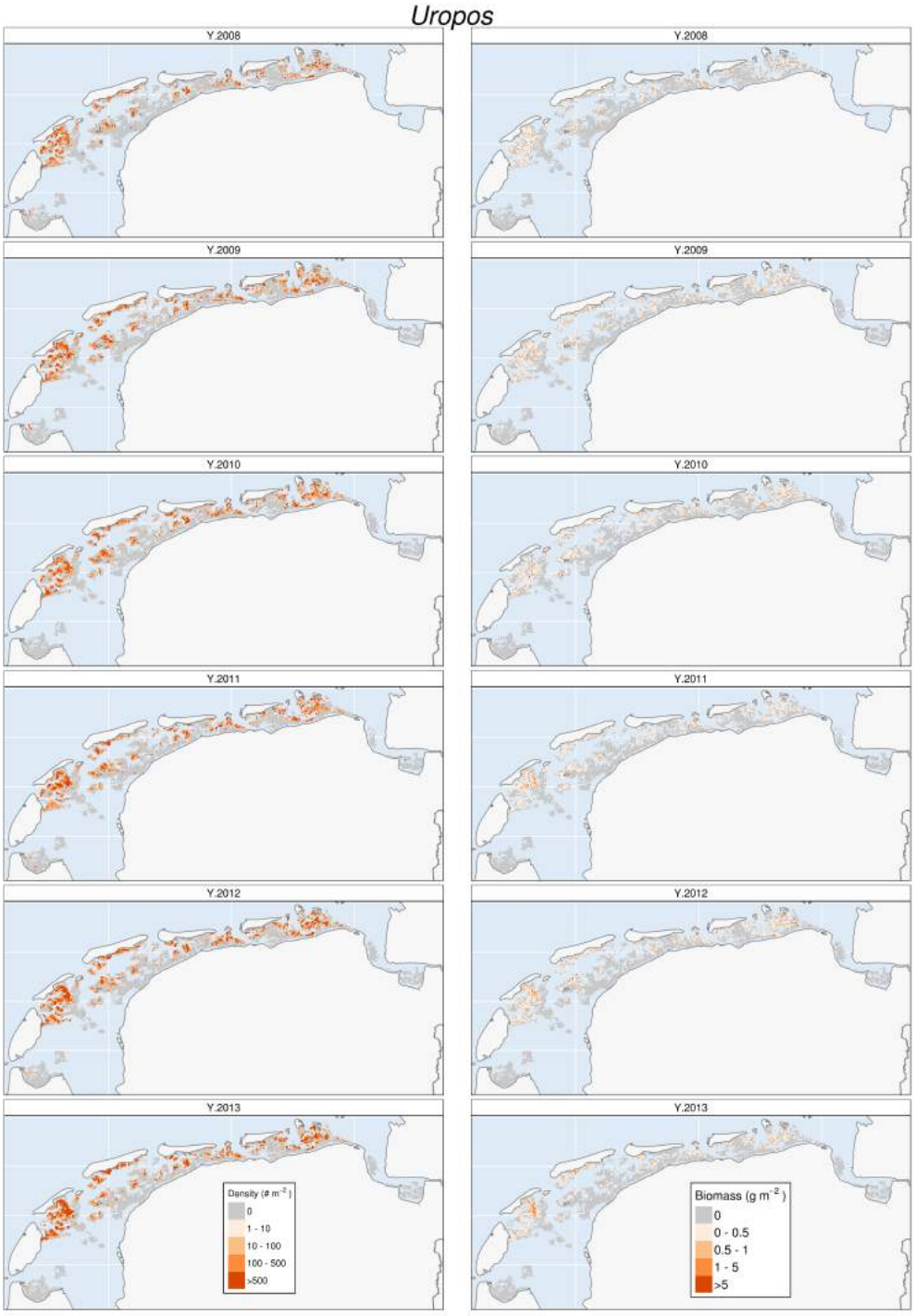

Figure 55: Spatial distributions of *Urothoe poseidonis* between 2008 and 2013 in the Dutch Wadden Sea.

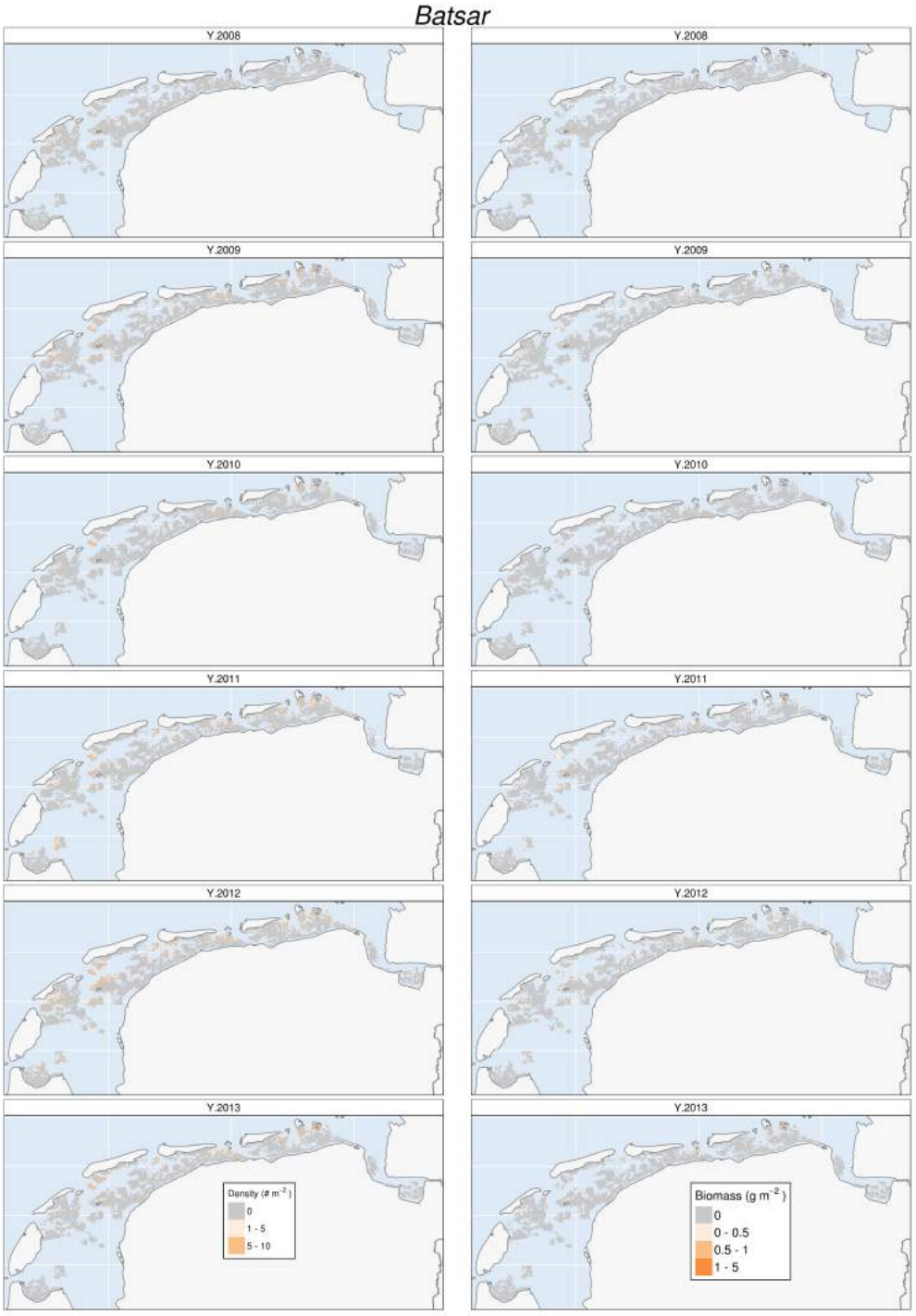

Figure 56: Spatial distributions of *Bathyporeia sarsi* between 2008 and 2013 in the Dutch Wadden Sea.

G Occupancy environment relationships

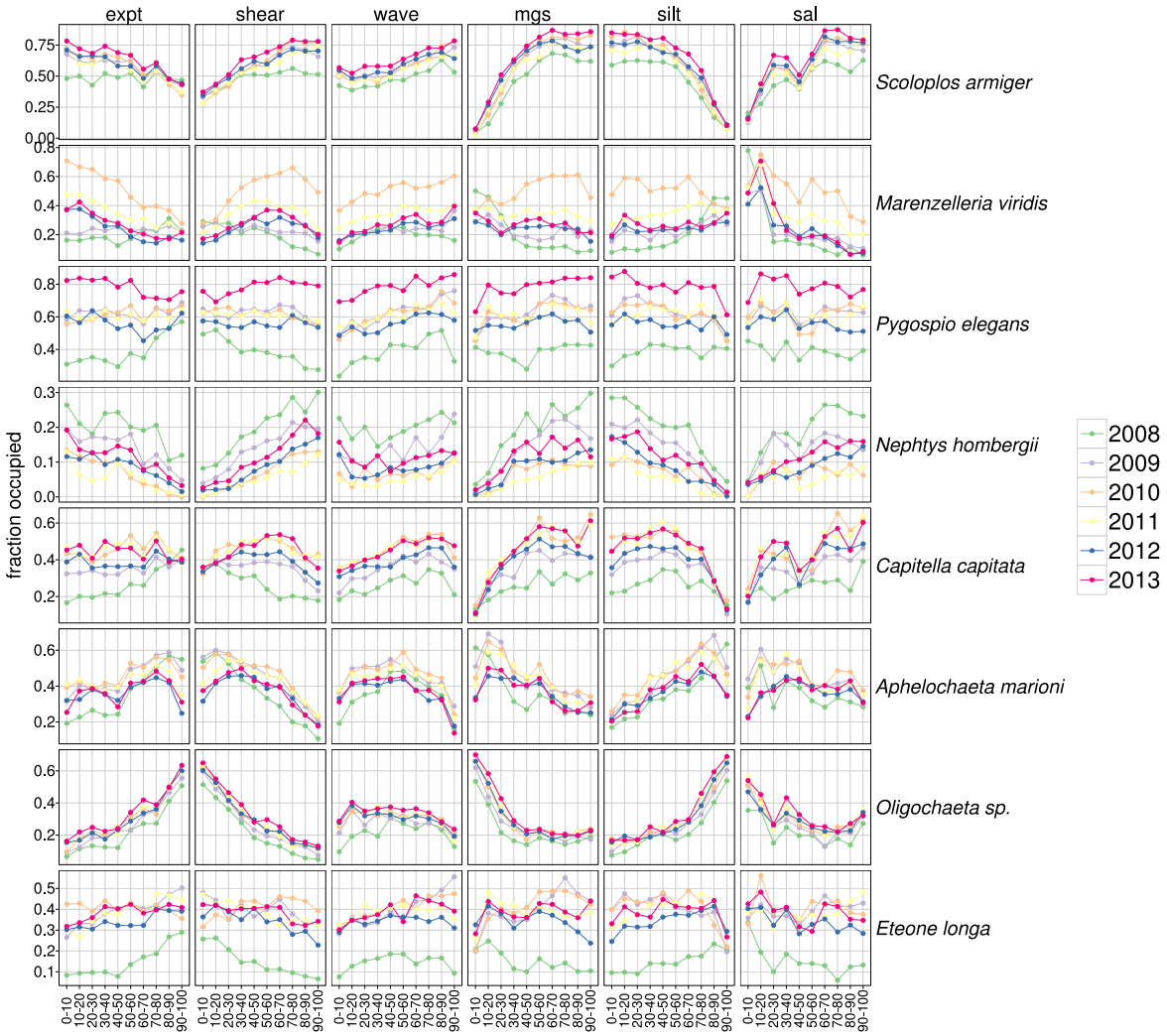

(a) Polychaete species 1-8

Figure 57: Fraction of benthos sampling sites that are occupied by polychaetes and oligochaetes against the 10 deciles of the predictor variables.

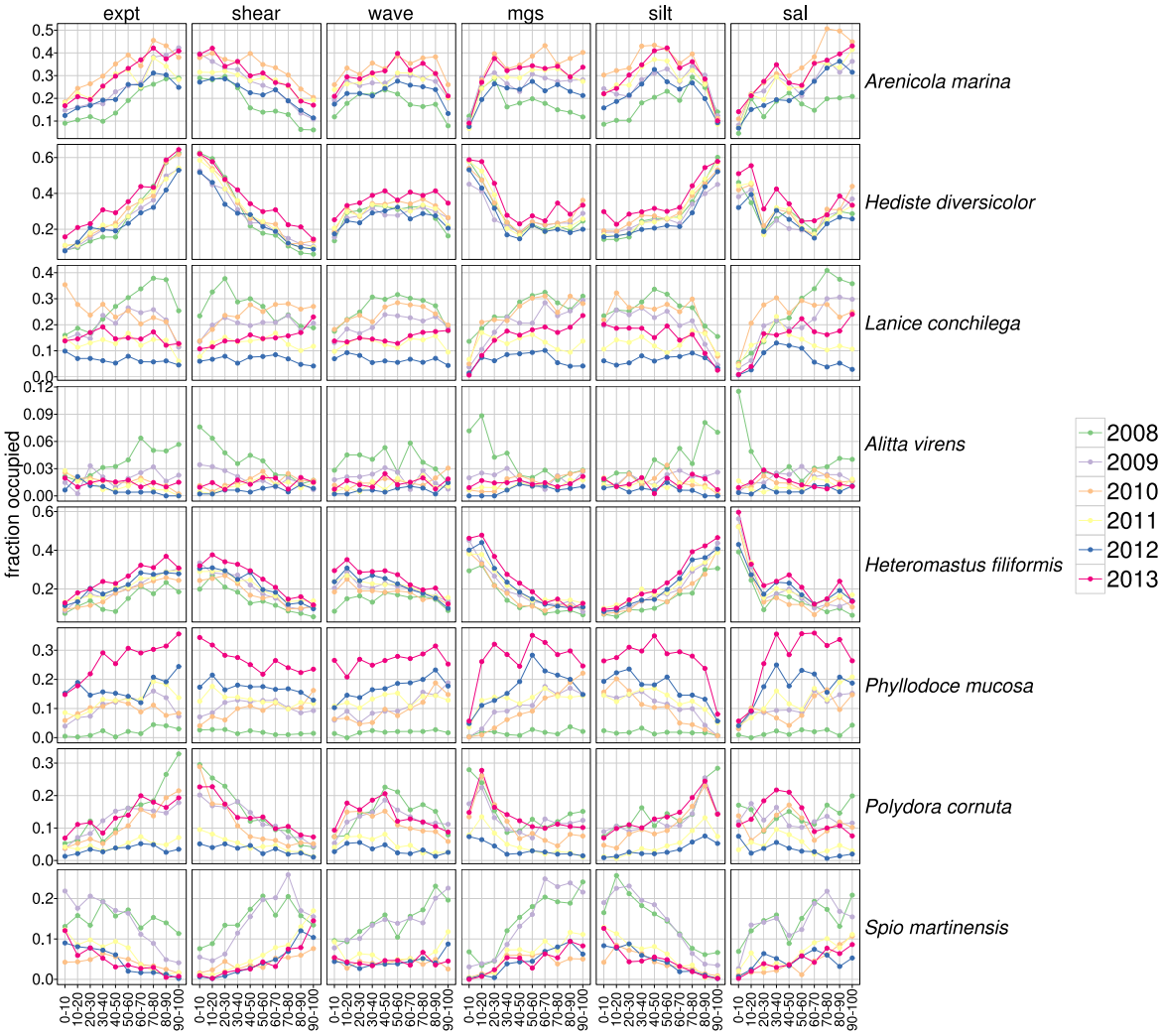

(b) Polychaeta species 9-16

Figure 57: Fraction of benthos sampling sites that are occupied by polychaetes and oligochaetes against the 10 deciles of the predictor variables.

Figure 58: Fraction of benthos sampling sites that are occupied by polychaetes and oligochaetes against the 10 deciles of the predictor variables.

H Species Distribution Models

This appendix presents the outcomes of the SDMs for the 27 benthos species.

H.1 SDM maps and spatial autocorrelation - Molluscs

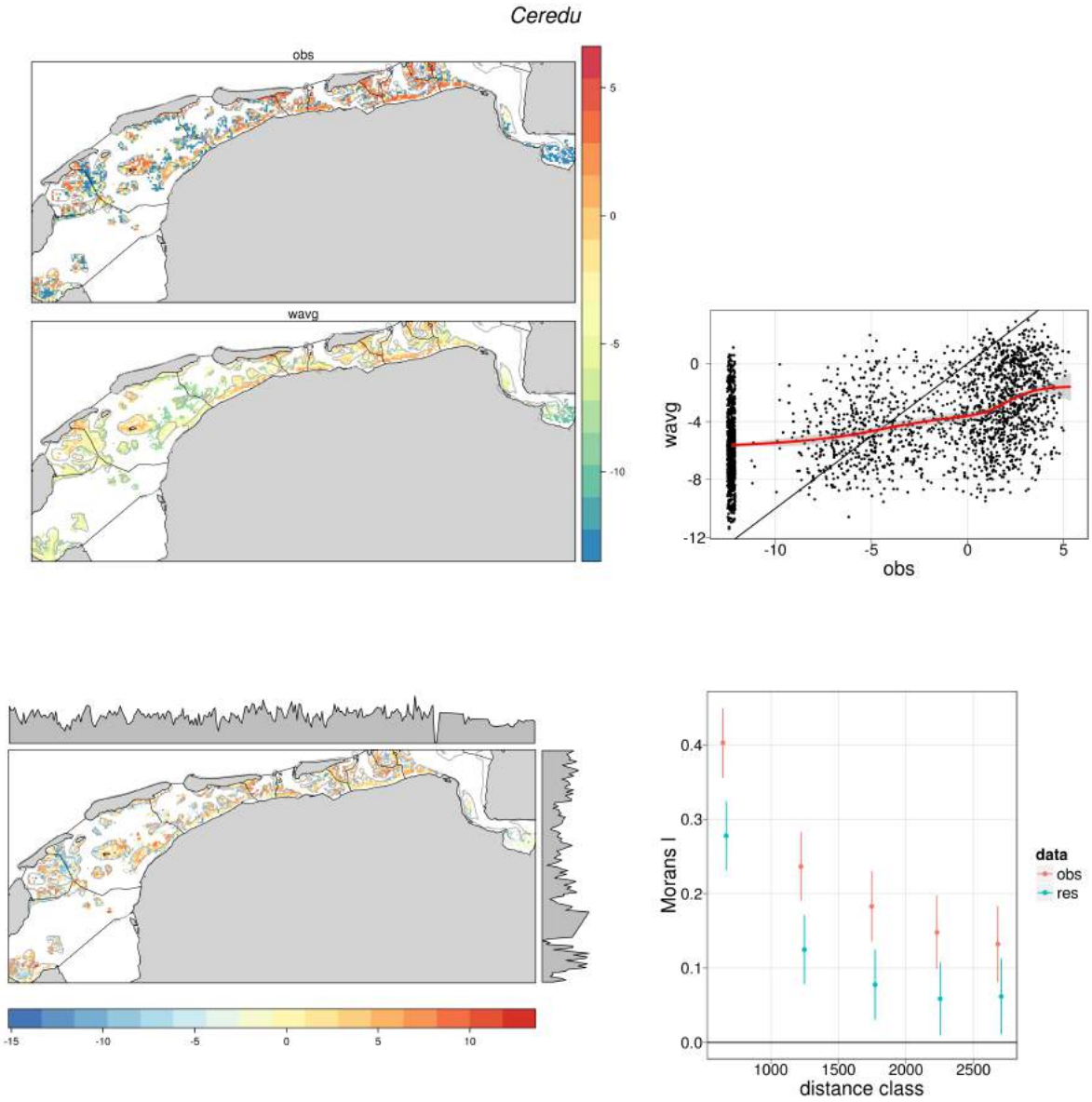

Figure 59: SDM results for biomass distributions of *Cerastoderma edule*. See caption in Figure 11 for further information.

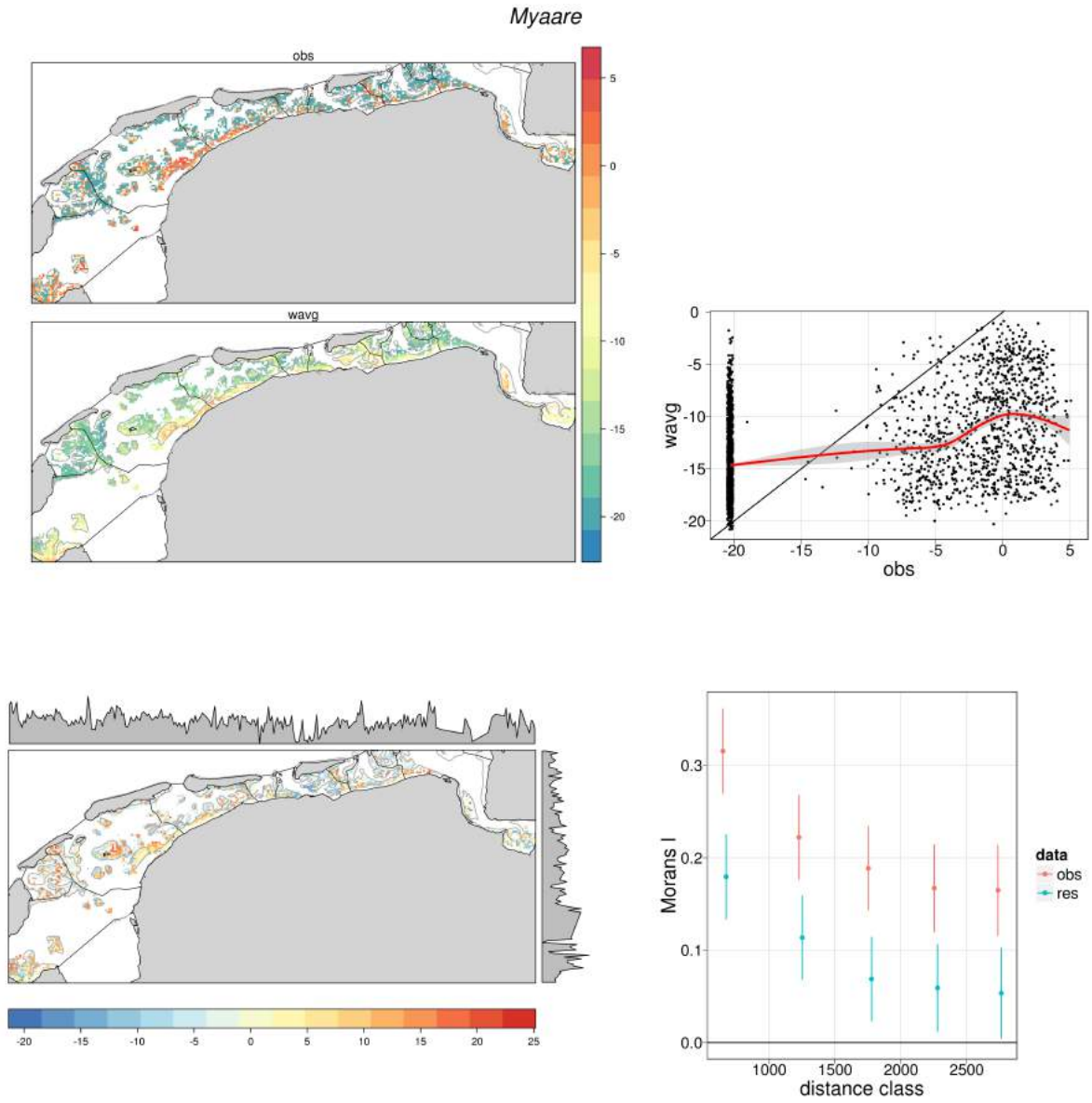

Figure 60: SDM results for biomass distributions of *Mya arenaria*. See caption in Figure 11 for further information.

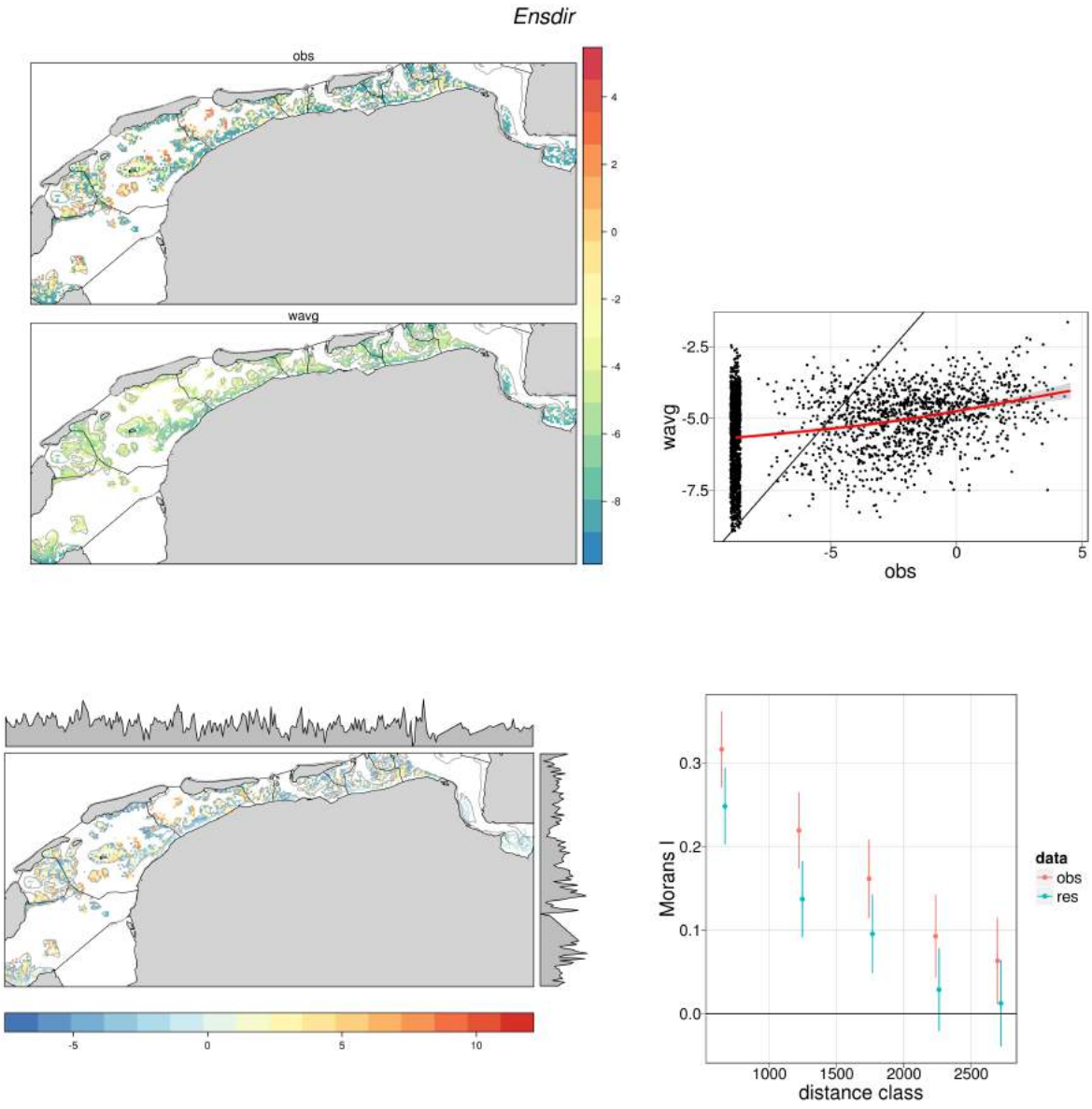

Figure 61: SDM results for biomass distributions of *Ensis leei*. See caption in Figure 11 for further information.

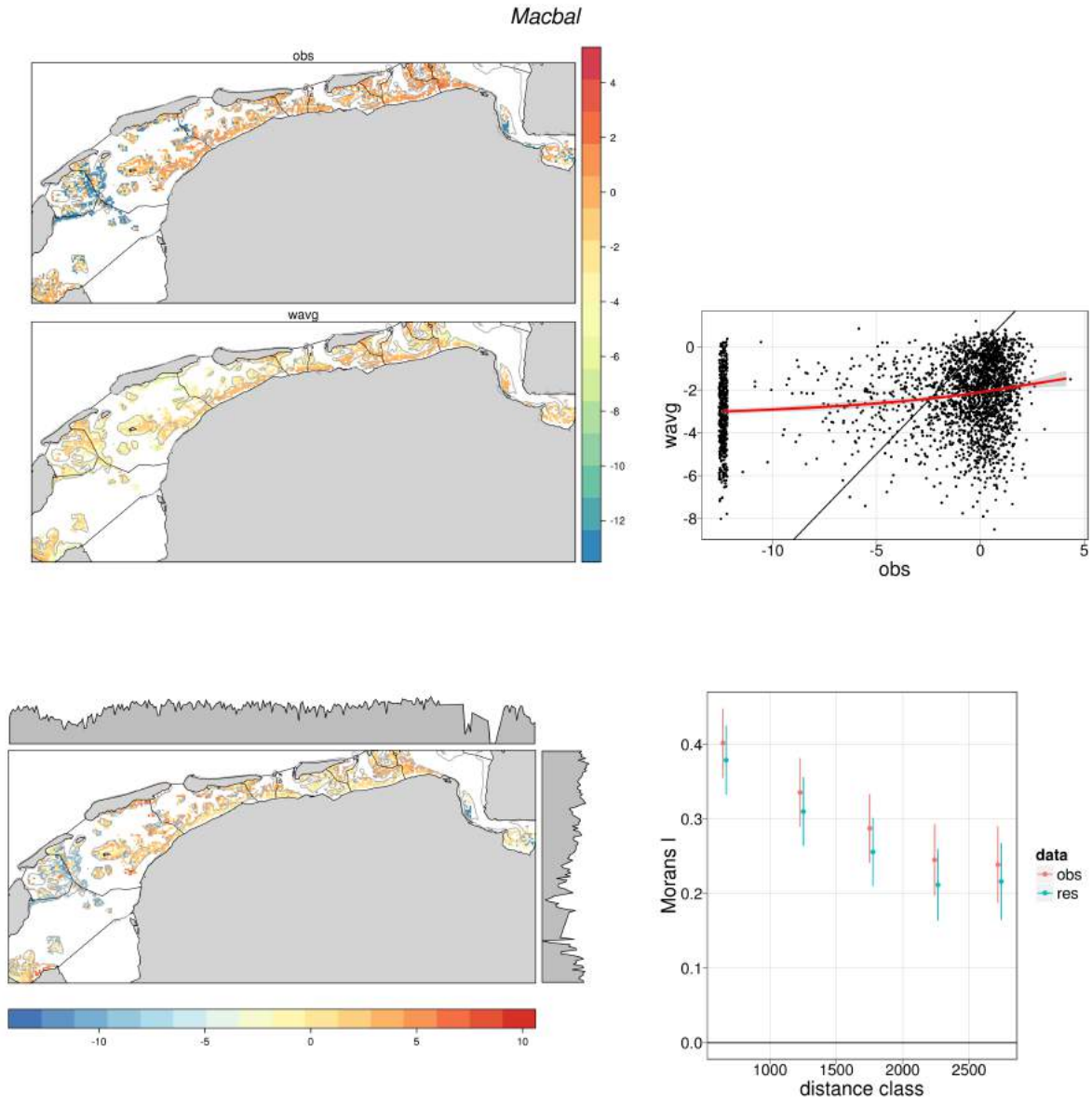

Figure 62: SDM results for biomass distributions of *Limecola balthica*. See caption in Figure 11 for further information.

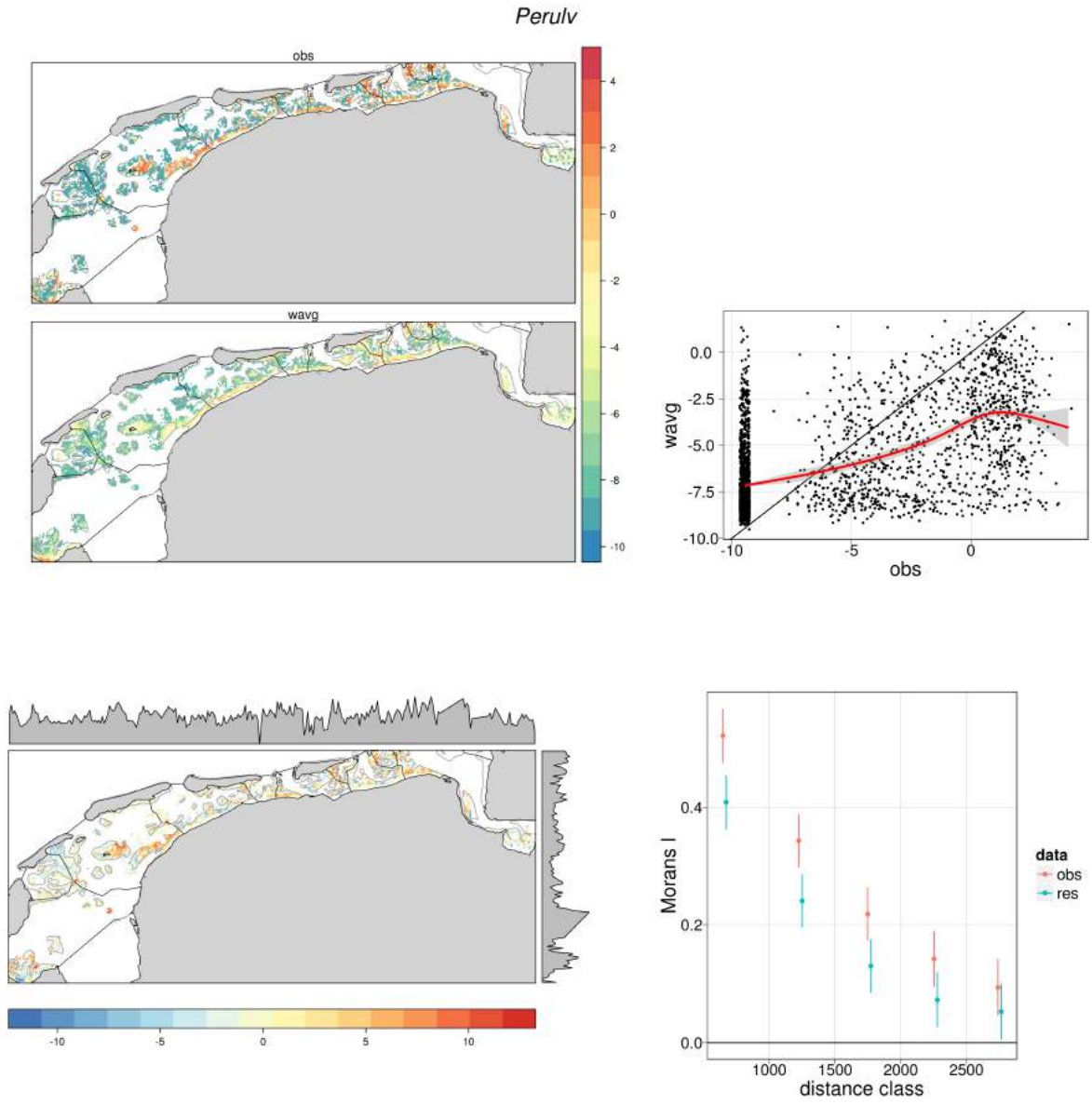

Figure 63: SDM results for biomass distributions of *Peringia ulvae*. See caption in Figure 11 for further information.

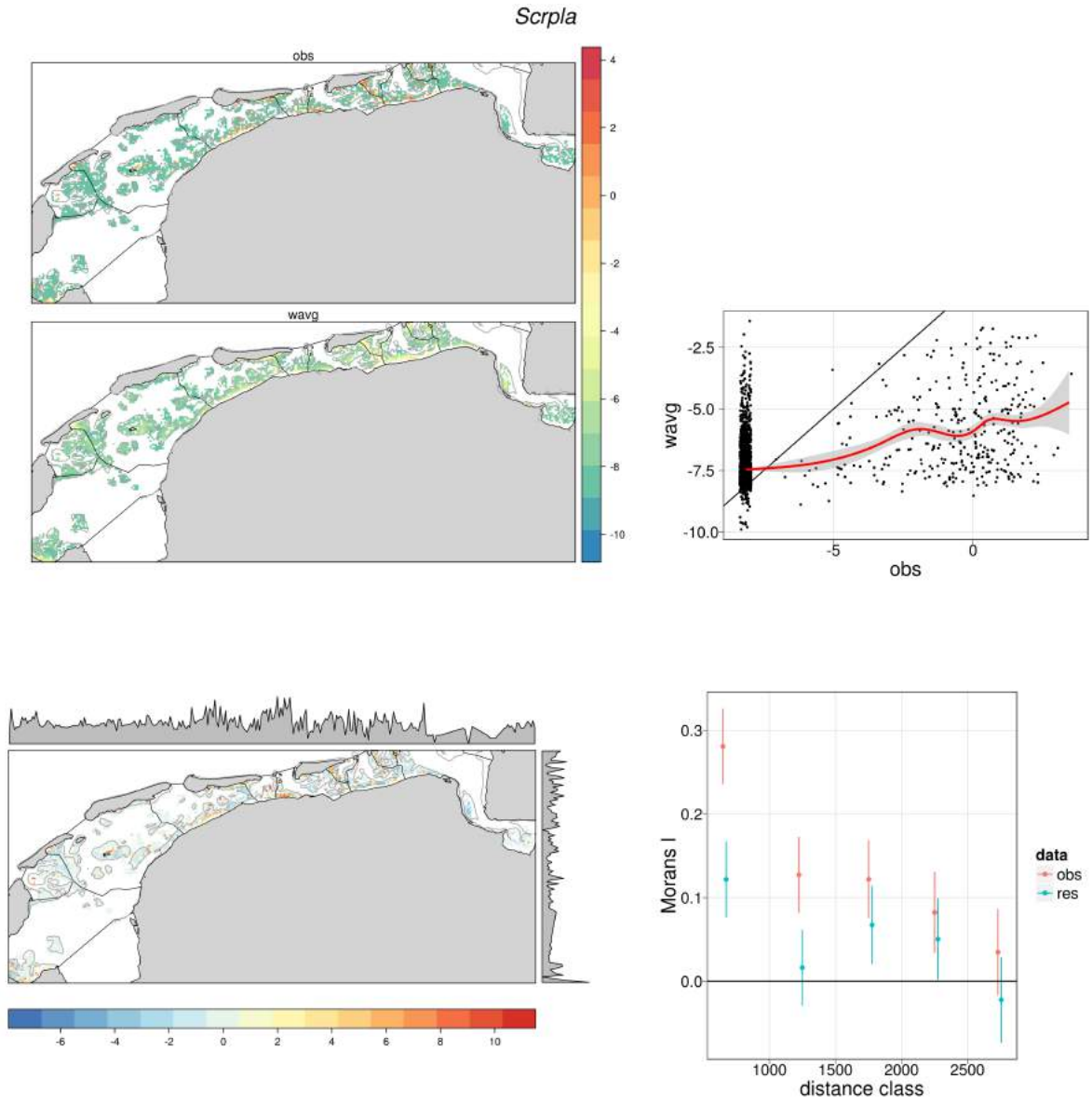

Figure 64: SDM results for biomass distributions of *Scrobicularia plana*. See caption in Figure 11 for further information.

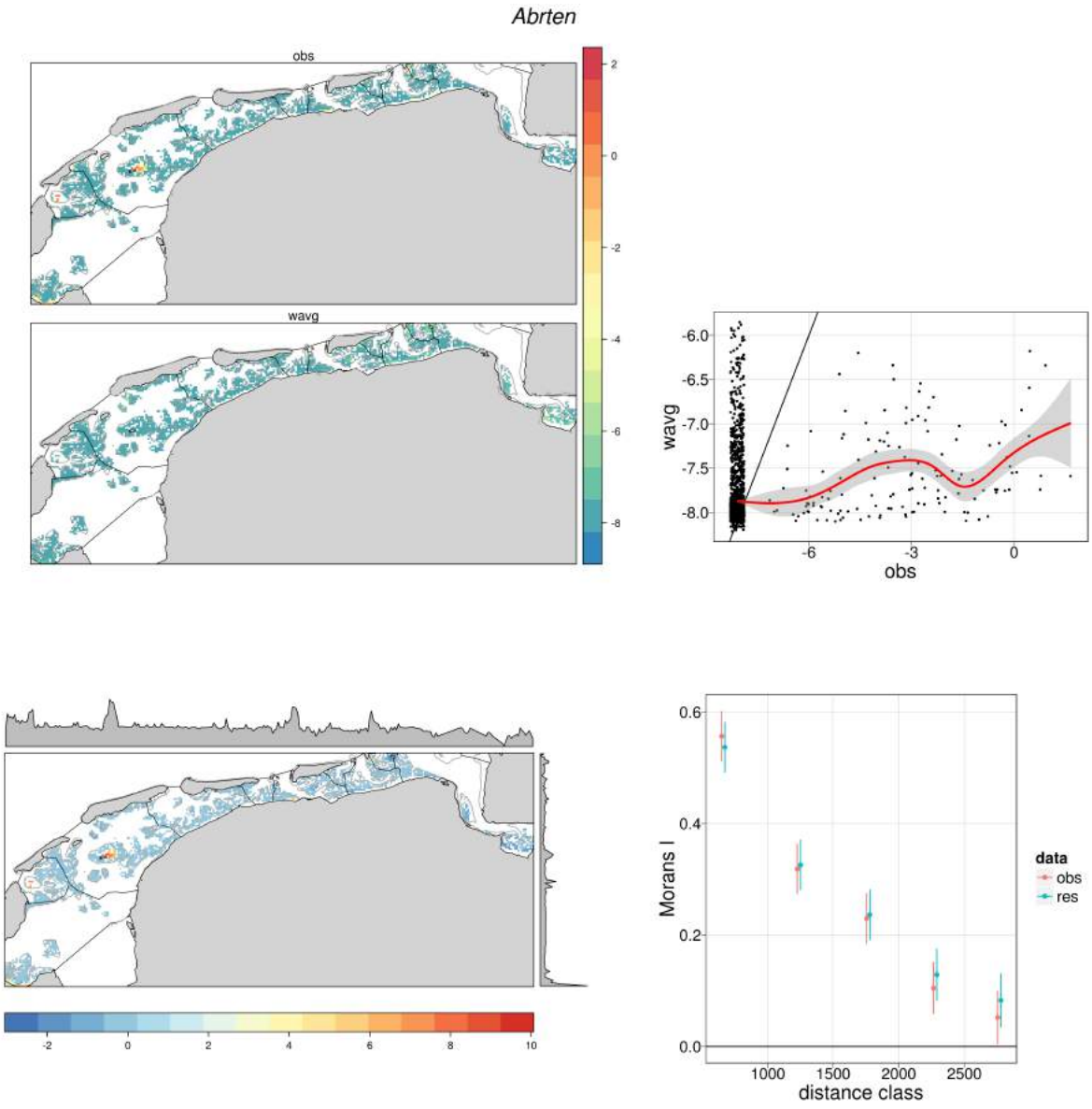

Figure 65: SDM results for biomass distributions of *Abra tenuis*. See caption in Figure 11 for further information.

H.2 SDM maps and spatial autocorrelation - Polychaetes

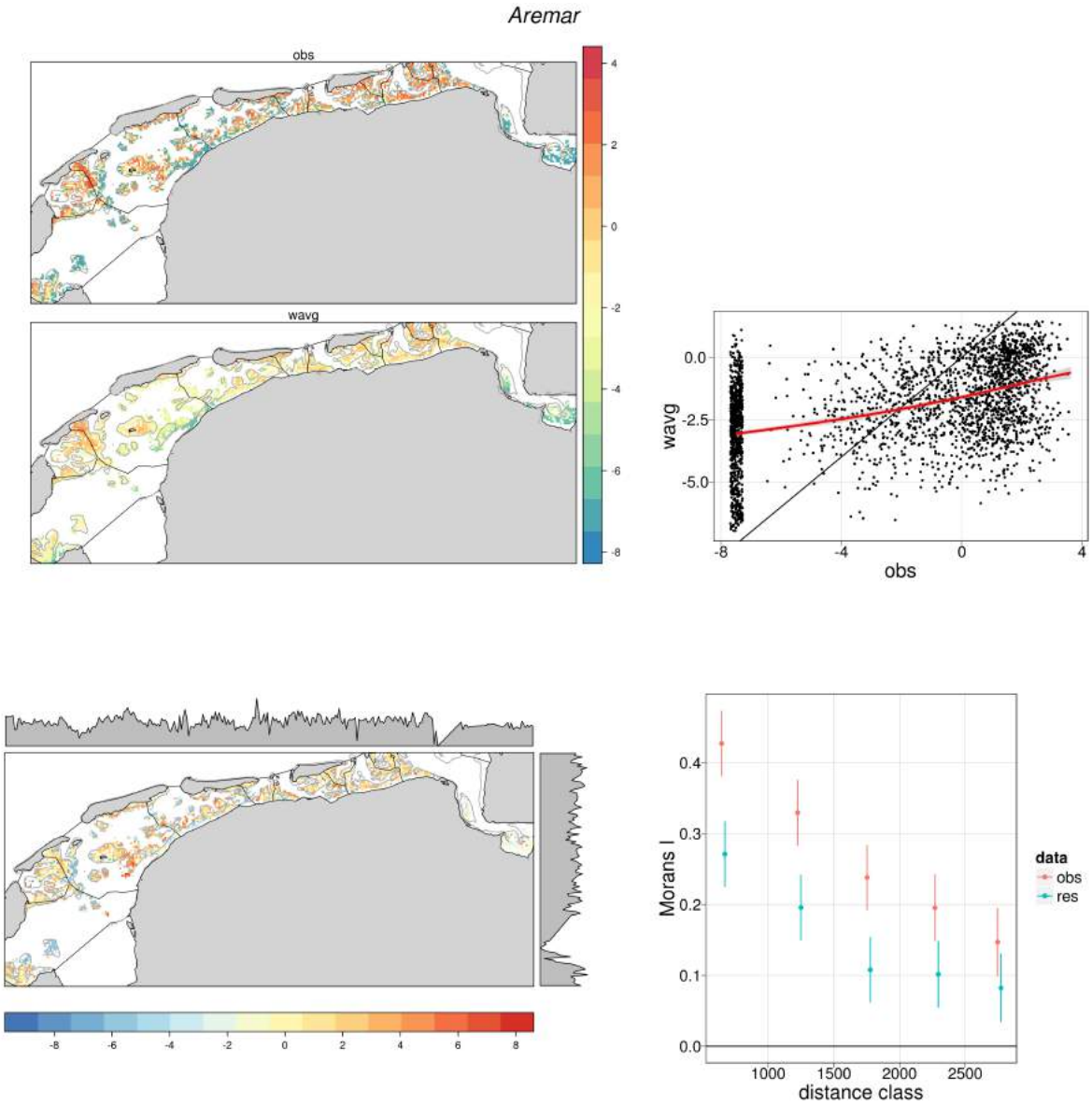

Figure 66: SDM results for biomass distributions of *Arenicola marina*. See caption in Figure 11 for further information.

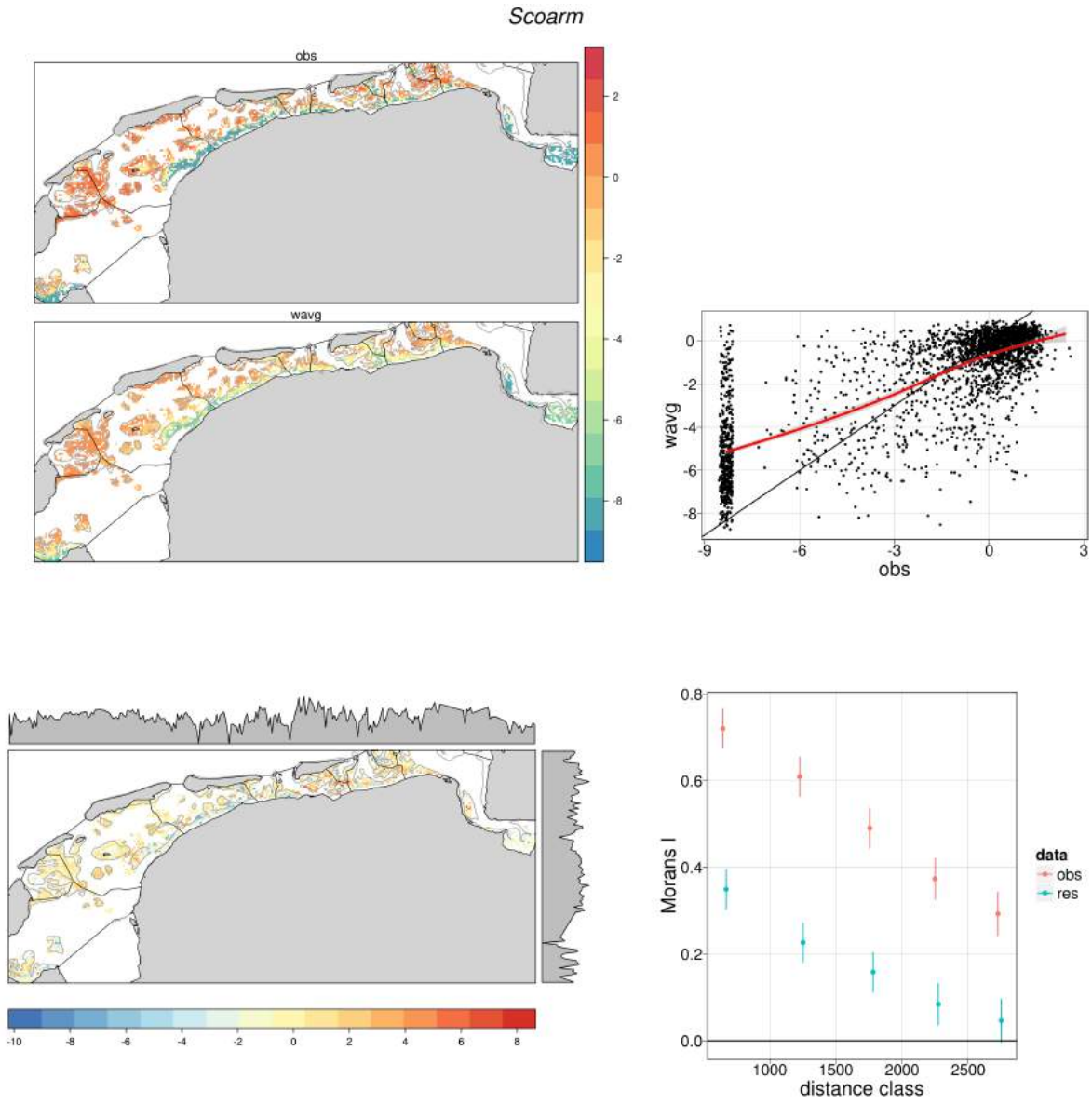

Figure 67: SDM results for biomass distributions of *Scoloplos armiger*. See caption in Figure 11 for further information.

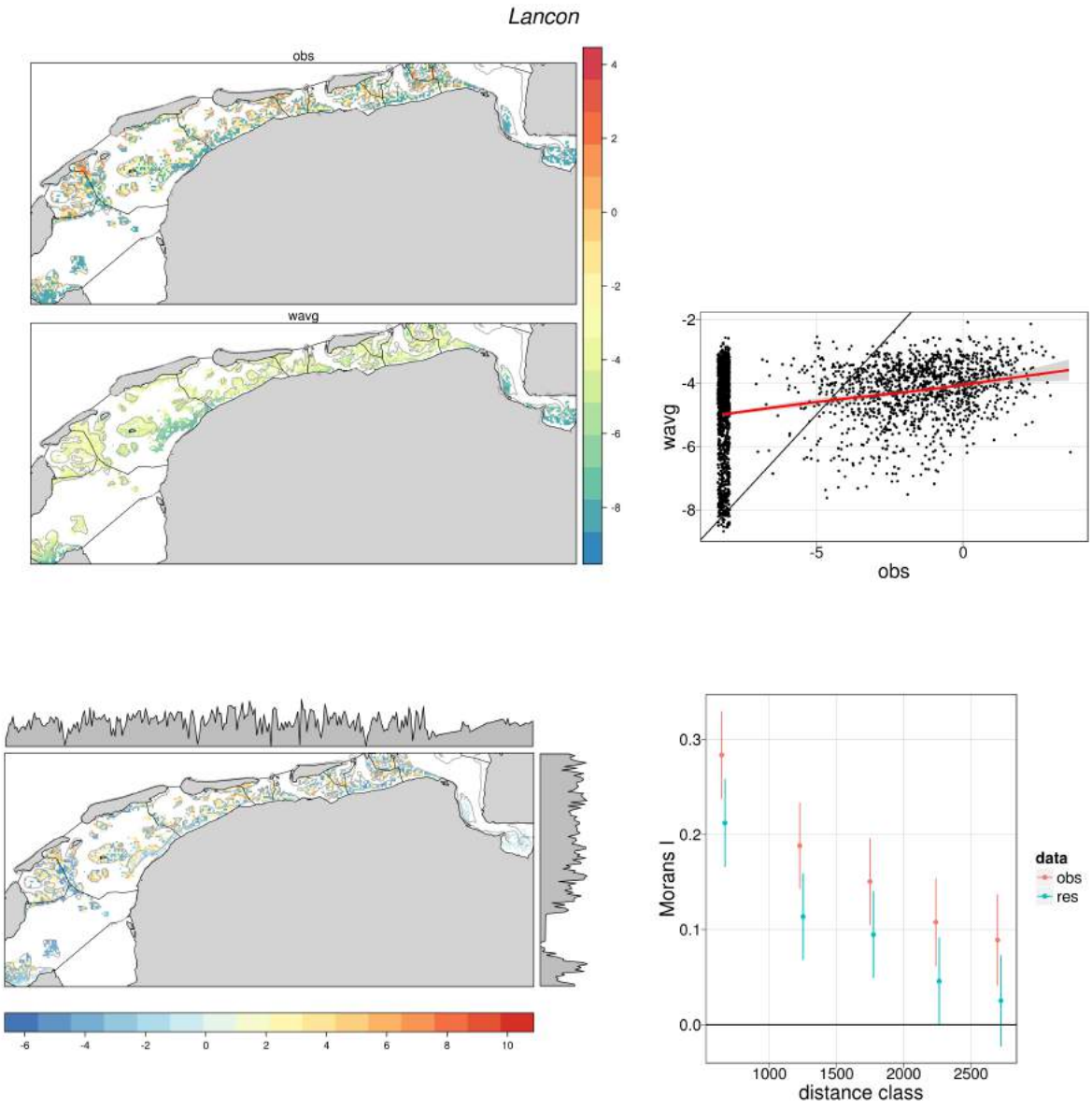

Figure 68: SDM results for biomass distributions of *Lanice conchilega*. See caption in Figure 11 for further information.

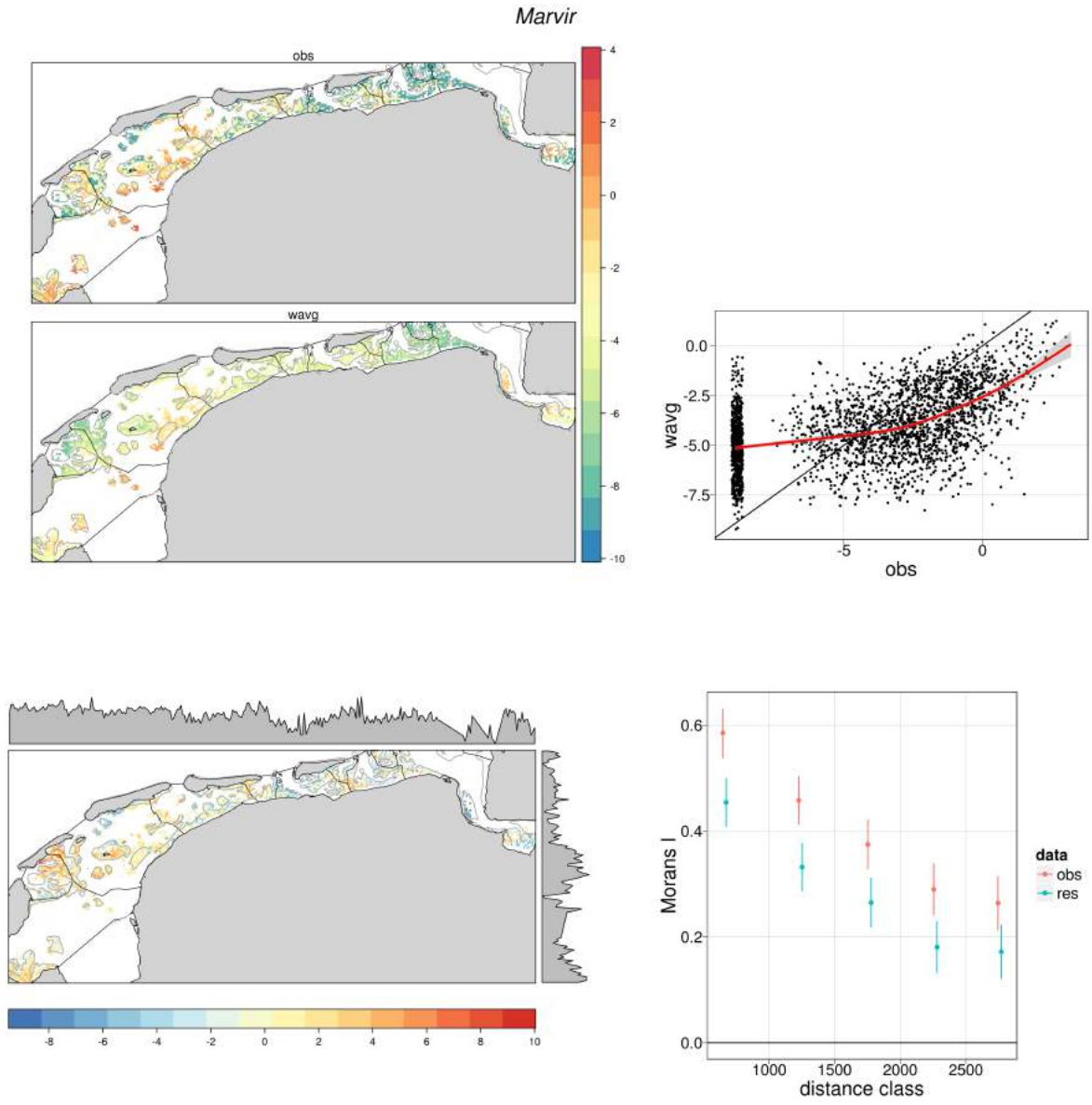

Figure 69: SDM results for biomass distributions of *Marenzelleria viridis*. See caption in Figure 11 for further information.

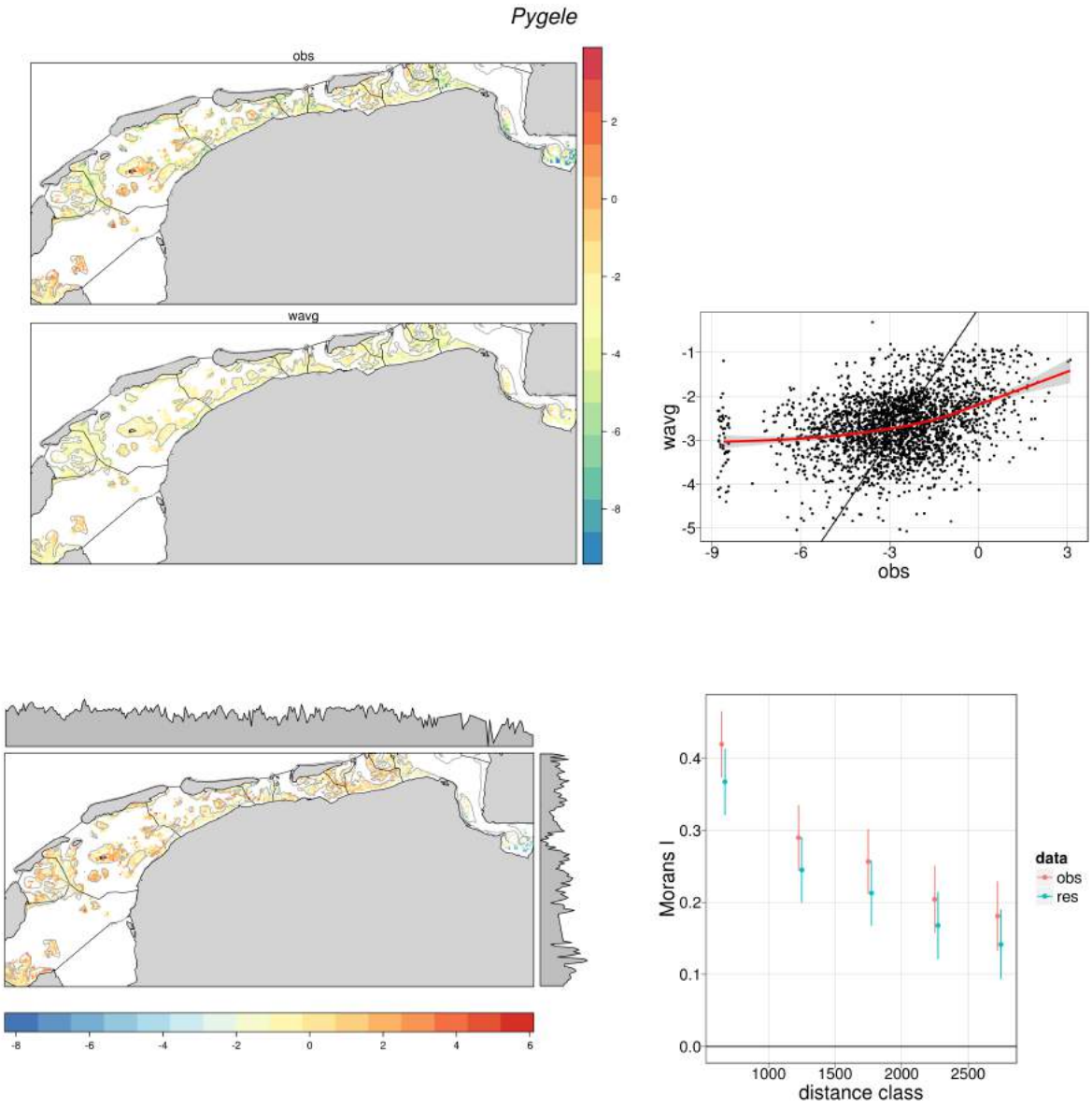

Figure 70: SDM results for biomass distributions of *Pygospio elegans*. See caption in Figure 11 for further information.

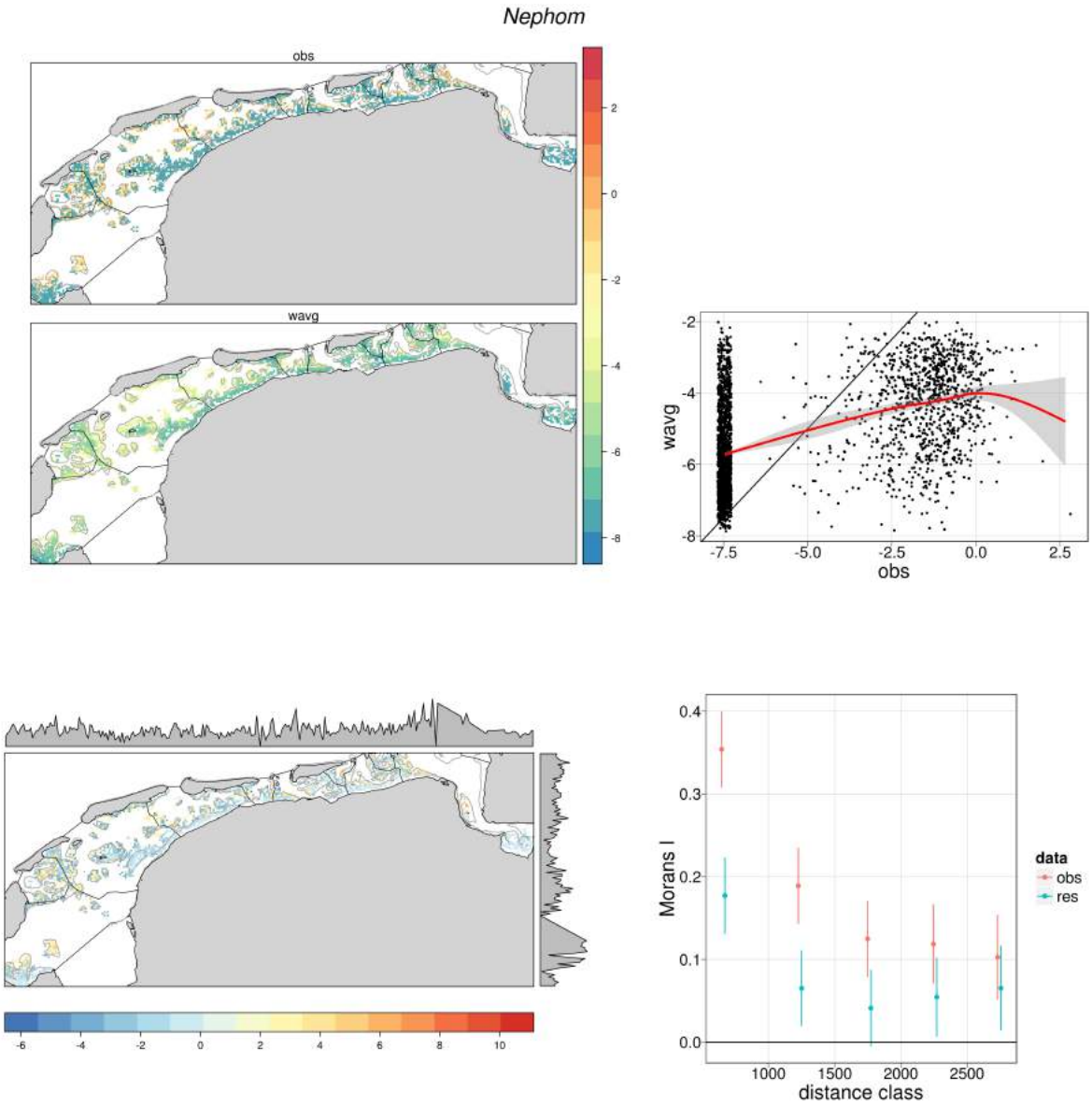

Figure 71: SDM results for biomass distributions of *Nephthys hombergii*. See caption in Figure 11 for further information.

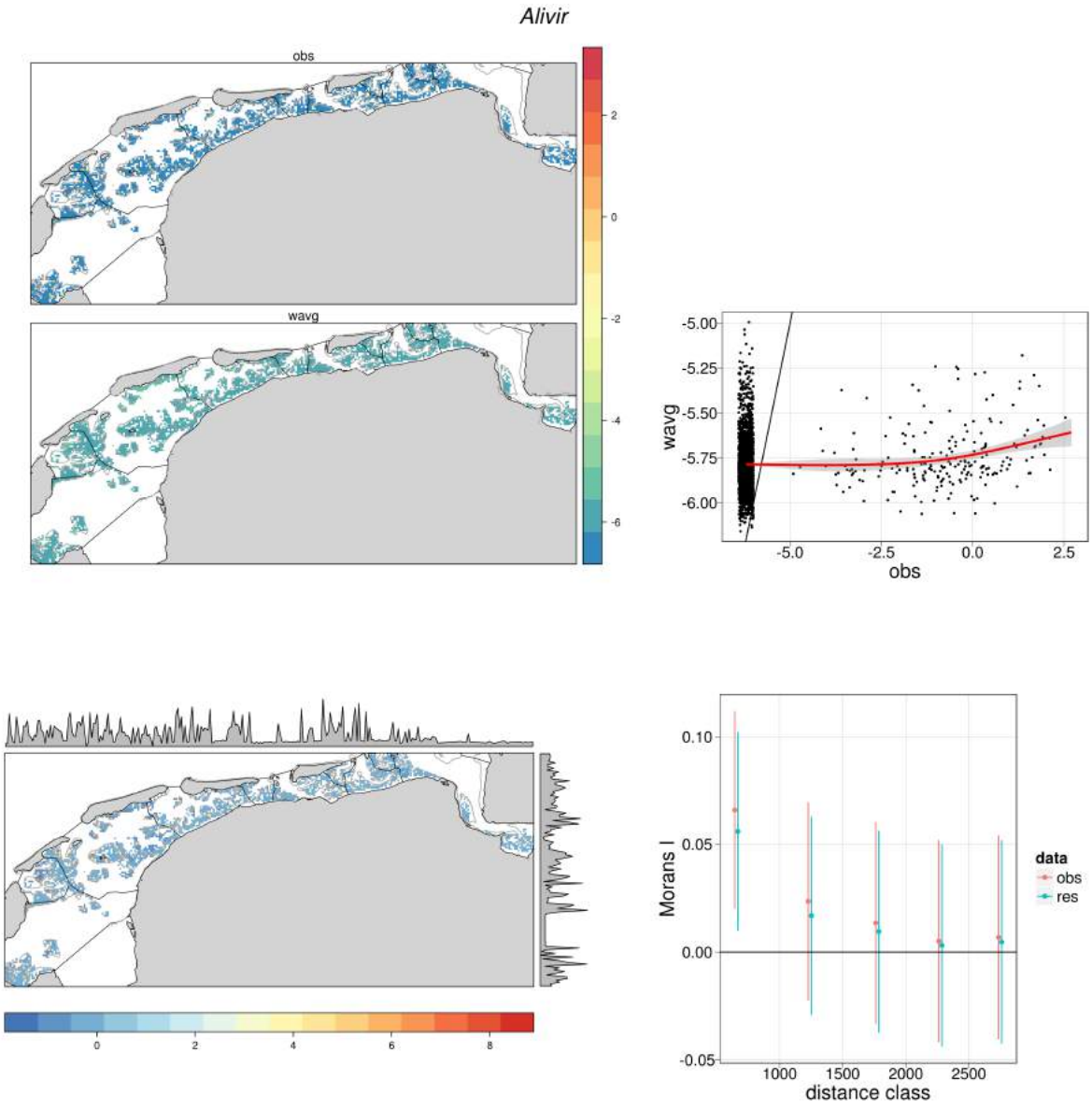

Figure 72: SDM results for biomass distributions of *Alitta virens*. See caption in Figure 11 for further information.

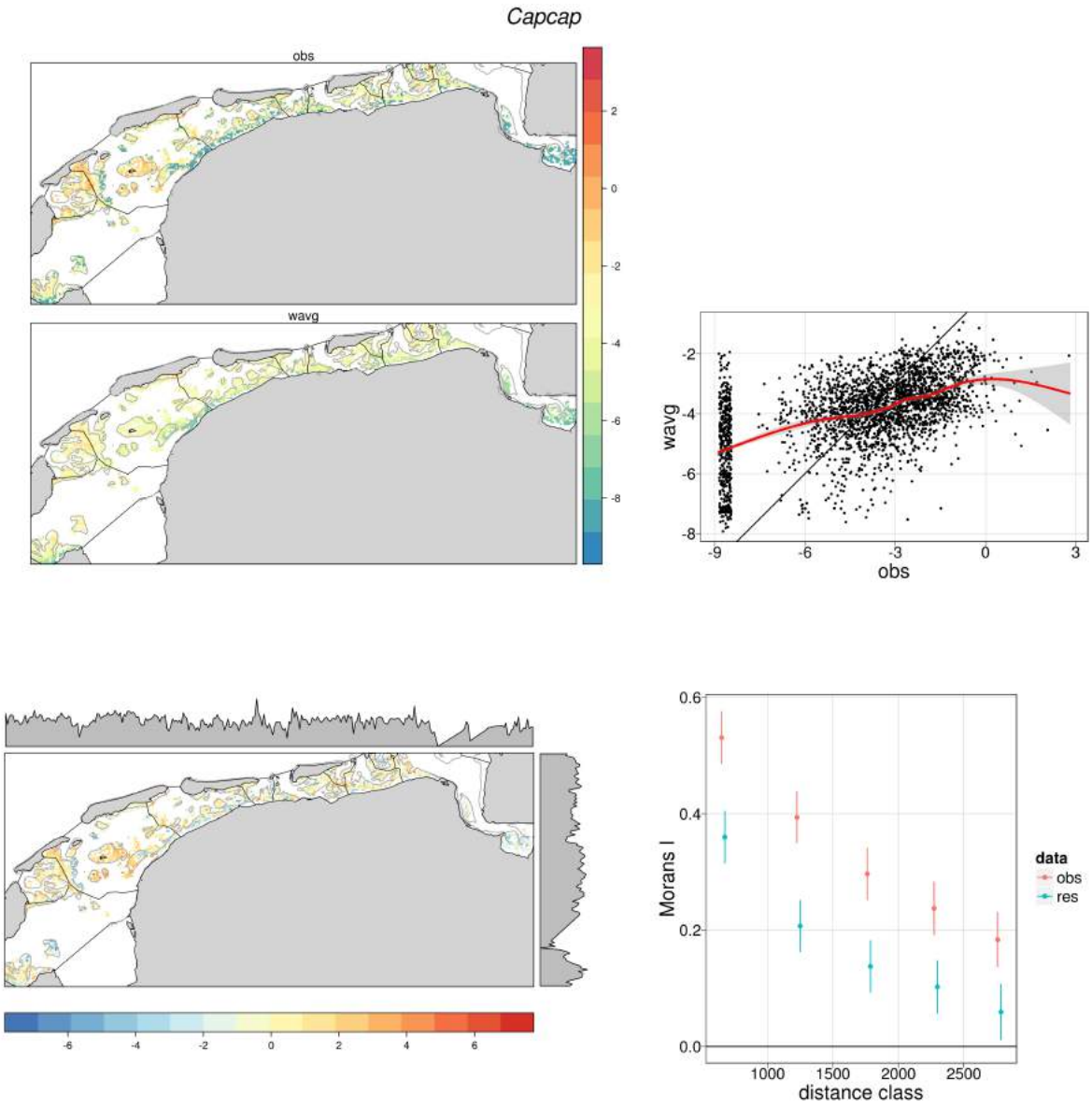

Figure 73: SDM results for biomass distributions of *Capitella capitata*. See caption in Figure 11 for further information.

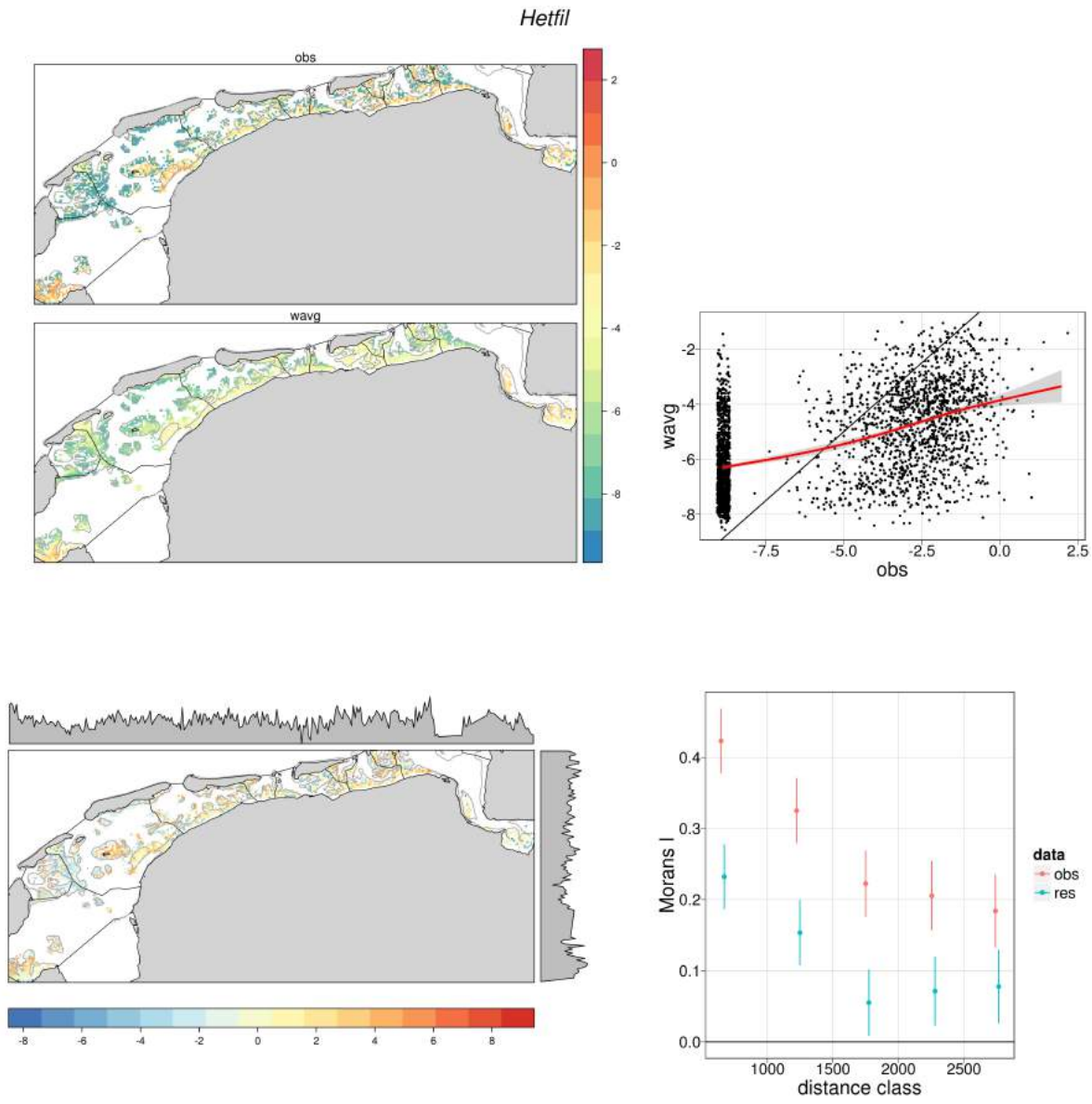

Figure 74: SDM results for biomass distributions of *Heteromastus filiformis*. See caption in Figure 11 for further information.

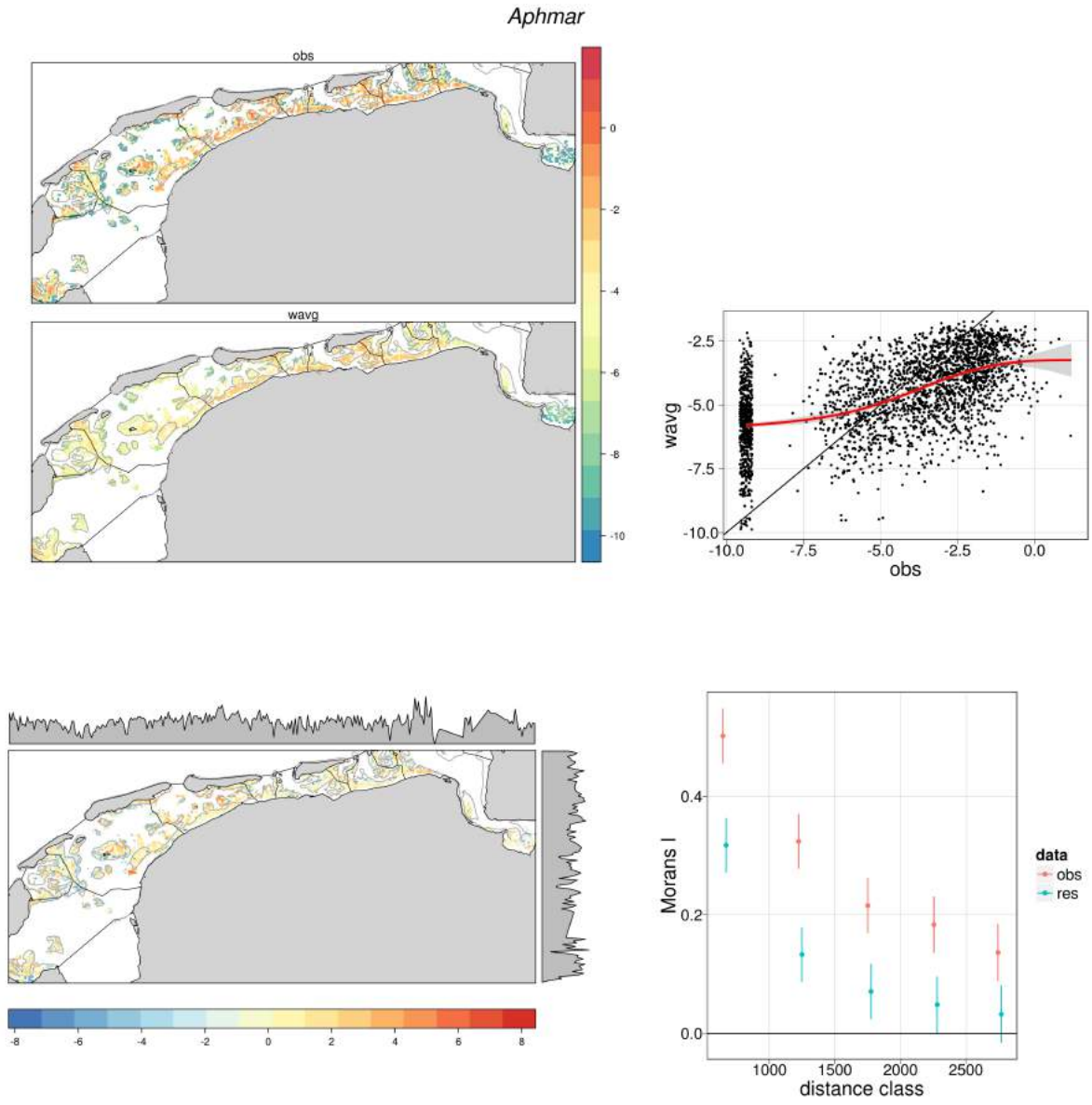

Figure 75: SDM results for biomass distributions of *Aphelochaeta marioni*. See caption in Figure 11 for further information.

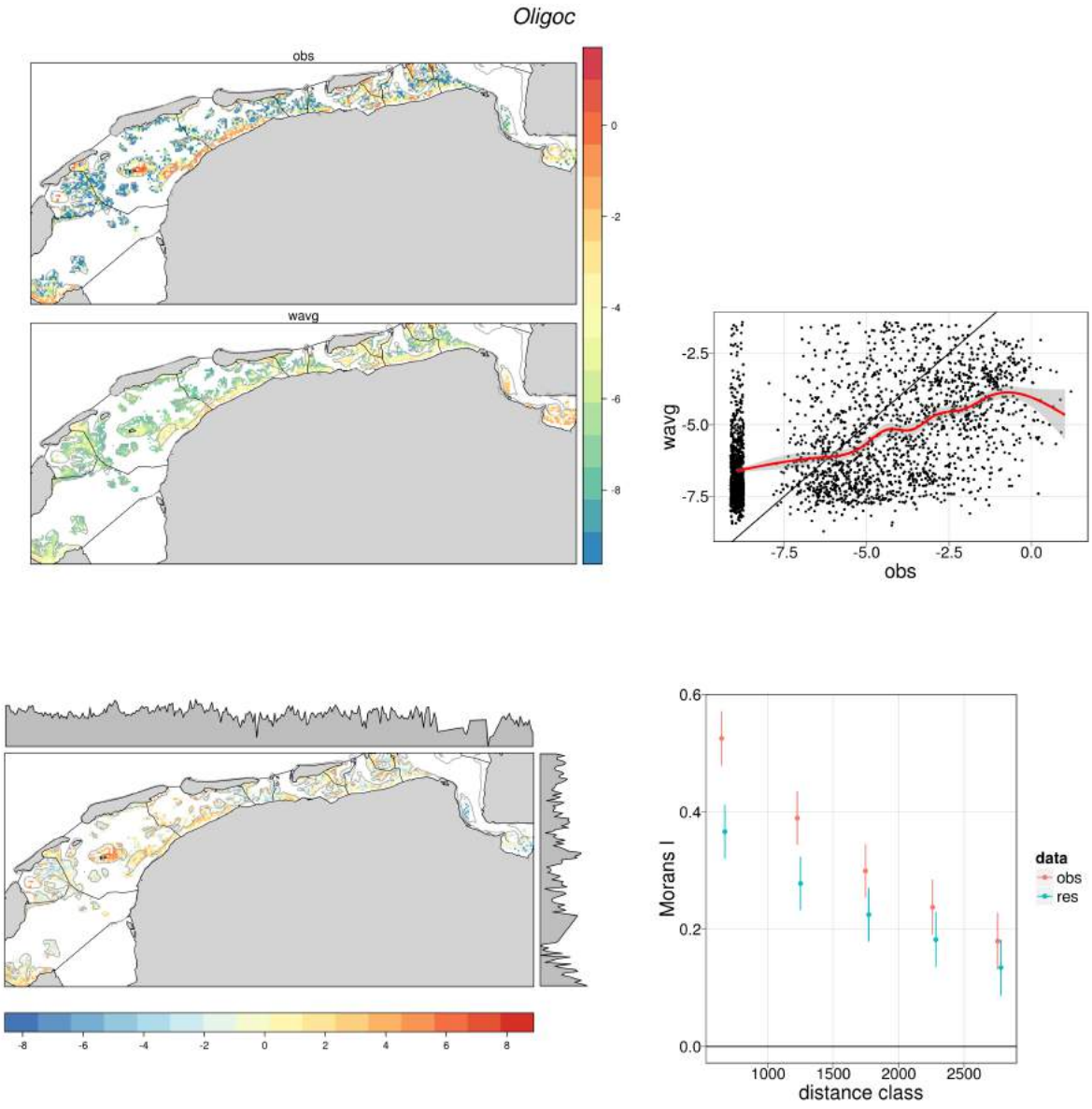

Figure 76: SDM results for biomass distributions of *Oligochaeta sp.*. See caption in Figure 11 for further information.

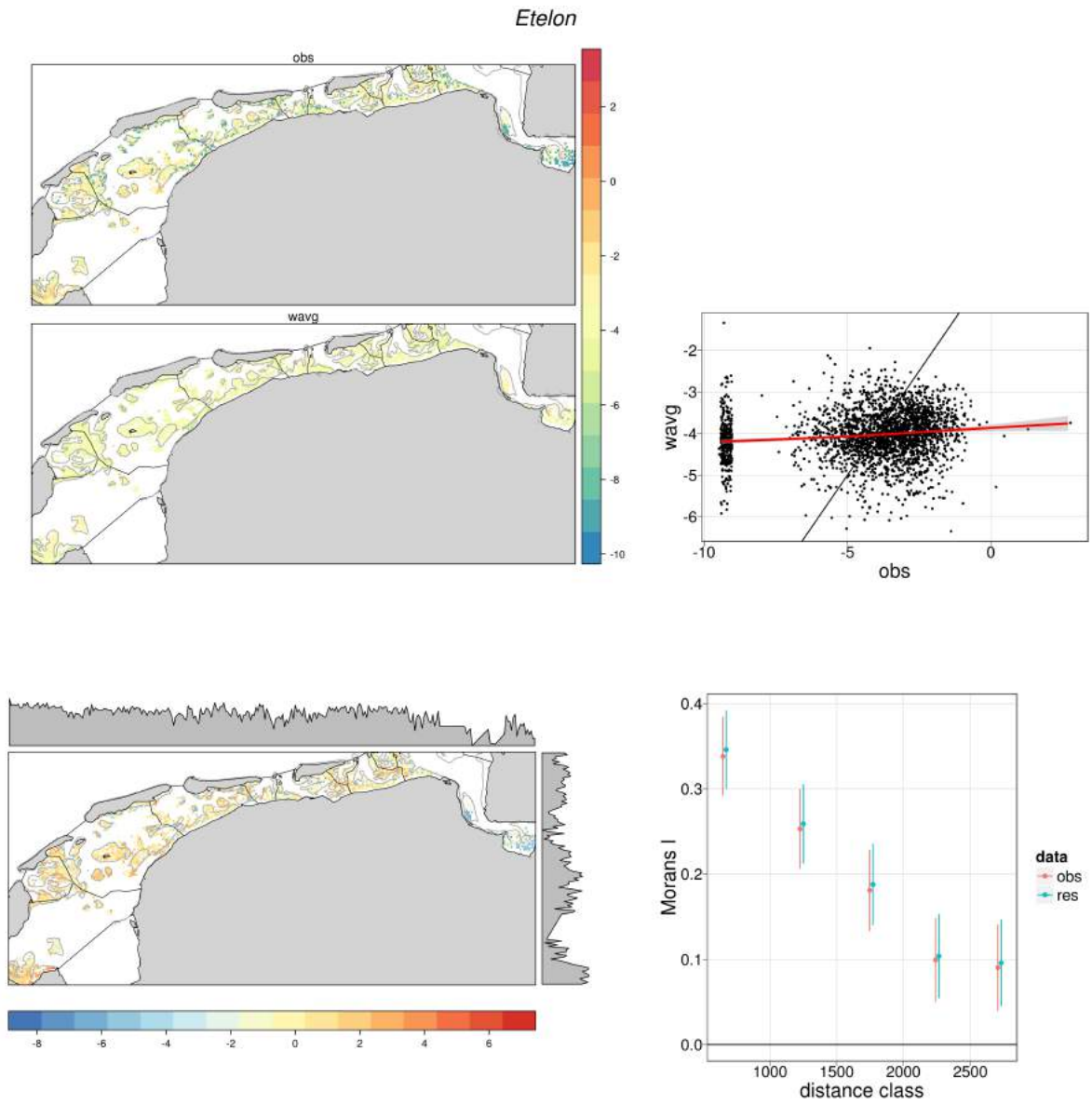

Figure 77: SDM results for biomass distributions of *Eteone longa*. See caption in Figure 11 for further information.

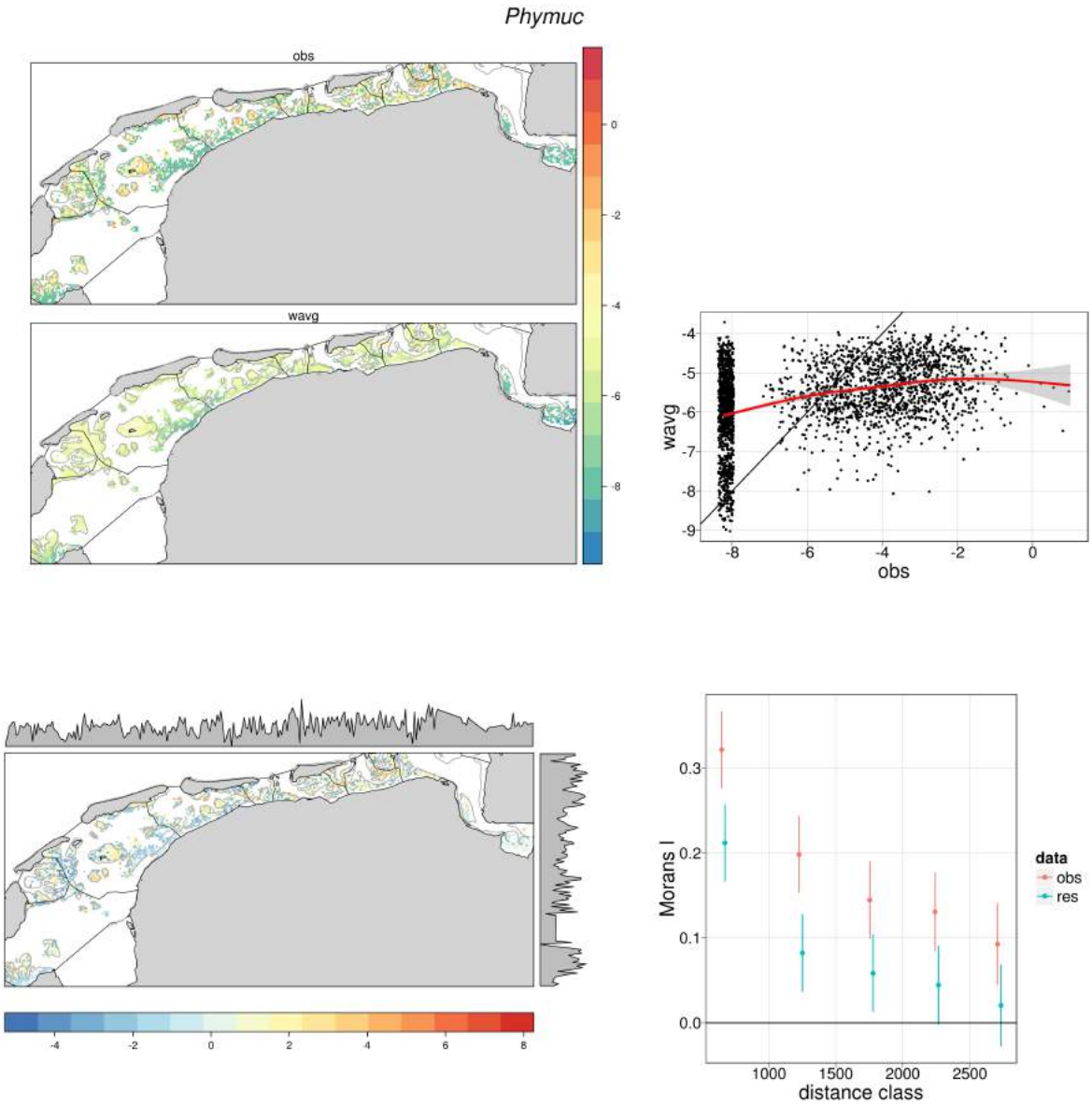

Figure 78: SDM results for biomass distributions of *Phylodoce mucosa*. See caption in Figure 11 for further information.

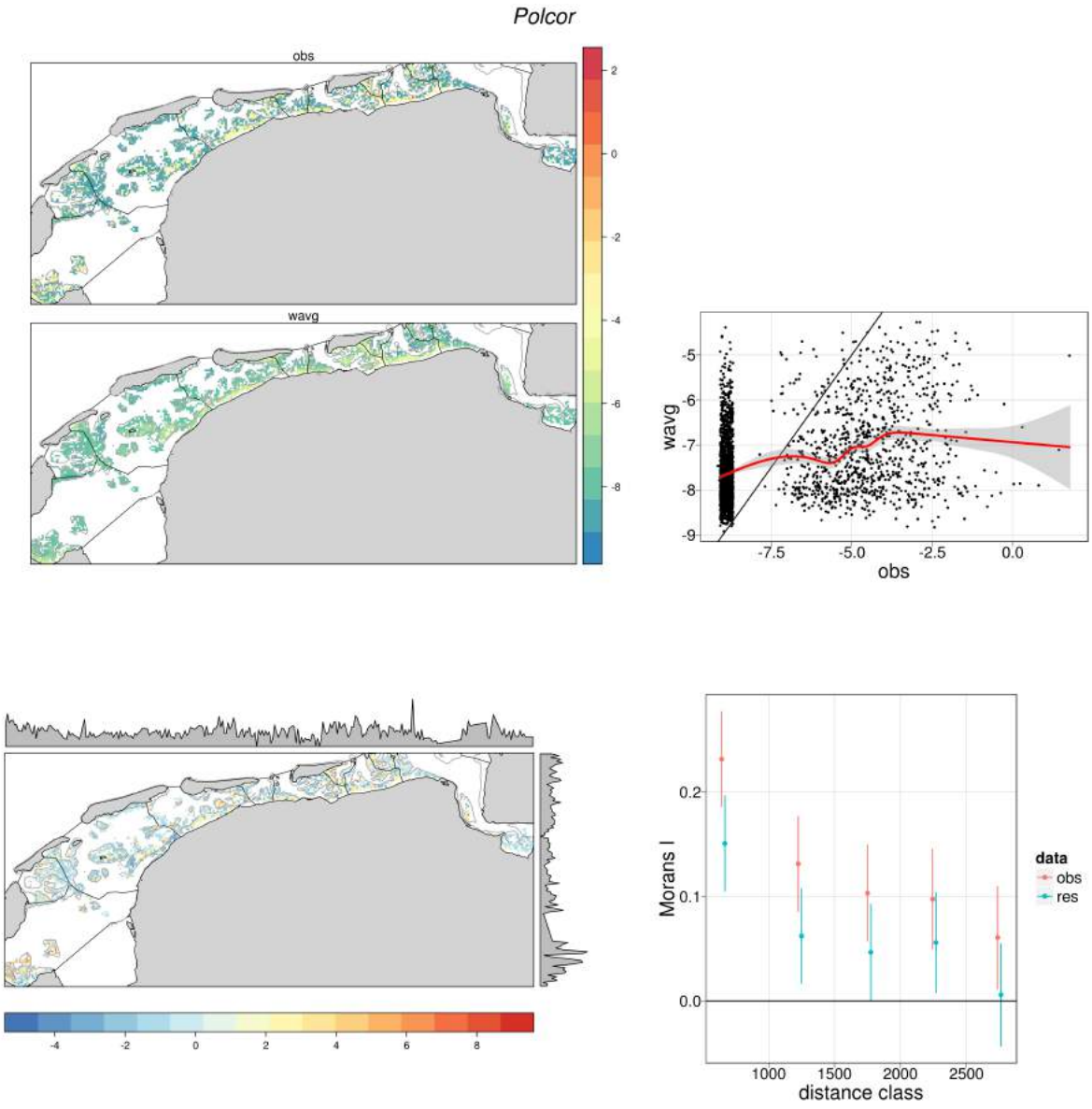

Figure 79: SDM results for biomass distributions of *Polydora cornuta*. See caption in Figure 11 for further information.

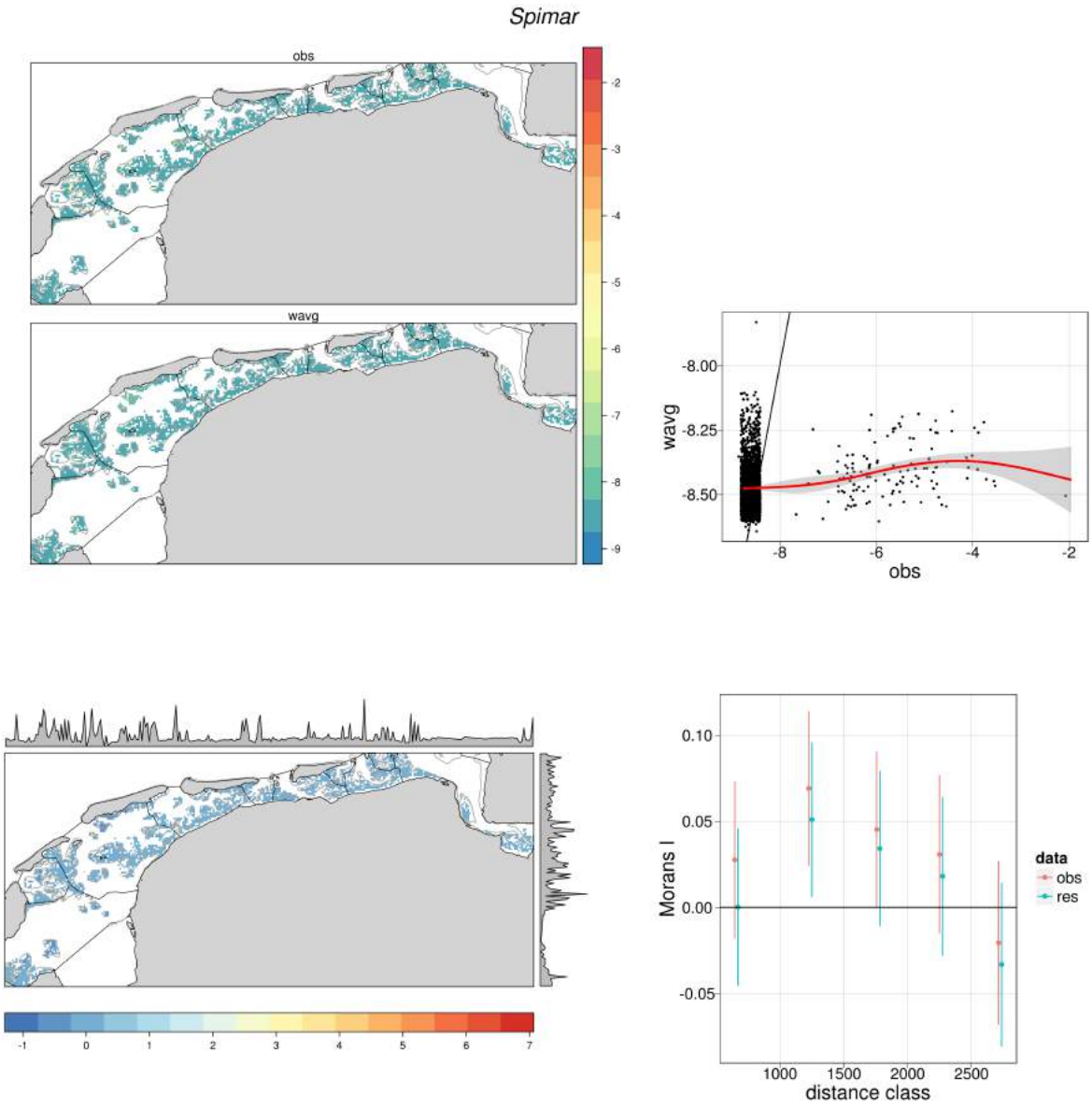

Figure 80: SDM results for biomass distributions of *Spio martinensis*. See caption in Figure 11 for further information.

H.3 SDM maps and spatial autocorrelation - Crustaceans

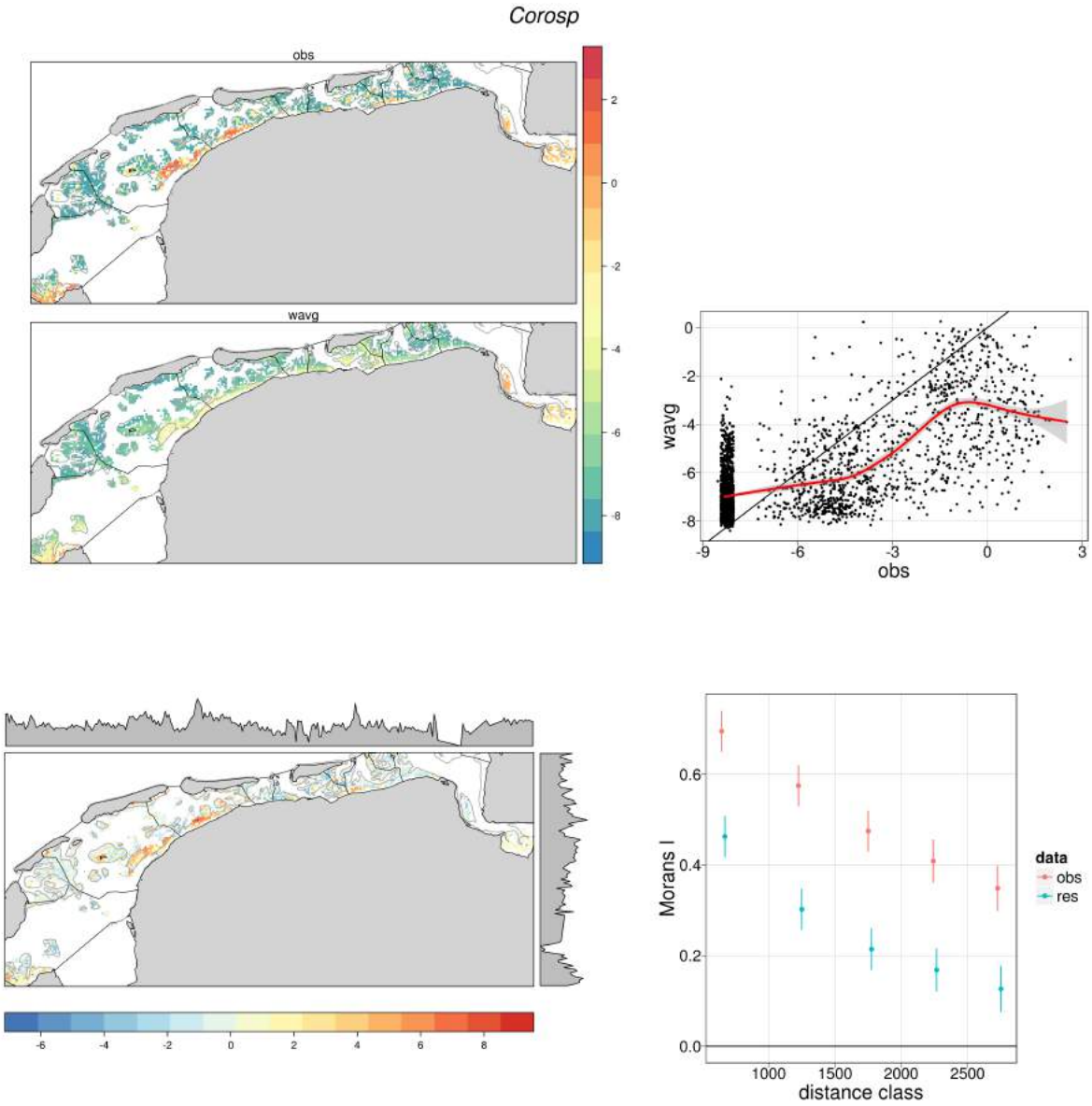

Figure 81: SDM results for biomass distributions of *Corophium sp.*. See caption in Figure 11 for further information.

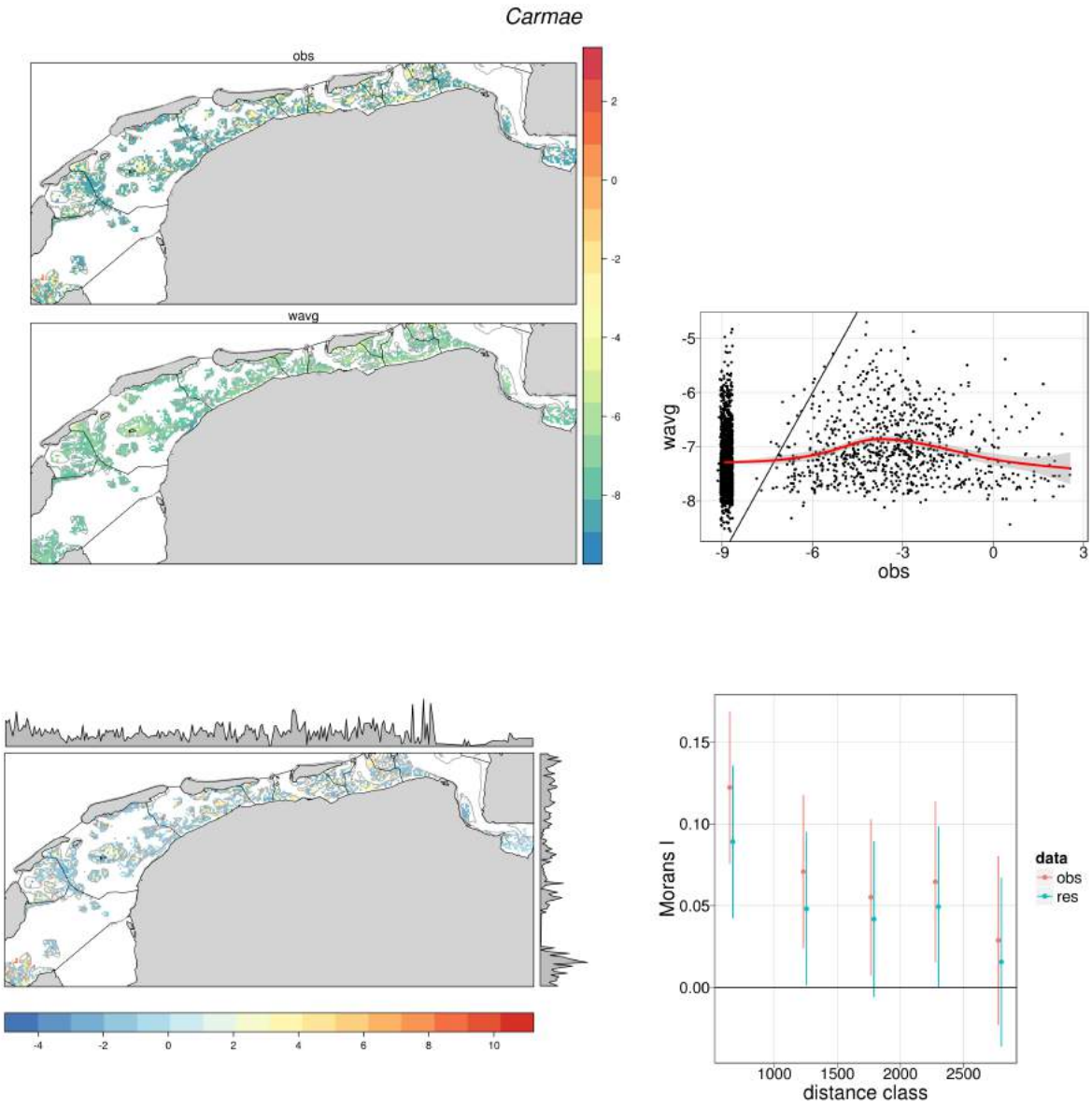

Figure 82: SDM results for biomass distributions of *Carcinus maenas*. See caption in Figure 11 for further information.

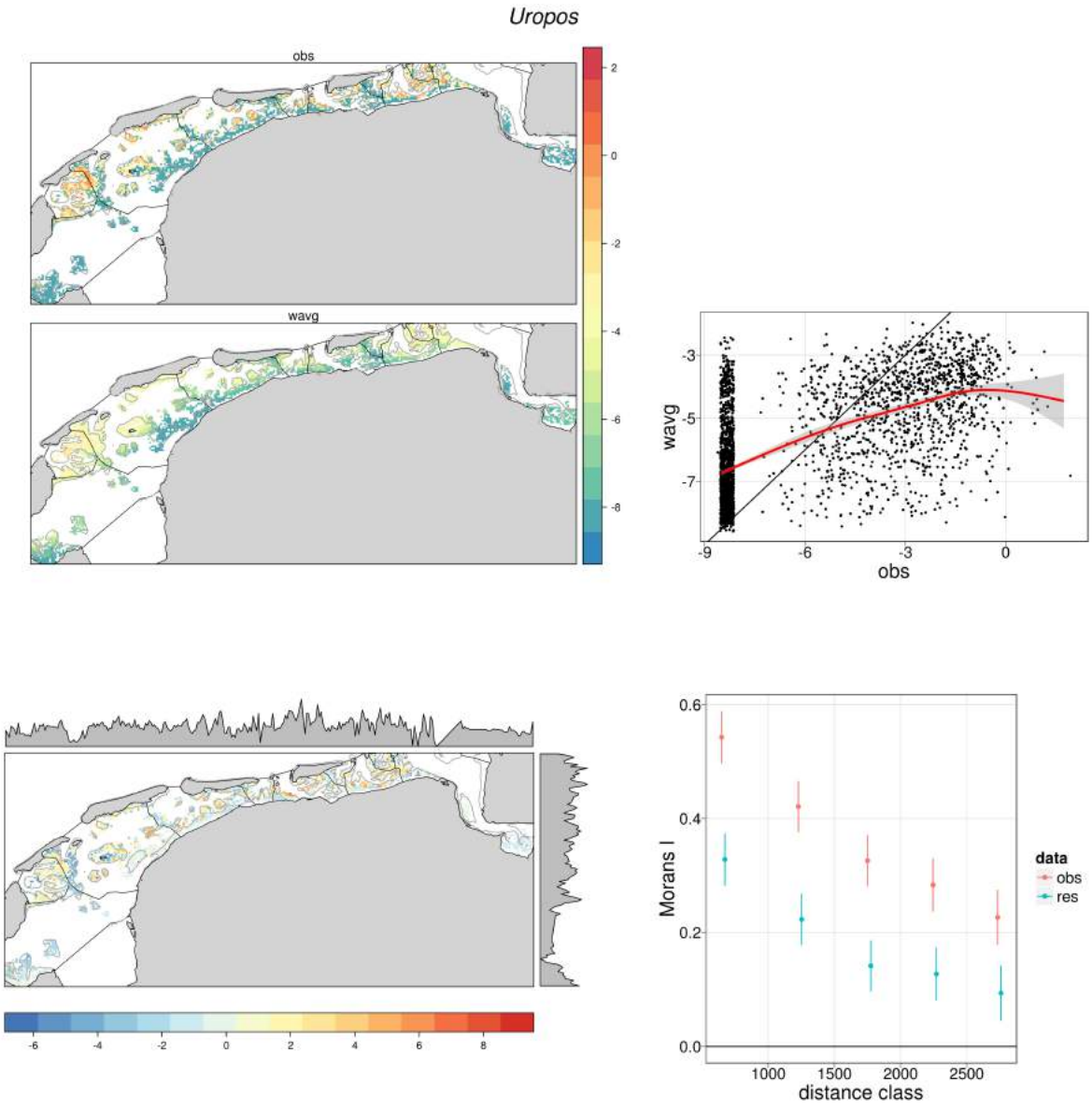

Figure 83: SDM results for biomass distributions of *Urothoe poseidonis*. See caption in Figure 11 for further information.

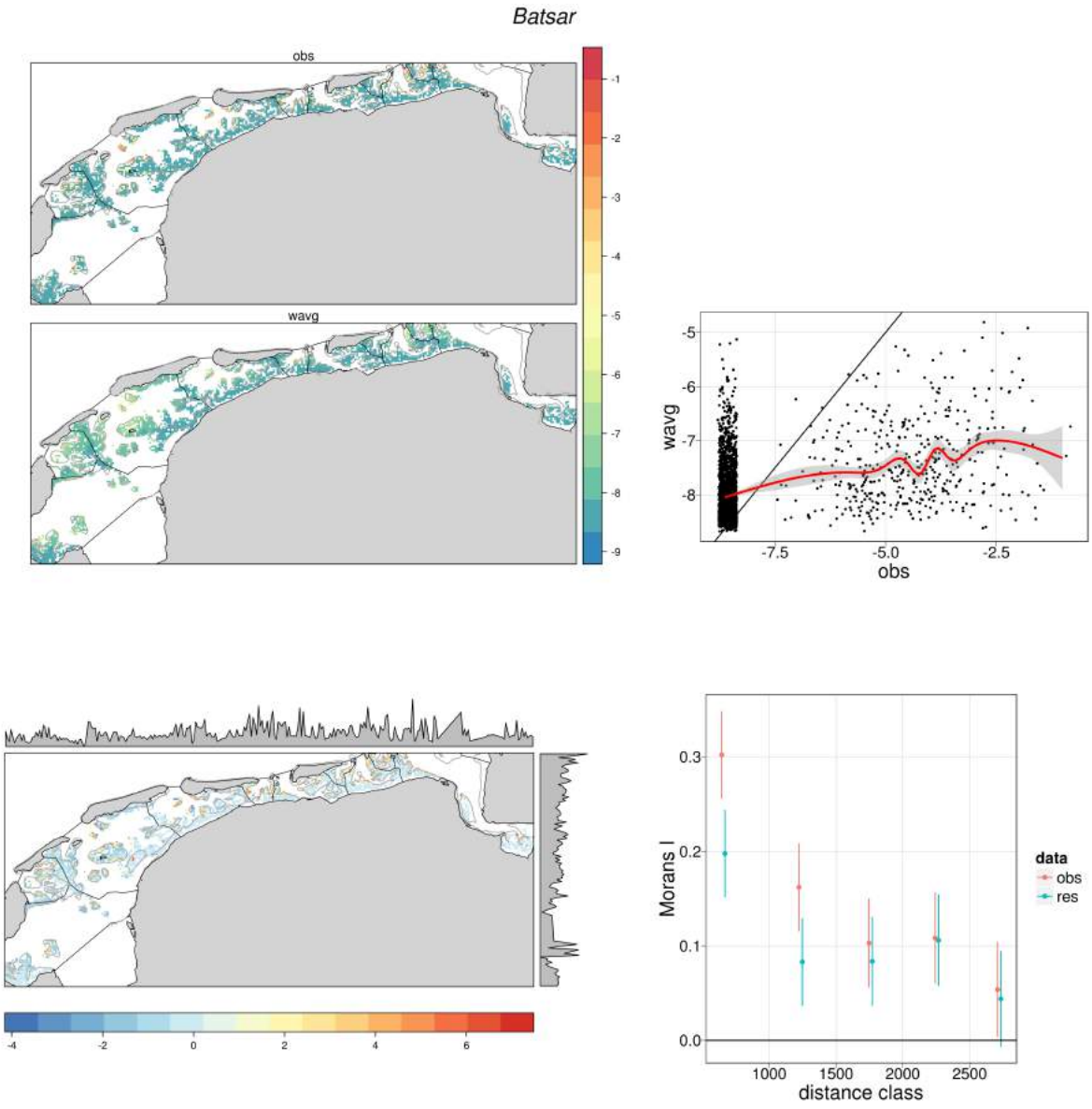

Figure 84: SDM results for biomass distributions of *Bathyporeia sarsi*. See caption in Figure 11 for further information.

NIOZ Royal Netherlands Institute for Sea Research is an Institute of the Netherlands Organization for Scientific Research (NWO).

NIOZ Texel
Landsdiep 4
1797 SZ 't Horntje, Texel

Postbox 59
1790 AB Den Burg, Texel
Nederland
Telephone: +31(0)222 - 369300
Fax: +31(0)222 - 319674

NIOZ Yerseke
Korringaweg 7
4401 NT Yerseke

Postbox 140
4400 AC Yerseke
Nederland
Telephone: +31(0)113 - 577417
Fax: +31(0)113 - 573616

www.nioz.nl

The mission of NIOZ is to gain and communicate scientific knowledge on seas and oceans for a better understanding and sustainability of our planet, to manage the national facilities for sea research and to support research and education in the Netherlands and in Europe.